Die Expedition ANTARKTIS X/4 mit FS "Polarstern" 1992

The Expedition ANTARKTIS X/4 of RV "Polarstern" in 1992

Herausgegeben von / Edited by
Peter Lemke
unter Mitarbeit der Fahrtteilnehmer /
with contributions of the participants

Ber. Polarforsch. 140 (1994)
ISSN 0176 - 5027

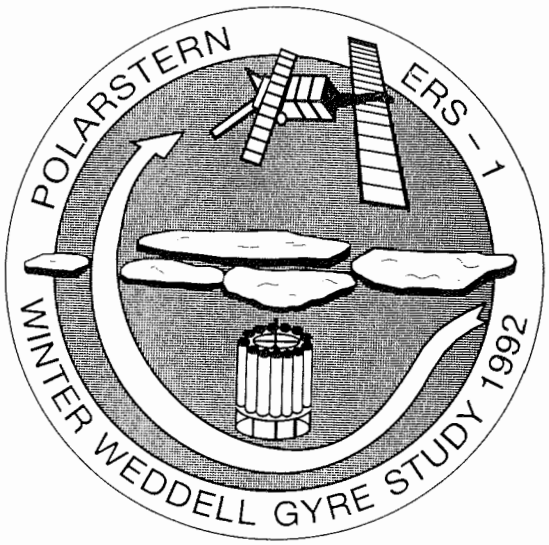

Peter Lemke
Alfred-Wegener-Institut für Polar- und Meeresforschung
Am Handelshafen 12
D-27515 Bremerhaven

Inhalt/Contents

1. Einleitung/Introduction

1.1 Wissenschaftliche Ziele und Fahrtverlauf

Der Fahrtabschnitt ANT X/4, die Winter Weddell Gyre Study 1992 (WWGS-92), umfaßte im wesentlichen zwei hydrographische Schnitte des World Ocean Circulation Experiments (WOCE), auf denen vertikale Profile von Temperatur, Salzgehalt, Sauerstoff, CO_2, Nährstoffen und einigen natürlichen und anthropogenen Spurenstoffen (Tritium, 3He, He, 18O, 16O, Ne, Freon-11 und Freon-12) gemessen wurden. Diese Arbeiten machten den gößten Teil des ozeanographischen Programms aus. Der erste Schnitt (SR2) verlief von Kapstadt im wesentlichen längs des Greenwich-Meridians zum antarktischen Kontinent (s. Fig. 1.1-1). Danach schloß sich eine Traverse durch den Weddell-Wirbel (SR4) von Kapp Norvegia nach King-George-Island an. Der Schnitt SR4 wurde - nach Sept. 89 und Dez. 90 - zum drittenmal durchgeführt und ermöglicht damit Abschätzungen zur Variabilität der Wassermassenproduktion im südlichen Weddellmeer. Die wesentlichen Ziele des ozeanographischen Programms waren die Bestimmung des baroklinen Massentransports und der damit verknüpften horizontalen Wärme- und Salzflüsse im Zirkumpolarstrom und im Weddell-Wirbel und die Abschätzung der Wassermassenumwandlung im südlichen Weddellbecken.

Im Zentrum der meteorologischen Meßprogramme stand die Energiebilanz der Meereisoberfläche. Dazu gehörte die Bestimmung der kurz- und langwelligen Strahlungsbilanz, der turbulenten Flüsse von Impuls, sensibler und latenter Wärme und des Wärmestromes durch Schnee und Meereis. Außerdem wurde die vertikale Struktur der gesamten Troposphäre mit Hilfe von Radiosonden und Omega-Windmeßsystemen erfaßt. Ferner wurden 6 ARGOS-Bojen auf Eisschollen ausgesetzt, von denen 2 außer Position, Luftdruck und Luftdrucktendenz noch vertikale Temperaturprofile in Luft, Schnee, Eis und Wasser, die Schneeakkumulation und den Salzgehalt in zwei Tiefen messen. Das Ziel der Meteorologen war, die thermodynamischen und auch dynamischen Randbedingungen für das Meereiswachstum und die Meereisbewegung zu bestimmen.

Ein wesentlicher Bestandteil dieses Fahrtabschnittes war das fernerkundliche Bodenmeßprogramm für das Synthetic Aperture Radar (SAR) und das Along Track Scanning Radiometer (ATSR) des europäischen Fernerkundungssatelliten ERS-1, sowie für infrarote, sichtbare und Mikrowellenkanäle anderer Satelliten. Aufnahmen des Real Aperture Radar (RAR) auf Satelliten der russischen OKEAN-Serie konnten leider nicht wie geplant empfangen werden, da ein neuer Satellit als Ersatz für den defekten OKEAN-3 nicht rechtzeitig in eine Umlaufbahn gebracht werden konnte.

Die Emissions- und Reflexionseigenschaften der Meereisoberfläche wurden mit Infrarot- und Mikrowellenradiometern und mit einem Scatterometer bestimmt. Referenzwerte (ground truth) der Meereiskonzentration lieferte eine digitale optische Zeilenrasterkamera. Eine neu entwickelte Infrarot-Zeilenrasterkamera wurde mit großem Erfolg erprobt. Die großskalige Oberflächenrauhigkeit (Preßeisrückenstatistik) erfaßte ein vom Hubschrauber betriebener Laserentfernungsmesser. Hauptziel des fernerkundlichen Programms war die Verbesserung der Algorithmen zur Bestimmung der Meereiskonzentration, der Meereisbewegung, des Meereistyps und der Oberflächenrauhigkeit, damit eine genauere Beschreibung dieser Variablen großflächig über einen längeren Zeitraum erfolgen kann. Dies ist für ein besseres Verständnis der Physik des Meereises und seiner Modellierung unerläßlich.

Außerdem wurden physikalische Eigenschaften von Schnee und Meereis untersucht. Dazu wurden Eiskerne gezogen und Dicke, Salz- und Temperaturprofile, Porengröße, Textur, Dichte, Dielektrizitätskonstante und die kleinskalige (mm-cm) Oberflächenrauhigkeit gemessen. Diese Daten ermöglichen eine verbesserte Analyse der Satellitenbeobachtungen des Meereises. In einem ersten Versuch wurde schließlich die Meereisdicke mit seismischen Mehrfrequenz Reflexionsverfahren auf größerer Distanz registriert.

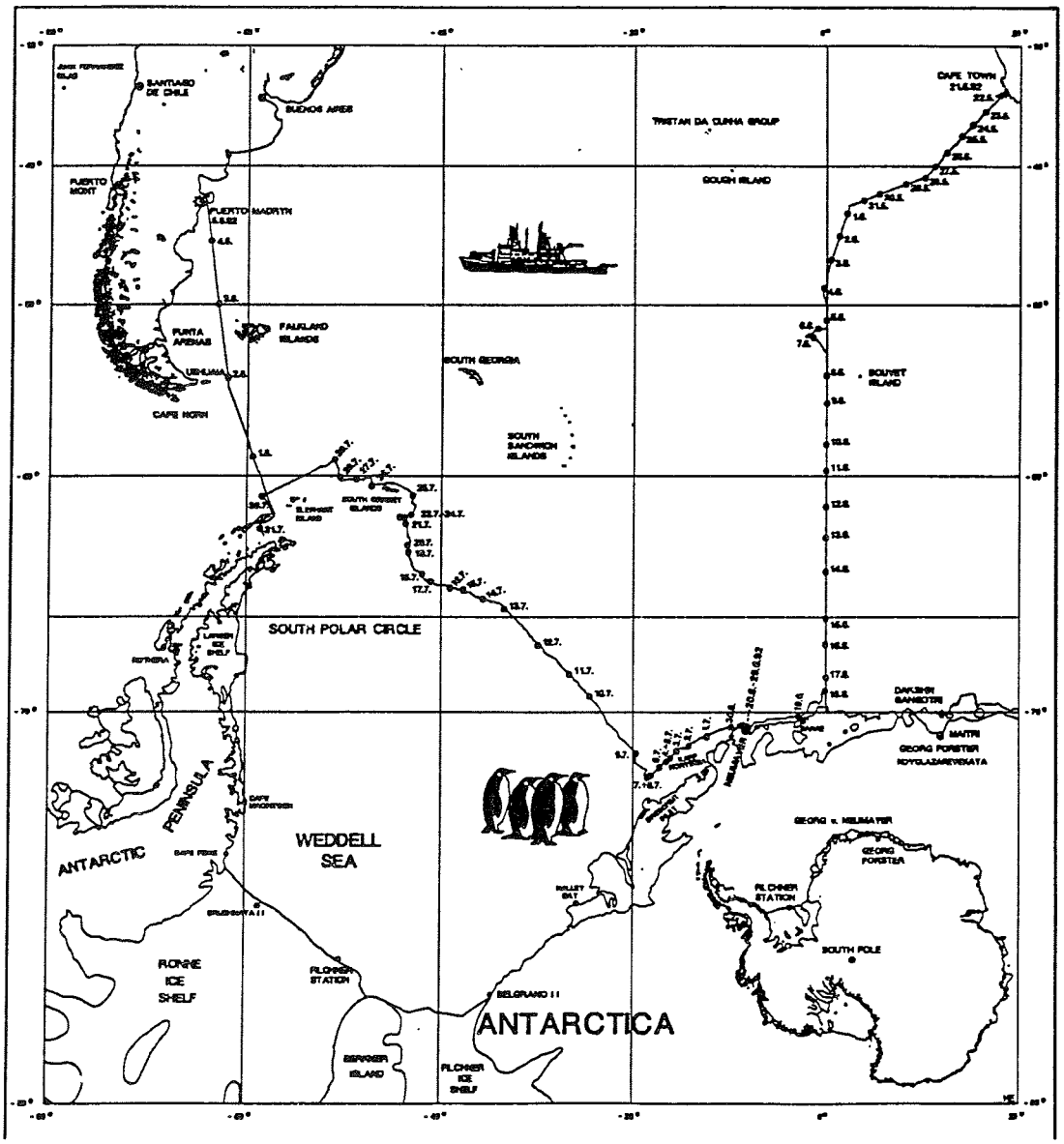

Fig. 1.1-1: Cruise track of RV "Polarstern" during ANT X/4

Im biologischen Programm wurde die Planktonökologie im Meereis und in den oberen Ozeanschichten untersucht. Insbesondere wurden Verteilungsmuster von Phyto- und Zooplankton, von partikulärem, organischen Kohlenstoff und Stickstoff und von Chlorophyll-a gemessen und mit den ozeanographischen Umgebungsbedingungen verglichen.

Die chemischen Messungen betrafen Lipiduntersuchungen, aus denen sich Rückschlüsse auf die physiologische Anpassung der Copepoden, die einen großen Anteil der Biomasse im Südlichen Ozean ausmachen, in Bezug auf Lebensraum und Nährstoffangebot ziehen lassen.

Schließlich wurden zwischen Kapstadt und der Meereisgrenze mit Hilfe eines unter der CTD-Rosette angebrachten Minicorers Oberflächensedimente gewonnen. Diese Proben sollen auf ihren Gehalt an kalkigen und kieseligen Mikrofossilien, sowie abiogenen Sedimentkomponenten analysiert werden. Sie bilden eine wichtige Grundlage für paläo-ozeanographische und paläo-klimatologische Rekonstruktionen.

"Polarstern" verließ Kapstadt am 21. Mai 1992 mit 42 Besatzungsmitgliedern und 45 Wissenschaftlern an Bord. Das ozeanographische Programm begann am 22. Mai früh morgens wenige Meilen südwestlich von Kapstadt mit der Aufnahme von vertikalen CTD- und Wasserschöpferprofilen (Rosette mit 24 Schöpfern) von der Meeresoberfläche bis zum Meeresboden in horizontalen Abständen von 30 bis 45 Seemeilen bis zum antarktischen Kontinent. Über den kontinentalen Schelfabhängen wurde ein engerer, an vorgegebenen Tiefenlinien orientierter Abstand gewählt.

Der Kurs führte zunächst nach Südwesten bis zum Greenwich Meridian. Auf dem Weg dorthin wurden die Subtropenfront (am 27. Mai bei 40°25'S, 10°50'E) und die Subpolarfront (am 2. Juni bei 45°50'S, 01°04'E) überquert. Auf dem Shannon Seamount (42°59.6'S, 02°20.3'E) wurden zwei Druckpegel in etwa 800 m Tiefe ausgesetzt. Auf dem Greenwich Meridian nach Süden fahrend wurden am 3. Juni die ersten Eisberge bei 47°30'S gesichtet. Am 5. Juni erreichte "Polarstern" die Polarfront bei 51°30'S. Nördlich der Polarfront begannen die Biologen mit ihren Untersuchungen, so daß nun zusätzlich zur CTD-Rosette täglich ein Bongo- oder ein Multinetz eingesetzt wurde.

Die Meereisgrenze erreichte "Polarstern" am 12. Juni bei 60°56.4'S. Das Meereis bestand im wesentlichen aus Pfannkucheneis, durchsetzt von Eisbrei und offenen Wasserflächen. Erst bei 68°S wurde die Meereisdecke dichter und dicker. Dort begannen am 17. Juni die Arbeiten der Eis- und Fernerkundungsgruppen auf dem Meereis. Vorher konnten einige kleinere Meereis-Pfannkuchen mittels Eiskorb an Deck gebracht werden und Eiskerne vom Kran aus geborgen werden.

Am 16. Juni begann die Polarnacht. Trotzdem war es in der Dämmerung häufig möglich, 2 bis 3 Stunden die Hubschrauber zu Forschungszwecken einzusetzen. So konnten im Umkreis von 10 bis 20 Seemeilen Schnee- und Eisproben genommen und die Infrarot-Rasterkamera sowie der Laser-Entfernungsmesser eingesetzt werden.

Am 19. Juni wurde der Schnitt SR2 mit der 71. CTD-Station vor der Schelfeiskante bei 69°42.6'S und 00°40.8'W beendet. Danach fuhr "Polarstern" durch die - wegen des Nachlassens der katabatischen Winde - gerade zufrierende Küstenpolynja zur Neumayer-Station, um dort einige Kisten mit Post, Ersatzteilen und frischem Obst und Gemüse per Hubschrauber abzuliefern.

Bei Ankunft in der Atka-Bucht am 20. Juni verschlechterte sich das Wetter derart, daß weder an einen Hubschrauberflug noch an einen Austausch per Skidoo gedacht werden konnte. Ein Schneesturm der Stärke 10 vereitelte alle größeren Außenaktivitäten. So wurde ein Depot mit Post und Ersatzteilen auf dem Meereis angelegt, in der Hoffnung, die Überwinterer könnten mit dem Skidoo in den nächsten Tagen dorthin gelangen. Der Sturm und auch der darauffolgende

stetige Ostwind preßten das Eis so stark in die Bucht, daß es "Polarstern" nicht gelang, aus der Bucht auszulaufen. Da in den nächsten Tagen die Sicht gut war, gelang endlich ein Hubschrauberflug mit Frischobst und -gemüse zur Station. Auch hatten die Überwinterer inzwischen das Depot per Skidoo erreicht. Erst nach einer Drehung des Windes auf Südost am 29. Juni - und einem damit verbundenen Nachlassen des Druckes im Meereis - konnte sich das Schiff befreien und nach Kapp Norvegia dampfen.

Nach einer CTD-Station vor Kapp Norvegia am 1. Juli vereitelte ein Orkan die weitere Fahrt nach Nordwesten. "Polarstern" wurde im dichten Preßeis des Küstenstromes gefangen, von starken Nordostwinden an die Küste gedrängt und so 140 Seemeilen nach Südwesten abgetrieben, ehe sie sich - wieder erst nach einer Winddrehung, diesmal auf Südwest - am 8.Juli aus dem Druck des Küstenstromes befreien konnte. Auf dem Weg zum Zentrum des Weddellwirbels wurden an 10. und 11. Juli zwischen 69°44'S, 23°47'W und 68°15'S, 27°35'W sechs Argos-Bojen und zehn Radarreflektoren (für das ERS-1 SAR) in Form eines Parallelogramms ausgesetzt.

Am 11. Juli endete die Polarnacht. Am 13. Juli begann am Polarkreis die geplante Arbeit mit Nordwestkurs auf dem vorgesehenen Schnitt von Kapp Norvegia zur Spitze der antarktischen Halbinsel. "Polarstern" geriet nun in Gebiete mit zunehmendem Anteil an zweijährigem Meereis mit Dicken von 150 - 250 cm. Die Lufttemperaturen sanken auf -32°C, so daß auch die letzten Rinnen zugefroren waren und die Navigation erschwerten. Mehrere Tage war nur eine Fahrt von durchschnittlich 2 Knoten möglich. Daher wurde am 19. Juli - mit Rücksicht auf die noch vorhandene Zeit und die Brennstoffvorräte - entschieden, den geplanten Kurs zu verlassen und entlang der wenigen, mit dünnem Eis überzogenen Rinnen nach Nordnordwesten auf South Orkney zuzuhalten.

Auf dem Schelf südöstlich von South Orkney fand vom 21. bis 24. Juli eine dreitägige Langzeitstation statt. Die Ozeanographen errichteten mehrere hundert Meter vom Schiff entfernt ihre Meßgeräte, mit denen sie durch ein Loch in der Eisscholle die Turbulenz in der obersten Ozeanschicht untersuchten. Die Eisgruppe war nicht nur mit dem üblichen Programm (Bestimmung der Eis- und Schneedicken und der vertikalen Temperaturprofile, Entnahme und Analyse von Eiskernen) beschäftigt, sondern hat auch versucht, mit Hilfe von seismischen Methoden etwas über die Elastizität des Eises und damit über die Eisdicke entlang einer größeren Strecke zu erfahren. Die Fernerkundler hatten endlich Gelegenheit, dasselbe Stück einer Eisscholle drei Tage lang bei unterschiedlichem Wetter mit aktiven und passiven Strahlungssensoren zu beobachten. Die Meteorologen haben während dieser Zeit die Energiebilanz der Meereisoberfläche gemessen. Dazu gehörten die Einstrahlung der Sonne, die Wärmeabstrahlung der Eisoberfläche, die Wärmestrahlung, die von den Wolken herunterkommt, der turbulente Wärmeaustausch zwischen Luft und Eis und der Wärmestrom vom Ozean durch die Eisscholle. Am ersten Tag herrschten Temperaturen um -22°C, dann sorgte eine Warmfront mit Windstärke 10 für Temperaturen um den Gefrierpunkt.

Nach Beendigung der Drei-Tage-Station fuhr "Polarstern" im Norden von South Orkney in westliche Richtung, um CTD-Stationen für die Bestimmung des ozeanischen Massentransportes zwischen Elephant Island und South Orkney durchzuführen.

Der letzte Einsatz der CTD-Rosette fand am 30. Juli über dem Südshetlandgraben nördlich von King-George-Island bei 5200 m Tiefe statt. Die Spurenstoffgruppe war insbesondere an dem unverschmutzten, FCKW-freiem Wasser interessiert, das sich hier in 2000 - 3000 m Tiefe befindet. Mit diesem reinen Wasser lassen sich Verunreinigungen der 24 Wasserschöpfer an der Rosette ausschließen.

Nach Beendigung der letzten Station - insgesamt waren es während dieser Fahrt 115 Stationen, an denen Geräte zum Einsatz kamen - dampfte "Polarstern" in die Maxwell-Bucht zur chilenischen Antarktis-Station Teniente Marsh an der Südküste von King-George-Island, wo am 31.

Juli die Bedienungsmannschaft der deutschen ERS-1 Satelliten-Empfangsstation auf O'Higgins per Flugzeug erwartet wurde. Leider war das Wetter schlecht. Es herrschte Nebel. Der Flug wurde abgesagt, und "Polarstern" mußte ohne Gäste nach Norden dampfen, da keine Wartezeit mehr zur Verfügung stand. Die Mannschaft mußte daraufhin mit einem Charterflug abgeholt werden.

Von King-George-Island ging es auf direktem Kurs zum Zielhafen Puerto Madryn. Von der Eiskante bis zum argentinischen Schelf wurden 23 vertikale Profile der Temperatur mittels XBT-Sonden und Profile der Strömung continuierlich durch ein ADCP (Accoustic Doppler Current Profiler) erfaßt.

Während der Fahrt wurden von der HRPT-Anlage an Bord 170 Infrarot-Aufnahmen der amerikanischen Wettersatelliten abgespeichert, die das Eis im Weddellmeer zeigen. Auf der deutschen ERS-1-Empfangsstation wurden 400 Überläufe des SAR aufgezeichnet. Außerdem stehen nach der Fahrt tägliche Mikrowellenbilder des SSM/I (Special Sensor Microwave Imager) des amerikanischen DMSP-Satelliten zur Verfügung. Durch den Vergleich dieser verschiedenen Sensoren wird eine Verbesserung der Algorithmen zur Bestimmung der Meereiskonzentration und Meereisbewegung erhofft.

Am 5. August 1992, um 6.oo Uhr, lief "Polarstern" planmäßig in den Hafen von Puerto Madryn ein.

1.2 Summary and itinerary

The expedition ANTX/4 - the Winter Weddell Gyre Study 1992 (WWGS-92) - consisted of two hydrographic sections of the World Ocean Circulation Experiment (WOCE), during which vertikal profiles of temperature, salinity, oxygen, CO_2, nutrients and several tracers (Tritium, 3He, He, 18O, 16O, Ne, Freon-11 and Freon-12) were taken. These activities represented the largest part of the oceanographic program. The first section (SR2) from Cape Town to Antarctica mainly followed the Greenwich Meridian. The second section (SR4) - a traverse of the Weddell Gyre - extended from Kapp Norvegia to King-George-Island. The section SR4 was taken for the third time after September 1989 and December 1990 and therefore allows estimates of the variability of the water mass production in the southern Weddell Sea. The main goals of the oceanographic program were the determination of the baroclinic mass transport from the horizontal heat and salt fluxes in the Antarctic Circumpolar Current and in the Weddell Gyre, and the water mass modification in the southern Weddell Sea.

The meteorological program focused on the energy balance at the sea ice surface. The activities consisted of the determination of the short- and long-wave radiation balance, the turbulent fluxes of momentum, sensible and latent heat, and the heat conduction through snow and sea ice. The vertical structure of the entire troposphere was determined from radio sonde ascents. Six ARGOS-buoys were deployed, two of which measured also the vertical temperature profiles in atmosphere, snow, ice and upper ocean, snow accumulation and salinity at two depths, in addition to position, air pressure and air pressure tendency. The goal of the meteorological program was the determination of the thermodynamic and dynamic boundary conditions for sea ice growth and motion.

One of the main components of the expedition was the remote "sensing ground truth" program for the Synthetic Aperture Radar (SAR) and the Along Track Scanning Radiometer (ATSR) of the european satellite ERS-1, and for infrared, visible and microwave channels of sensors on other satellites. Data of a Real Aperture Radar (RAR) on board a satellite of the russian OKEAN series could not be received as planned since a replacement for the defective OKEAN-3 satellite was not launched in time.

Emission, reflection and scattering properties of the sea ice surface were determined with infrared and microwave radiometers and with a scatterometer. Ground truth data of sea ice concentration were obtained with a line-scan camera operated from a helicopter. The sea ice surface topography (pressure ridges) was measured with a helicopter-borne laser-altimeter. The main goal of the remote sensing program was the improvement of algorithms for determining sea ice concentration, motion, ice type and surface roughness on larger scales in space and time. These data sets are required to improve our understanding of the physics of sea ice and to provide observations to test and verify sea ice models.

Measurements of the physical properties of snow and sea ice included the sea ice thickness, vertical profiles of density, salt, temperature, pore size, and texture, and the dielectric constant and small-scale (mm-cm) surface roughness. These data will be used to better interprete satellite observations. Finally, a first attempt was undertaken to determine sea ice thickness with a seismic multifrequency reflection method.

The main goal of the biological program was the plancton ecology within the sea ice and the upper ocean. Measurements of the distribution of phyto- and zoo-plankton, of particulate organic carbon and nitrogen and of chlorophyll-a were taken, and were compared to the properties of the oceanographic environment.

The chemical measurements consisted of lipid investigations undertaken to obtain information on the physiological adaptation of copepods, which represent a large fraction of the biomass in the Southern Ocean, with respect to environment and nutrient supply.

Within the geological programm surface sediments were investigated between Cape Town and the sea ice edge using a minicorer fixed under the CTD-rosette. Data from these samples represent the basis for paleo-oceanographic and paleo-climate reconstructions.

"Polarstern" left Cape Town on 21 May 1992 with 42 crew members and 45 scientists aboard. The oceanographic program started on 22 May in the morning a few miles south-west of Cape Town with the beginning of the section SR2. Stations were taken with a distance of 30 to 45 nm. Above the continental shelf slopes the station distance was smaller depending on given depth intervals.

In the beginning the course led south-west to the Greenwich Meridian passing the subtropical front on 27 May at 40°25'S, 10°50'E and the subpolar front on 2 June at 45°50'S, 01°04'E. Above the Shannon Seamount (42°59.6°S, 02°20.3'E) two pressure gauges were deployed at a depth of about 800 m. Steaming south along the Greenwich Meridian the first icebergs were sighted on 3 June at 47°30'S. On 5 June "Polarstern" crossed the polar front at 51°30'S. North of the polar front the biology program started with a daily bongo- or multinet tow.

The ice edge was crossed on 12 June at 60°56.4'S. The sea ice was mainly pancake and grease ice up to 68S where the ice got thicker and more compact. Here the work of the sea ice and remote sensing group started on the ice floes on 17 June.

On 16 June the sun set for the polar night. Nevertheless, helicopter work was generally possible for two hours during the twilight at noon for taking snow and ice samples or obtaining data from the infrared line scanner or the laser altimeter in the vicininity of the ship.

The section SR2 was completed on 19 June with the 71st station off the shelf ice at 69°42.6S, 0°40.8'W. "Polarstern" steamed through the freezing coastal polynya towards Neumayer-Station. Entering Atka Bay on 20 June the weather conditions deteriorated such that a supply of the station with helicopter or skidoo was impossible. A depot was put on the sea ice, which was visited from the station later during calm weather. "Polarstern" tried to leave Atka Bay but the pressure in the sea ice cover due to the strong easterly winds was too high. It was only after a

turning of the wind to south-east on 29 June that "Polarstern" was able to escape the dense pack ice in Atka Bay and steam towards Kapp Norvegia.

After finishing a CTD-station off Kapp Norvegia on 1 July a hurricane stopped the continuation of the section towards the north-west. "Polarstern" was forced to shut off the engines, and drifted due to continuing strong north-easterly winds passively with the sea ice in the coastal current 140nm to the south-west. After a turning of the wind towards south-west on 8 July the ship escaped the coastal current. On course to the center of the Weddell Gyre six ARGOS-Buoys and ten radar reflectors were deployed on 10 and 11 July between 69°44'S, 23°47'W and 68°15'S, 27°35'W.

The polar night ended on 11 July. The section work continued on the planned cruise track on 13 July. "Polarstern" now entered regions with increased concentration of multiyear sea ice with thicknesses of 150 to 250 cm. The temperature decreased to -32°C such that most leads were frozen. The average speed of the icebreaker reduced to 2 knots. Considering the remaining time and fuel it was decided on 19 July to leave the planned cruise track in northward direction following the lead pattern towards South Orkney.

On the shelf south-east of South Orkney a three-day ice-station took place from 21 to 24 July. The oceanographers performed turbulence measurements in the mixed layer under the sea ice. Besides the general program of measuring sea ice and snow thicknesses and profiles of temperature, salinity and porosity, the sea ice group investigated the elasticity of the ice floe - and hence its thickness - with seismic methods. The remote sensing group was glad to view the same piece of sea ice with their sensors under different weather conditions. The meteorologists were able to collect a longer data set for the energy balance at the sea ice surface. The first part of the station took place under cold conditions (-22°C). Then a passing warm front with Beaufort 10 winds raised the temperature up to the freezing point.

After the long station "Polarstern" steamed westward north of South Orkney taking CTD-stations in order to determine the baroclinic flow between South Orkney and Elephant Island. The last CTD-station was taken on 30 July 1992 above the South Shetland Trench north of King-George-Island at a water depth of 5200 m. This station with a freon-blanc at depths between 2000 and 3000 m was used for calibration of the tracer data. In total 115 stations were taken during the cruise.

After the last CTD-station "Polarstern" steamed into Maxwell Bay off the chilean station "Teniente Marsh", where the crew of the german ERS-1 receiving station was supposed to board the ship. Unfortunately, the weather was bad. The flight from O'Higgins was cancelled, and "Polarstern" had to leave for Puerto Madryn without taking the crew aboard.

From the sea ice edge up to the argentinian shelf 23 XBT-profiles were taken, and the vertical current shear was recorded continuously with an Accoustic Doppler Current Profiler (ADCP).

During the cruise 170 infrared images of the Weddell Sea region from US weather satellites were recorded. At the german receiving station at O'Higgins 400 passes of the ERS-1 SAR were received. Furthermore, after the cruise daily microwave images of the SSM/I will be available. From the comparison of the different sensors an improvement of the algorithms for sea ice concentration and motion are expected.

On 5 August 1992 at 6:00 GMT "Polarstern" arrived at Puerto Madryn as planned.

1.3 Wetterchronik

E. Röd, H. Köhler (SWA), O. Schulze (IMH)

Auf dieser Winterreise stellten sich fünf ausgeprägte Sturmlagen ein, die von wesentlichem Einfluß auf den Fahrtverlauf und die wissenschaftlichen Arbeiten waren. Sie liefen nach unterschiedlichen Mechanismen ab und hatten jeweils andere Auswirkungen.

Der erste Sturm entwickelte sich am 4./5. Juni auf 50S/00E,W. Das auslösende Zentraltief war bei der Bouvet-Insel zu erkennen, der orkanartige Sturm war jedoch hauptsächlich durch einen kleinen Randwirbel verursacht, der genau über "Polarstern" hinweg nach Osten zog. Der Kerndruck von 962 hPa konnte daher recht exakt festgelegt werden. An der Rückseite setzte von SW Kaltluftadvektion ein und ließ von jetzt an bis zum Verlassen des Eises die Temperatur nicht mehr deutlich über den Gefrierpunkt steigen.

Bei dieser Zyklogenese handelte es sich um eine durch Advektion positiver Vorticity an der Polarfront eingeleitete Entwicklung, die ausschließlich durch das geostrophische Gleichgewicht bestimmt war. Ein zweites Sturmtief an der Polarfront blieb über dem Fahrtgebiet wirkungslos, da ein anderes Tief bei der Schiffsposition einen Sattelpunkt mit schwachen Gradienten hatte entstehen lassen.

Die 2. Starkwindlage war hingegen schon ganz dem antarktischen Regime zuzuordnen. Das auslösende Tief auf 66S/25W war von der Atka-Bucht noch so weit entfernt, daß bei einem Kerndruck von 975 hPa der hier beobachtete 50 Knoten-Wind nicht als Gradientwind erklärt werden konnte. Am Abend des 22. Juni schwenkte die Kaltfront dieser Zyklone über "Polarstern" hinweg: innerhalb weniger Minuten drehte der Wind von ESE auf NW und nahm gleichzeitig von Sturmstärke auf 3-4 Bft ab. Offenbar handelte es sich bei dem E-Sturm um einen föhnartigen katabatischen Wind (die Temperatur stieg von -15° bis -6° C und sank hinter der Kaltfront in der schwachen NW-Strömung wieder bis -24° C) der durch das Tief in Gang gesetzt worden war und sich dann autonom entwickelte, bevor ihn die Kaltfront beendete. Die schwache postfrontale NW-Strömung zeigte, daß wieder das geostrophische Regime bestimmend geworden war. Dieser Fall demonstriert besonders gut die komplizierte Verquickung geostrophischer und katabatischer Antriebe, die oft nicht voneinander getrennt werden können, wodurch die Analyse des Windfeldes aus Windbeobachtungen wesentlich erschwert wird.

Der 3. schwere Sturm wurde durch ein Tief ausgelöst, das von South Georgia anfangs nach E zog, bei den South Sandwich-Inseln dann aus der zonalen Zugbahn nach SE ausscherte und sich unter Vertiefung auf 950 hPa dem bei Kapp Norvegia operierenden Schiff am 1.Juli bis auf 300 SM näherte. Die hier gemessene Windgeschwindigkeit von durchschnittlich 60 Knoten ließ sich diesmal zwanglos aus den beobachteten Druckdifferenzen erklären, allenfalls die Orkanböen von 85 Knoten können als katabatische Komponente gedeutet werden.

Am 2. Juli hatte kräftiger Druckfall bis 962 hPa bei "Polarstern" die Druckdifferenz gegenüber dem Tiefkern auf ca. 14 hPa verringert, ohne daß der Wind zunächst deutlich abnahm. Der weiter anhaltende E 10 Bft muß demnach als katabatische Fortsetzung des geostrophisch eingeleiteten Sturmes angesehen werden. Katabatische Winde im engeren Sinne, die örtlich begrenzt abrupt einsetzen und aufhören oder sprungartige Temperaturänderungen herbeiführen, wurden nicht beobachtet. Ein weiterer antarktischer E-Orkan mußte aufgrund der dramatischen 108 Stunden-Vorhersage des ECMWF für den 27./28. Juni prognostiziert werden. Die spätere 60 Stunden-Vorhersage für denselben Tag brachte hingegen eine gänzlich andere harmlose Version, während nach den US-Prognosen die Zeichen weiterhin auf Sturm standen. Tatsächlich trat an den fraglichen Tagen nur Windstärke 7 auf. Dieser prognostische Fehlschlag zeigt, daß in der Antarktis, die oft fast ein No-Data-Gebiet ist, die numerischen Modelle vielfach überfordert sind und besonders die längerfristigen Vorhersagen mit viel Kritik und Vorsicht verwendet werden müssen.

Interessant waren die wiederholten Zyklogenesen über der westlichen Weddell-See, die durch Tiefs induziert worden waren, die sich von W der Halbinsel genähert und dann dort aufgelöst hatten. Ein solches war für die 4. Sturmlage verantwortlich, die sich am 23. Juli entwickelte. "Polarstern" hatte die Antarktis auf Heimatkurs bereits verlassen, auf 62S bei den South Orkneys die Westwindzone erreicht und die subpolare Tiefdruckrinne durchquert. Bei hohem Druck über dem südlichen Südamerika baute der Druckfall über der Weddell-See von der Drake-Passage über das Fahrtgebiet hinweg eine sehr scharfe Frontalzone auf. Die Warmfront des Weddell-See-Tiefs ließ die Temperatur vom 23. zum 24. Juli von -22° C auf 0° C steigen, während der Wind gleichzeitig zum schweren NW-W-Sturm wurde. In der Nähe der South Orkneys zeigten sich deutliche orographische Effekte: im Windschatten der Inseln flaute der Wind auf 6 Bft ab, um nördlich davon an der strömungsparallelen Küste unvermittelt auf W 9-10 zuzunehmen.

Die fünfte und letzte Starkwindlage war am 31. Juli die Ursache des Fehlschlagens der geplanten Abholaktion bei der Station Teniente Marsh auf King George Island. Das wirksame Tief war an der Nordspitze der Halbinsel bei hohem Druck über der Bellingshausen See offenbar rein dynamisch durch die Orographie erzeugt worden und entfernte sich langsam zur zentralen Weddell-See. Diese Zyklogenese folgte somit einem ganz anderen Mechanismus als die zuletzt beschriebene. Anzeichen für eine Induzierung durch Advektion positiver Vorticity waren nicht zu erkennen. Das Windfeld dieses Tiefs war in Nähe der Inseln sehr uneinheitlich. Der schwere Weststurm mit Böen bis 10 Bft flaute im Windschatten rasch auf W 7 ab und hätte den Helikoptereinsatz nicht mehr wesentlich behindert, doch wollte der Pilot des Flächenflugzeuges wegen der auf die Leeseite der Insel übergreifenden tiefen Staubewölkung und schlechter Kontraste in leichtem Schneefall den Flug von O'Higgins nach Teniente Marsh nicht riskieren. Vom 1. August an nahm der Wind rasch ab, doch war "Polarstern" bereits in der Drake Passage unterwegs zum Zielhafen.

Zu erwähnen ist, daß in antarktischen Breiten "polar lows" weder direkt beobachtet noch im Satellitenbild gefunden werden konnten. Vielleicht deshalb, weil während der Polarnacht nur Bilder im Infrarotbereich aufzunehmen und die von diesen subskaligen Zirkulationen erfaßten unteren Schichten durch hohe Wolken verdeckt waren. Trotz ztw. erhöhter solarer Aktivität war überraschenderweise sogar auf der südlichsten Position auch nicht die Andeutung von Südlicht am sternklaren Himmel zu entdecken.

Unerwartet war die hohe interdiurne Variabilität der Temperatur, die durch häufige, z.T. drastische advektive Vorgänge bedingt war. Nicht nur Fronten, die in ausgeprägter Form die antarktischen Breiten erreichen konnten, brachten rasche und kräftige Temperaturänderungen, oft genügte dafür eine Winddrehung. Die Temperaturvorhersage reduzierte sich somit vielfach auf eine Windvorhersage. Die vertikale Temperaturschichtung war besonders während der anhaltenden Ostlagen durchweg inversionell. Die schärfste Inversion betrug 18° C, der stärkste vertikale Temperaturgradient 2.4° C /100 m.

Eine Zusammenfassung des Wettergeschehens während der Expedition ist in Tables 1.3-1, 1.3-2 und in Figs. 1.3-1a-c und 1.3-2 dargestellt.

1.4 Weather Conditions

During this winter cruise five marked storm events occurred which had a strong influence on the ship's operations and the scientific work. The first storm developed on 4/5 June at 50S,0E with 11 Bft winds. The cyclogenesis was driven by advektion of positive vorticity at the polar front, and the wind was geostrophically balanced. During the storm "Polarstern" had to stop all station work and was forced off course.

The second storm event (22 June, 10 Bft) confined "Polarstern" to Atka Bay. This time the wind speed could not be explained by geostrophy alone, but by an additional strong katabatic wind component. The third storm (1 July, 12 Bft) forced "Polarstern" off course into the densely packed coastal current. This storm was basically in geostrophic balance. Only the gusts of up to 85 knots were probably katabatically induced.

The fourth storm event (23 July, 10 Bft) showed a typical cyclogenesis in the western Weddell Sea influenced by low pressure systems dissolving at the Antarctic Peninsula. This storm was associated with a warm front which initiated a strong temperature change during the long ice station. The fifth storm (31 July, 10 Bft) which seemed to be orographically induced was mainly responsible for the failure to take the crew of the german receiving station aboard. A summary of the weather conditions during the expedition is shown in Tables 1.3-1 and 1.3-2 and Figs. 1.3-1a-c and 1.3-2.

Table 1.3-1: Extrema of several meteorological parameter measured during WWGS-92:

	Extrema	
Parameter	Maximum/date	Minimum/date
air pressure	1016.1 hPa/22.07.	961.2 hPa/11.06
air temperature	1.1° C/25.07.	-32.0° C/14.07
windspeed (10 min. mean)	64.3 kn/01.07.	

Maximum air pressure decrease:	01.07. - 02.07.	47 hPa in 32 hours (1009 hPa to 962 hPa)
Maximum temperature rise:	17.07.	23.4 K in 27 hours (-24.6° C to -1.2° C)
Maximum temperature decrease:	22.06.	18.3 K in 11 hours (-5.0° C to -23.3° C)

Table 1.3-2: Temperature statistics for the cruise track within the ice cover:

Number of days with minimum	< 0.0° C:	46
Number of days with maximum	< 0.0° C:	42
Number of days with minimum	≤ -10.0° C:	38
Number of days with minimum	≤ -20.0° C:	21
Number of days with minimum	≤ -30.0° C:	2
Number of days with maximum	≤ -10.0° C:	23
Number of days with maximum	≤ -15.0° C:	14
Number of days with maximum	≤ -20.0° C:	6

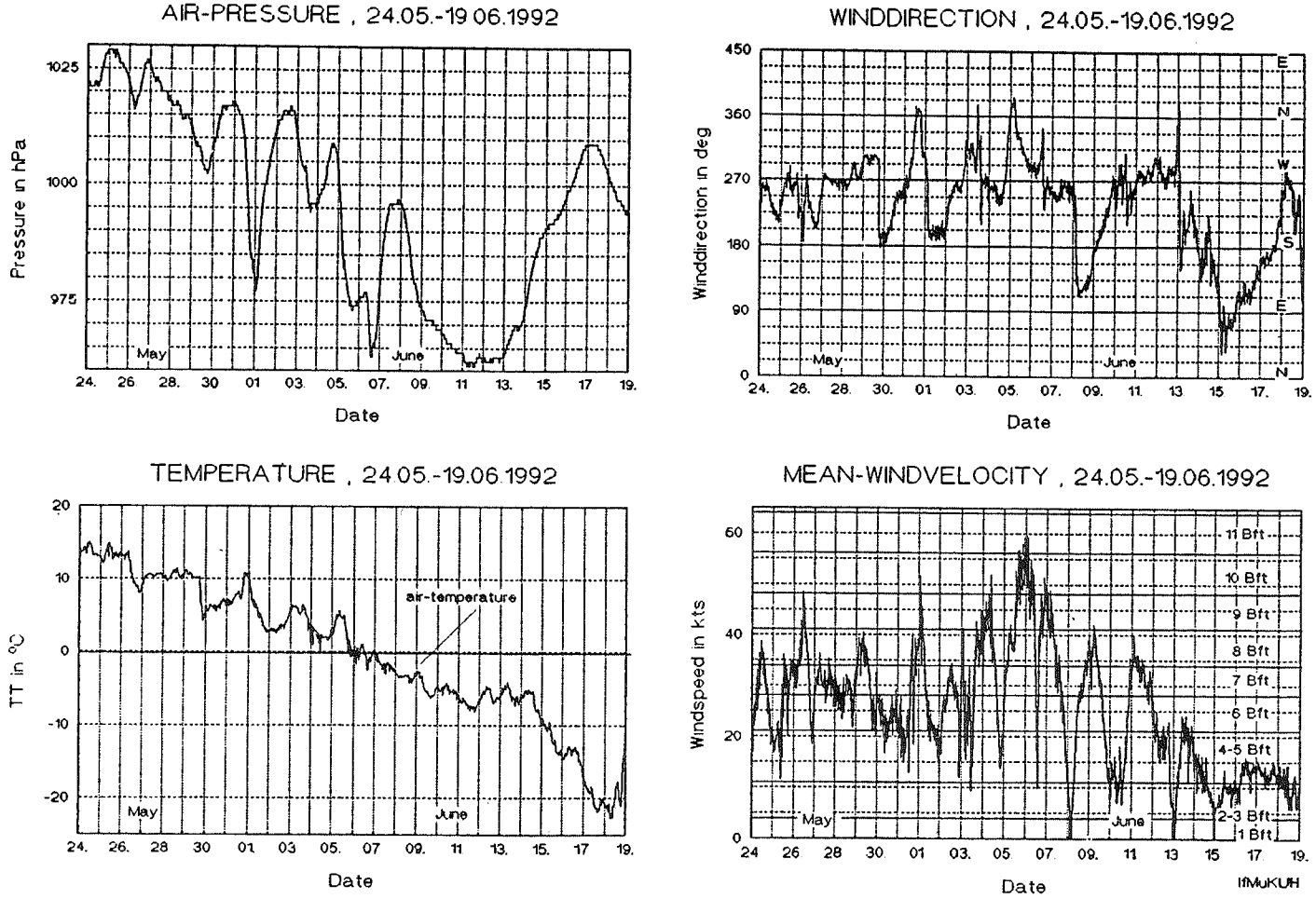

Fig. 1.3-1a: Plot of air pressure, temperature, wind direction and wind velocity for the time periods 24 May - 19 June 1992

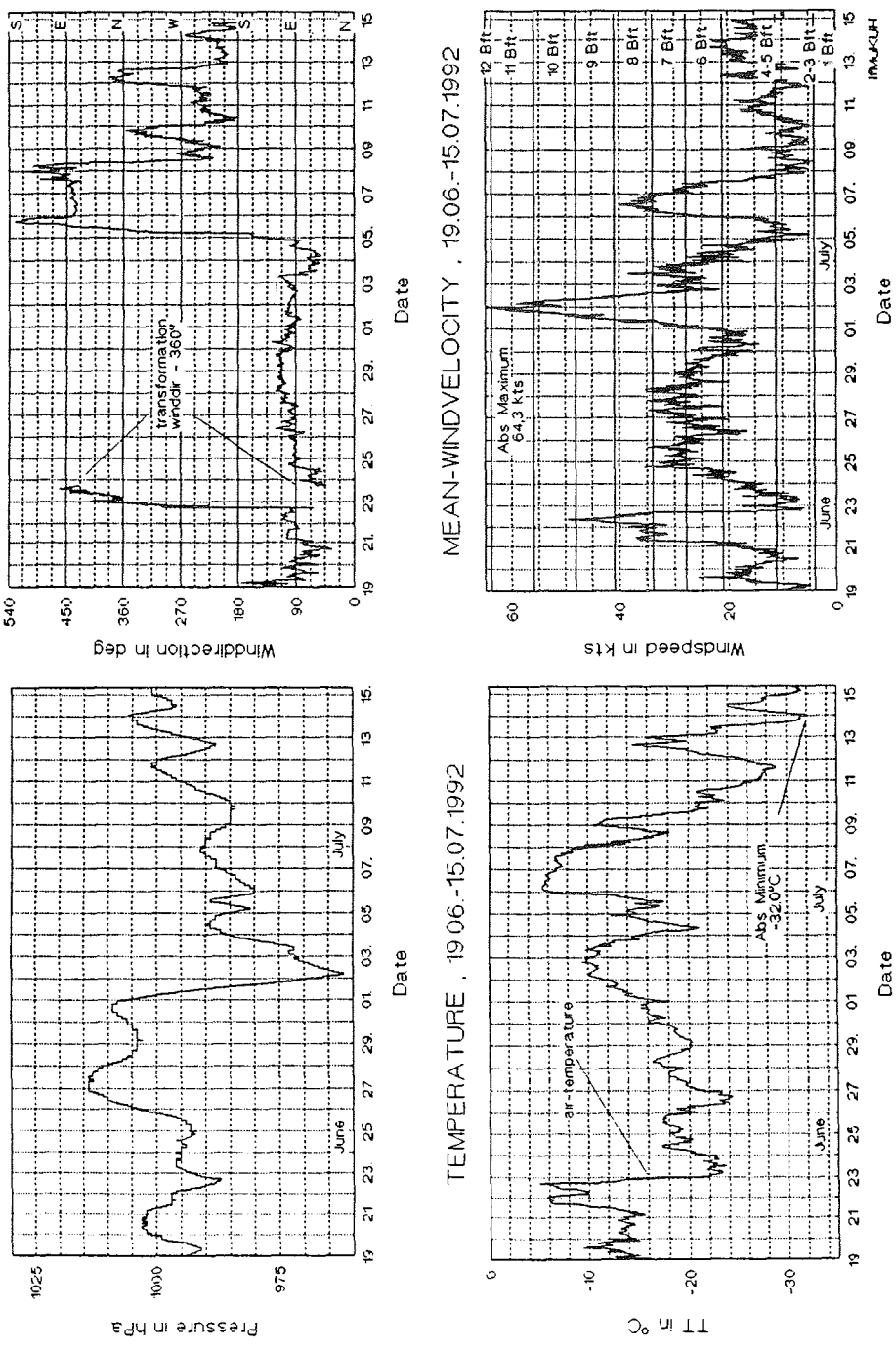

Fig. 1.3-1b: Plot of air pressure, temperature, wind direction and wind velocity for the time periods 19 June - 15 July 1992

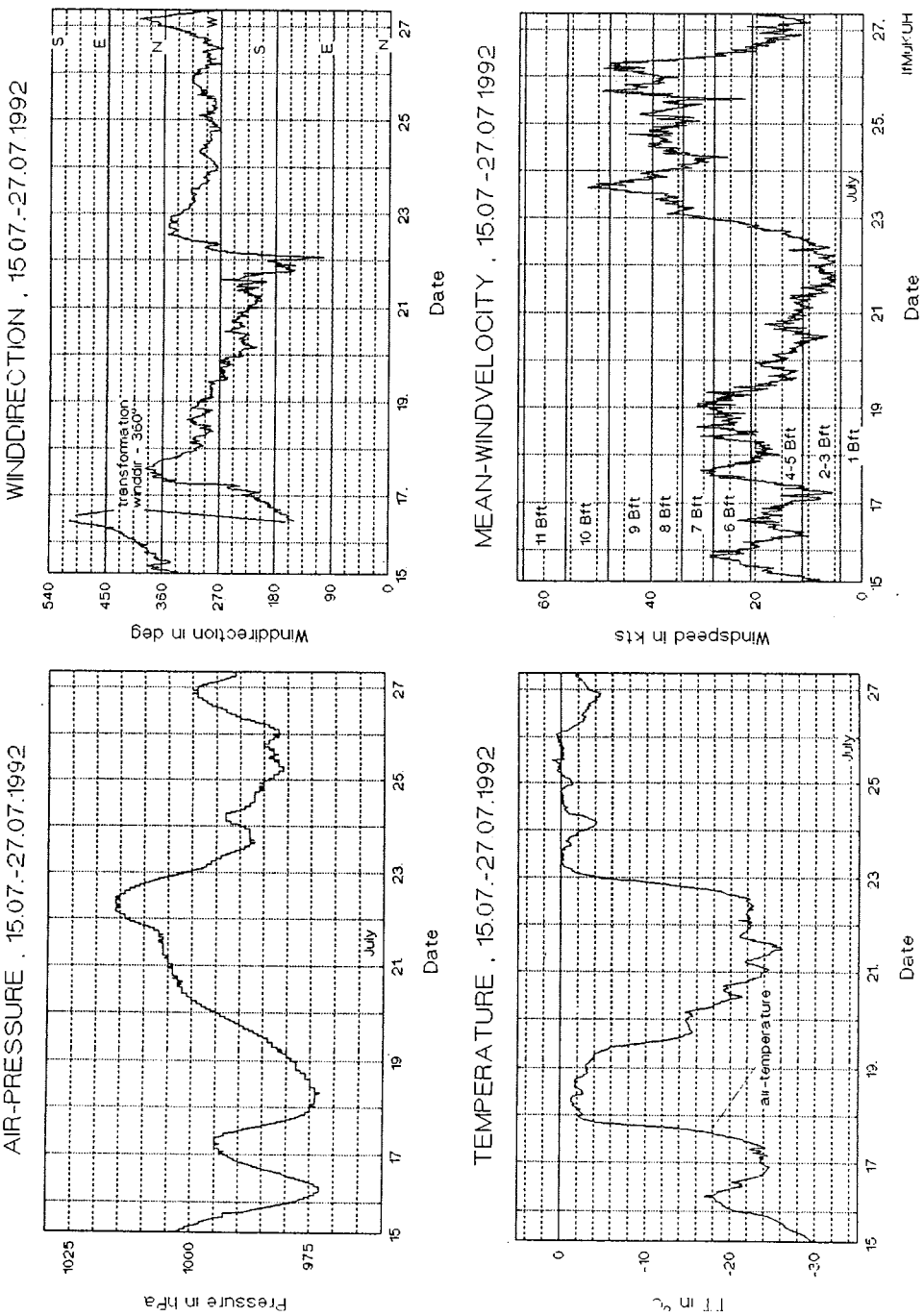

Fig. 1.3-1c: Plot of air pressure, temperature, wind direction and wind velocity for the time periods 15 July - 27 July 1992

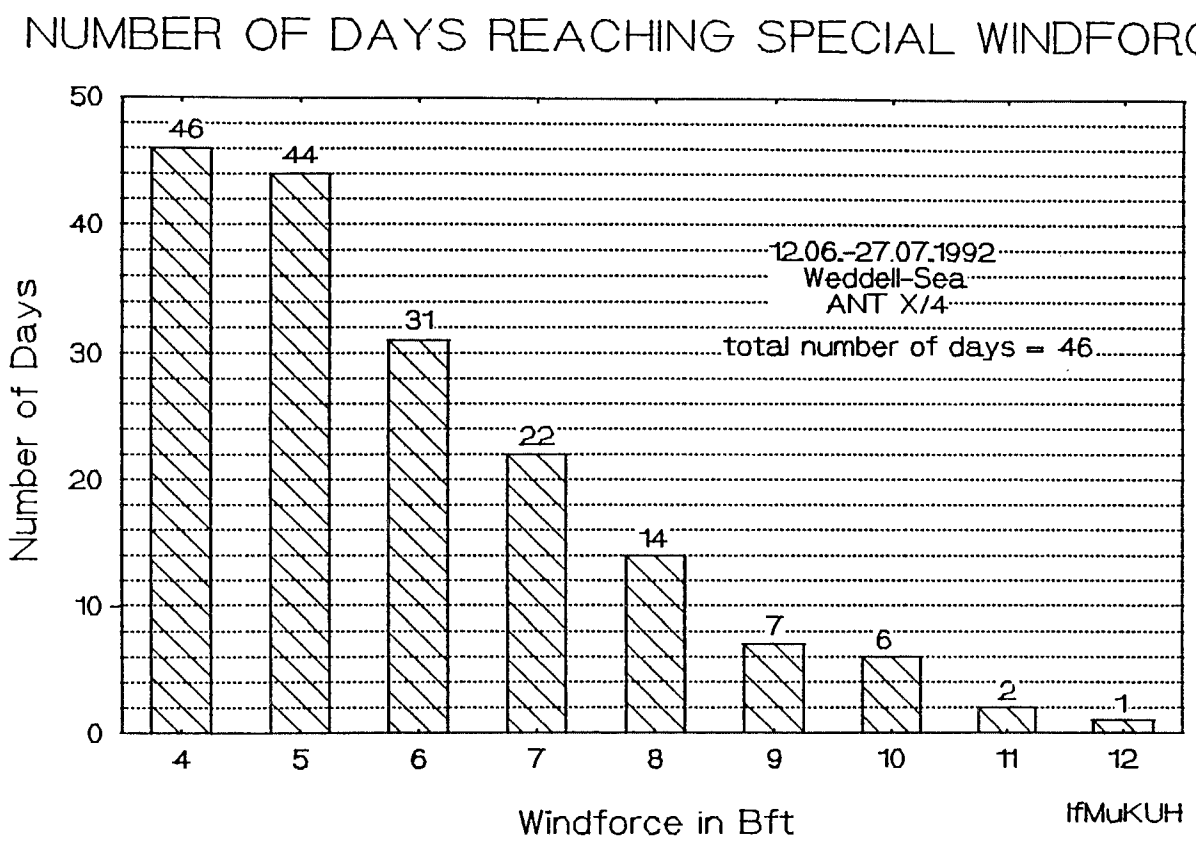

Fig. 1.3-2: Wind statistics

2. Research Program

2.1. Oceanography

2.1.1 Physical ceanography and nutrients

M. Schröder, A. Wisotzki, N. Brunken, I. Hansen, P.Heil, M. Kreyscher, S. Moschner, N. Steiner, U. Sterr, K.U. Richter, H. Diedrich (AWI)

As part of the World Ocean Circulation Experiment (WOCE) the oceanographic program focussed on two hydrographic sections: SR2, between South Africa and the Antarctic continent, and SR4 in the Weddell Sea, connecting Kapp Norvegia and the tip of the Antarctic Peninsula. For both sections the oceanographic measurements represent the first mid-winter realisation.

The objectives of the oceanographic program were:

- Calculation of volume, heat, and salinity fluxes between Atlantic and Indian ocean and within the regime of the Weddell Gyre.
- Calculation of the geostrophic shear in the different current bands of the Antarctic Circumpolar Current (ACC) and the Coastal Current (CC) along the eastern and western Antarctic shelf.
- Definition of water mass characteristics within the circumpolar belt and the Weddell Sea, including the variability of natural and anthropogenic tracers.
- Detection of the variability of the ACC with an ADCP along the Greenwich Meridian and across the Drake Passage.
- Description of the variability of the ACC across the Drake Passage with temperature profiles from XBTs and comparision of seasonal changes with other XBT cruises.
- Measurement of the turbulent heat- and momentum fluxes in the oceanic boundary layer below the sea-ice during winter conditions.

The intrumentations used were:

- CTD (NB Mk III B), General Oceanic-Rosette (24*12 l), XBT (T 7), Salinometer (Autosal), ADCP (RDI, 150 kHz).
- Autoanalyzer (Technicon System II).
- During the long ice station:
  CTD plus three component acoustic current meter (Simtronix UCM-40 Mk II).

The oceanographic program included (for location of stations see also Figs. 2.1-1 and 2.1-2):

- 115 CTD-stations in total.
  101 casts of full hydrographic work, which includes 24 water samples of temperature, salinity, oxygen, silicate, phosphate, nitrate, nitrite and
  14 special biological casts. Additional tracer measurements were done including Tritium, Helium, F-11, F-12 and oxygen isotopes O16/O18 (see also 2.1.2).
  The section SR2 along the Greenwich Meridian consisted of 71 deep casts and 8

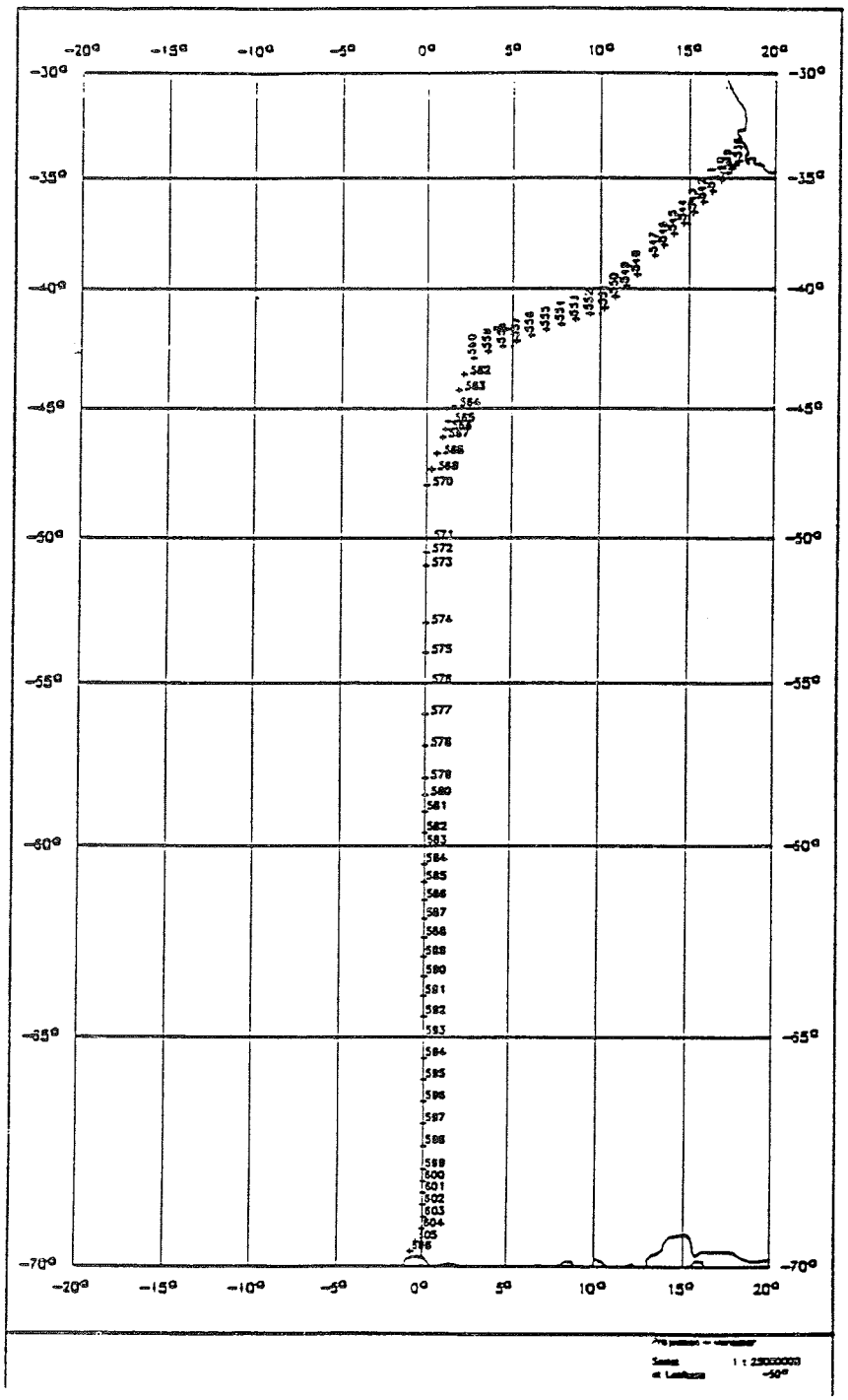

Fig. 2.1-1: ANT X/4 cruise track and station map between Cape Town and Antarctica along the Greenwich meridian

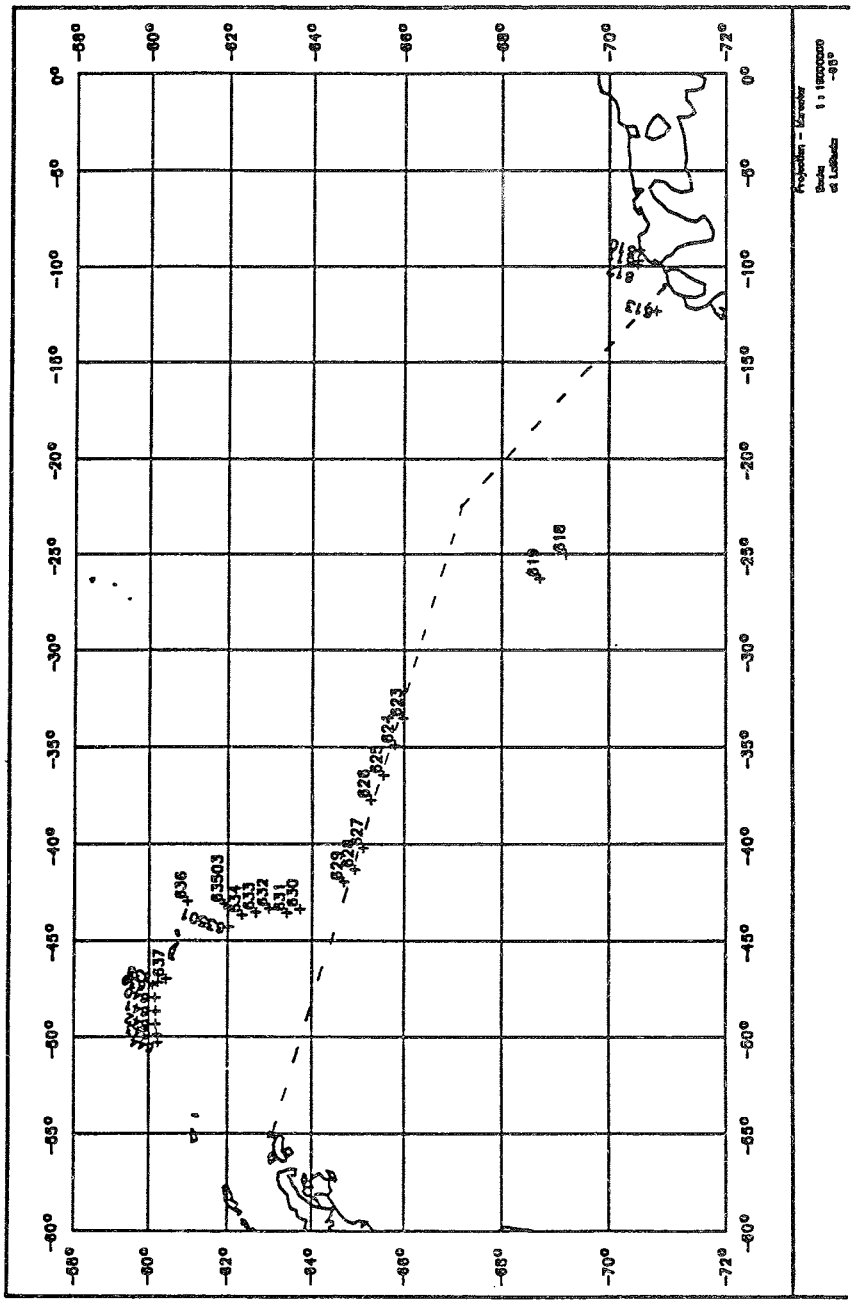

Fig. 2.1-2: Map of CTD Stations in the Weddell Sea.
The broken line denotes the planned cruise track.

biological casts to 300 m depth. The section SR4 across the Weddell Sea included 28 full depths and 6 biological casts to 300 m depth. For calibration 2 deep casts were taken.

- Enroute measurements of velocity profiles with an ADCP in ice free regions along the Greenwich Meridian (2090 nm) and across the Drake Passage (680 nm).

- Enroute registration of surface temperature and salinity with a vessel mounted thermosalinograph (only in regions without sea-ice cover).

- 23 XBT-profiles across the Drake Passage.

- On the long ice station a mobile system of current meters was used from a sea ice floe.

Greenwich Meridian (SR2):
Oceanographic work started on 22 May with a test-station in 2100 m water depth at the shelf break southwest of Cape Town. After steaming back to the beginning of the first transect the routine CTD work began with a normal distance of 40 nm between stations, decreasing to 15 nm at the slopes of the continental shelf breaks. Additionally, enroute registrations of the ADCP and thermosalinograph were done. The ADCP-data set had to be carefully analysed at home whereas the surface values of temperature and salinity (at 8 m depth) provided a useful tool in detecting frontal systems during the cruise (Fig. 2.1-3). The position of the oceanic fronts, the Subtropical Front (STF), the Subantarctic Front (SAF), the Polar Front (PF), and the Continental Water Boundary (CWB) were dominated by large horizontal gradients in T and S which amount to the following winter values:

	Δ-T (°C)	Δ-S (psu)
STF:	7.0	1.0
SAF:	3.5	0.4
PF:	1.5	0.2

Except for the Polar Front these gradients were higher than in the summer season (Bathmann U., et al, 1992). In ice covered regions the thermosalinograph did not work because of freezing within the pump system. Therefore, values for the gradient at the CWB could not be detected. The oceanographic fronts and the main water mass characteristics in the Atlantic sector of the Southern Ocean along the Greenwich Meridian are shown in Figs. 2.1-4a, b, c, d. The hydrographic parameters of potential temperature (Θ), salinity (S), phosphate (PO_4), and silicate (SiO_3) are chosen as examples, which can be used to identify the different water masses in this part of the ocean. The vertical extent of these water masses can also clearly be seen in CTD profiles as for example in Figs. 2.1-5a and 2.1-5b. An overview of the important features, like position of fronts, mean values, and surface elevation due to the density variations of water types is given in Fig.2.1-6. North of 56°S, which is the southernmost extension of the mid-ocean ridge in this area, the different water masses could most easily be traced by salinity, whereas in the Weddell Gyre the temperature is the better parameter to identify specific water types on a large scale. Looking from north to south the upper water column (0-1000 m) is dominated by the surface waters of the subtropical gyre (north of the STF) and Subantarctic Surface Water (SASW) between STF and SAF, which are high in salinity and temperature but poor in oxygen and nutrients. The belt of strong winds and high precipitation between Subantarctic and Polar Front is the source region of the Antarctic Intermediate Water (AAIW) which is characterized by low salinity and high oxygen values. This tongue sinks towards the north and spreads into the southern Atlantic at a depth range of 500-1200 m.

In the upper 200 m south of the PF the water is cold, fresh, rich in oxygen and high in nutrients as compared to the SASW. It is composed of Antarctic Surface Water (AASW) and/or Winter Water (WW) which is cooled down to the freezing point. Near the continent, the

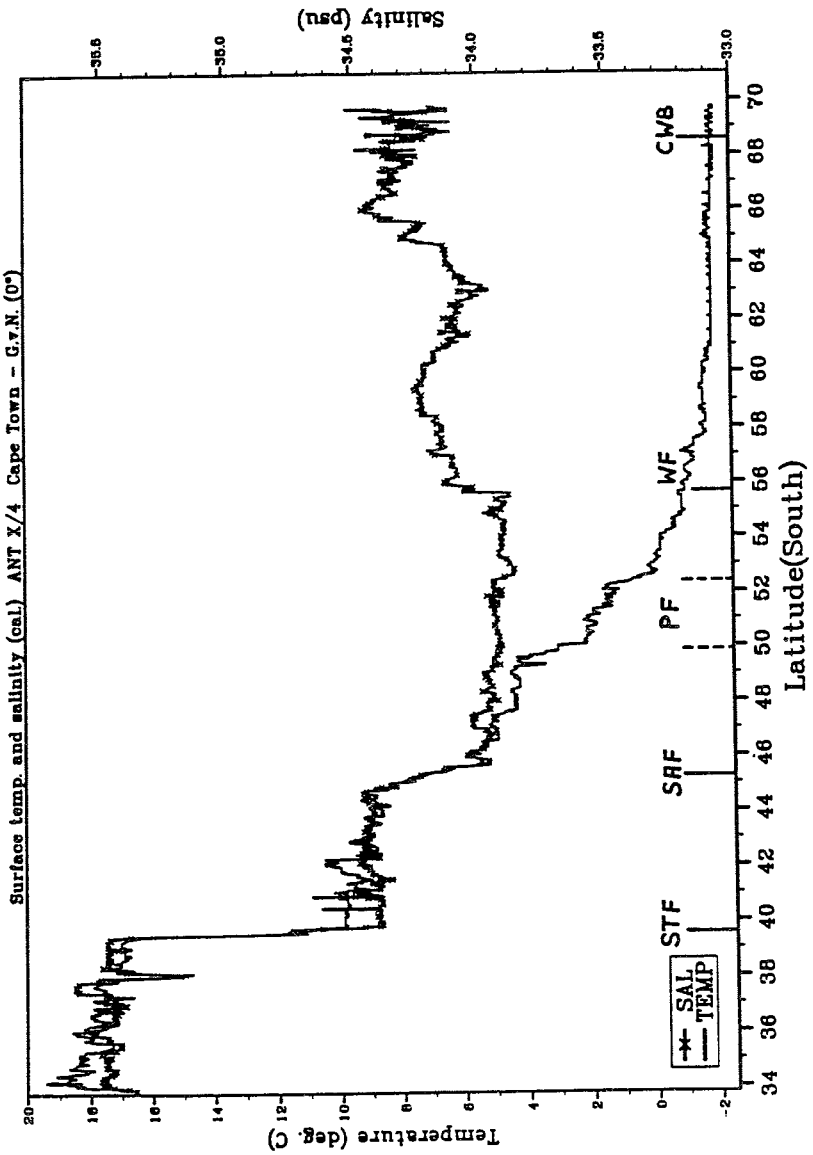

Fig. 2.1-3: Surface temperature and salinity measured with the ship's thermosalinograph at 0°E. Marked are the position of fronts: STF = Subtropical Front, SAF = Subantarctic Front, PF = Polar Front, WF = Weddell Front, CWB = Continental Water Boundary.

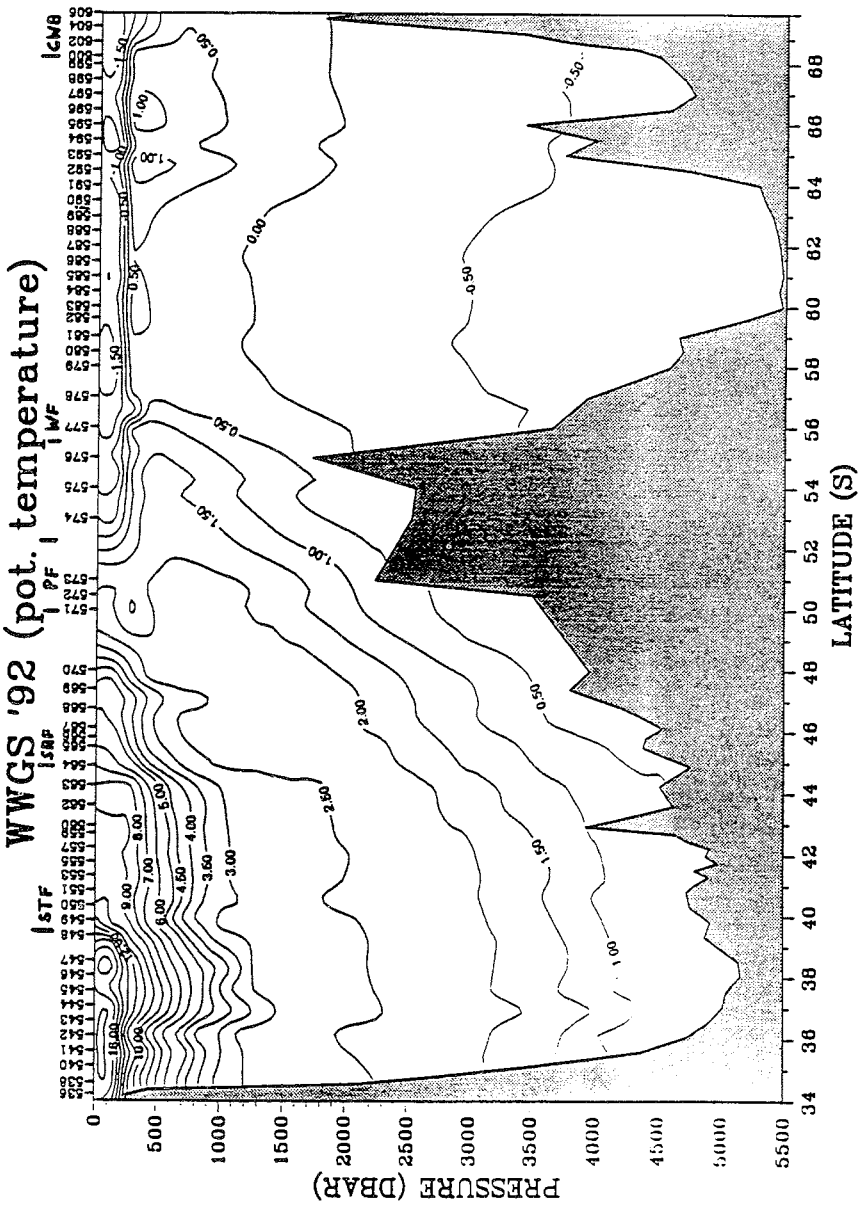

Fig. 2.1-4a: Section of potential temperature along 0°E together with frontal positions

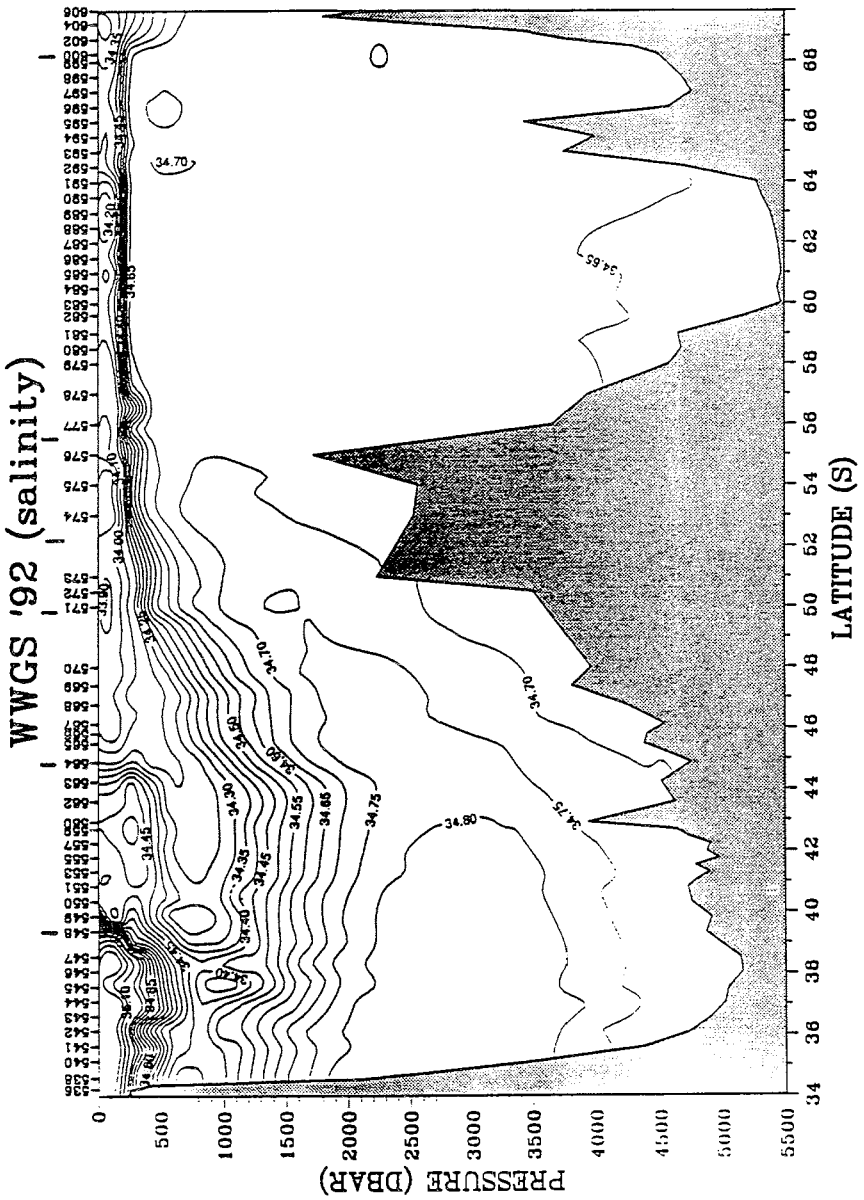

Fig. 2.1-4b: Section of salinity along 0°E together with frontal positions

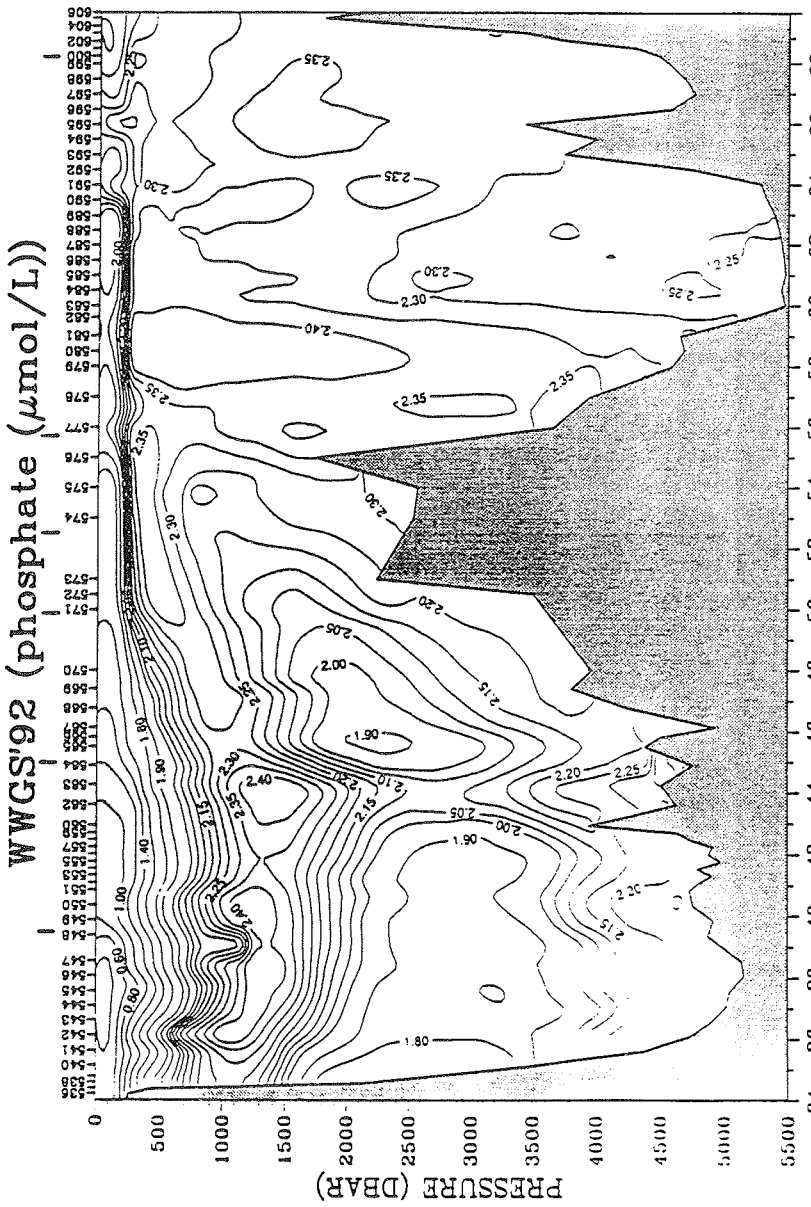

Fig. 2.1-4c: Section of phosphate along 0°E together with frontal positions

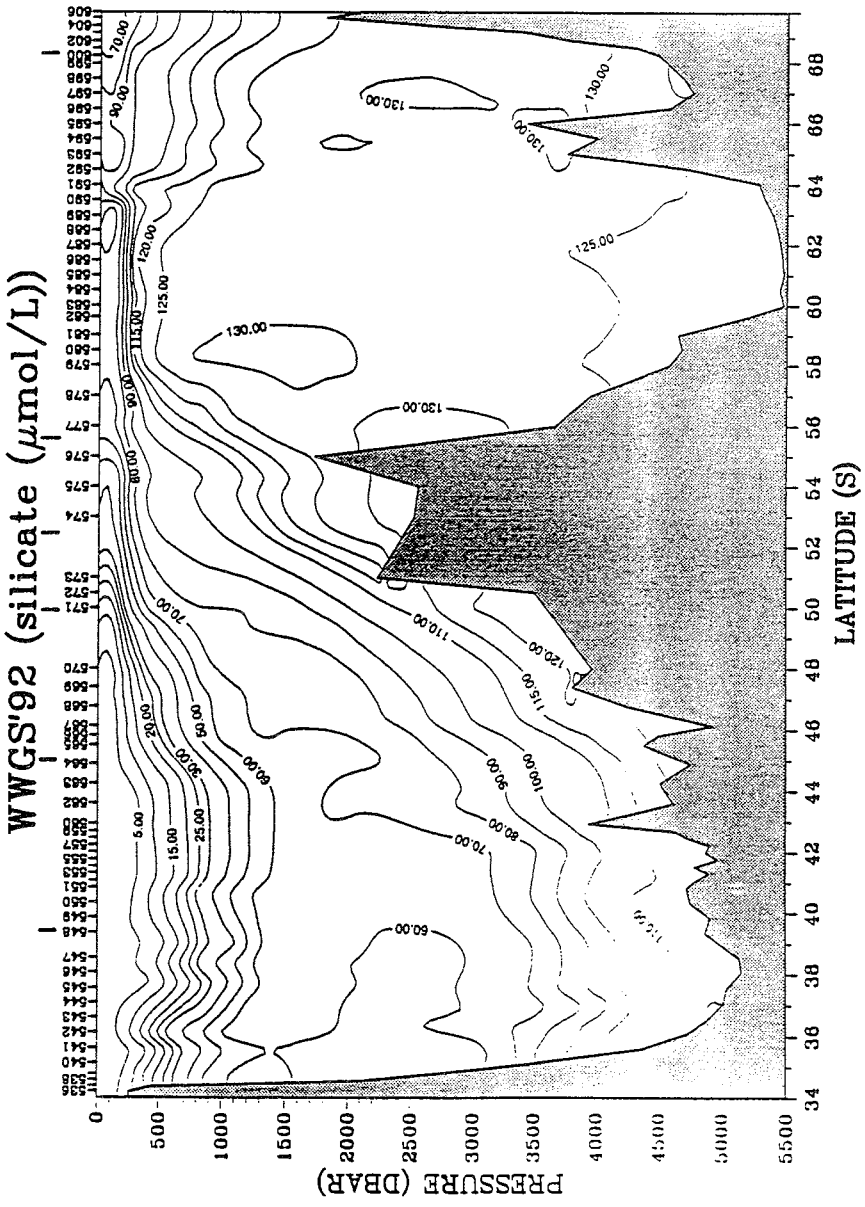

Fig. 2.1-4d: Section of silicate along 0°E together with frontal positions

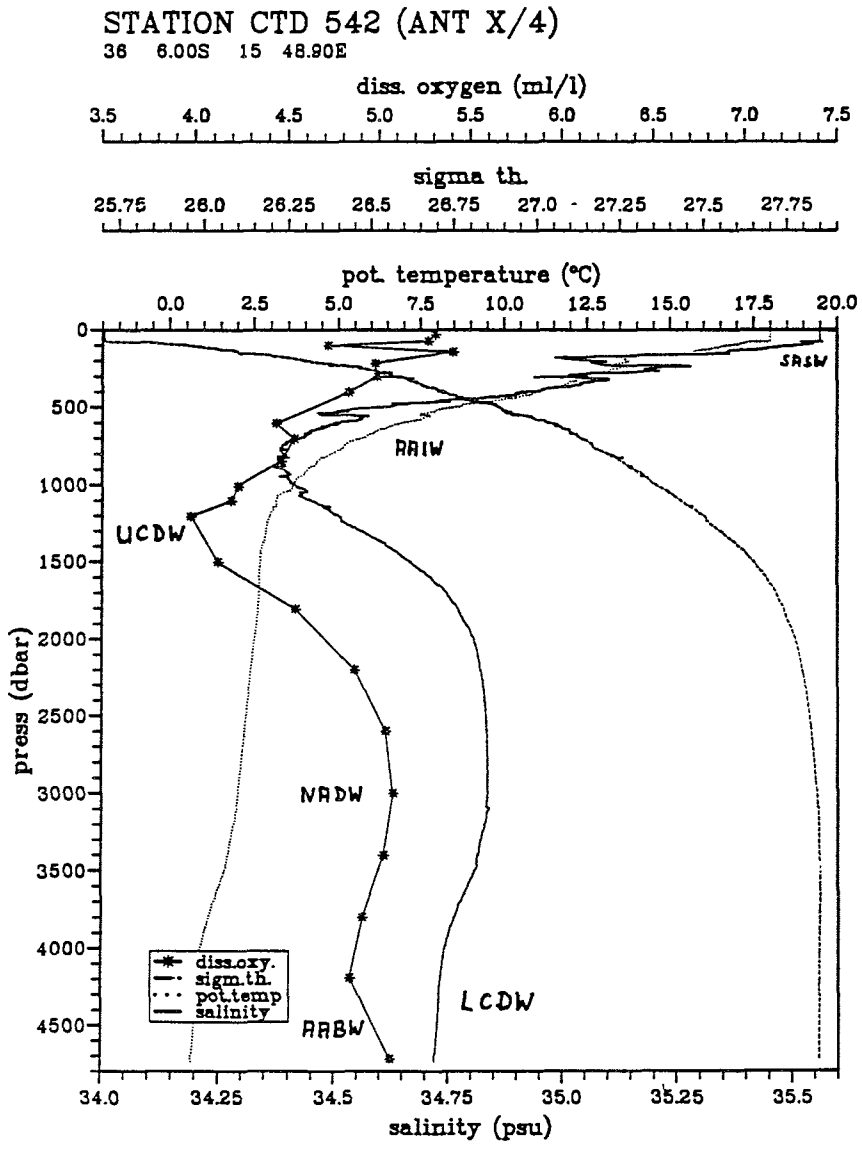

Fig. 2.1-5a: Profiles of potential temperature, salinity, dissolved oxygen, and density of station a) 542, and b) 601 which show some of the main water masses and their vertical extent in the Southern Ocean and the Weddell Gyre

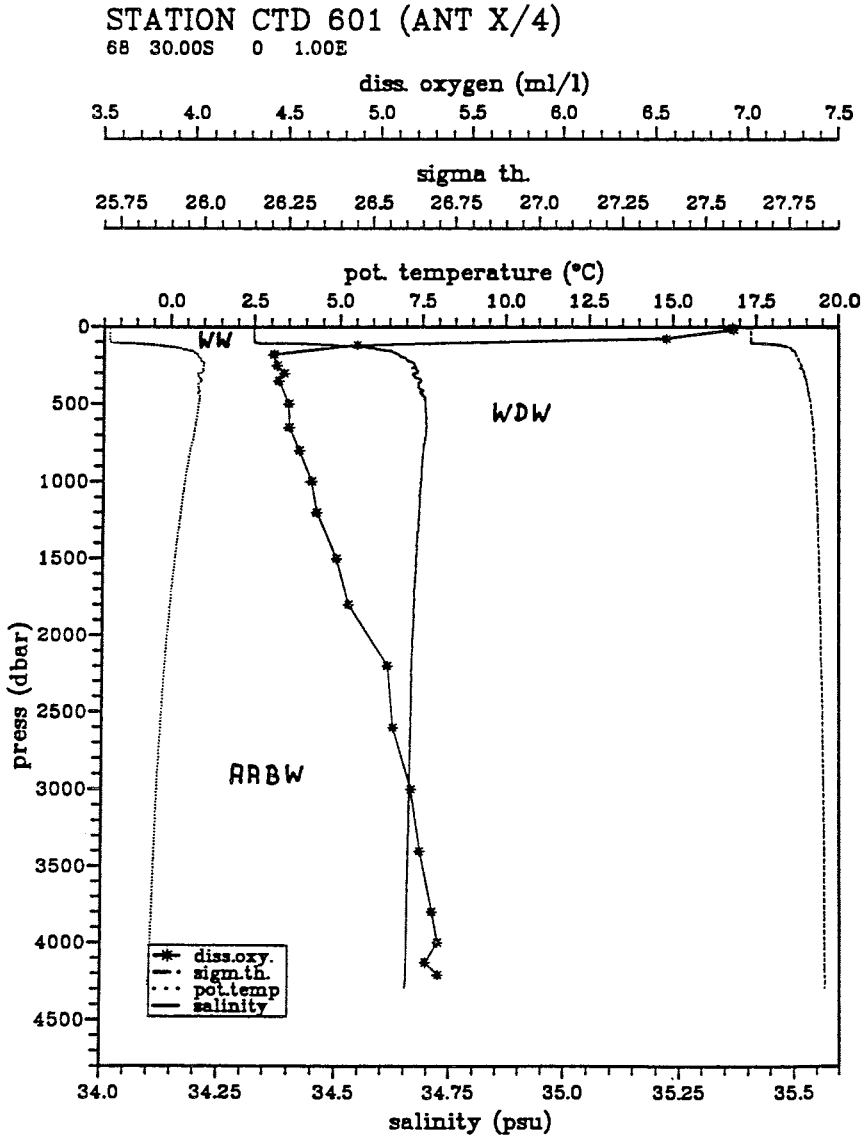

Fig. 2.1-5b: Profiles of potential temperature, salinity, dissolved oxygen, and density of station a) 542, and b) 601 which show some of the main water masses and their vertical extent in the Southern Ocean and the Weddell Gyre

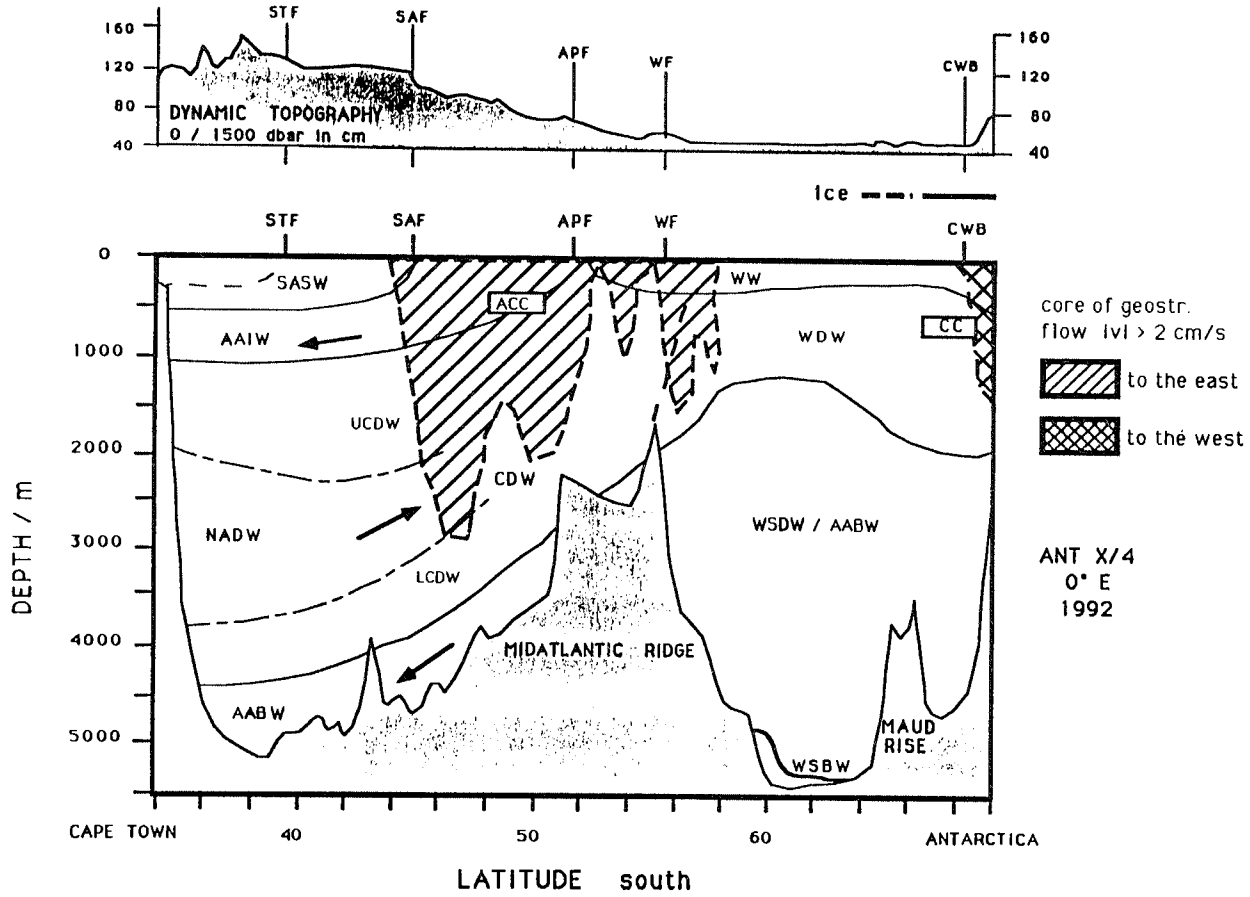

Fig.: 2.1-6: Overwiew of the horizontal distribution water masses along 0°E.SASW: Subantarctic Surface Water, AAIW: Antarctic Intermediate Water, NADW: North Atlatnic Deep Water, AABW: Antarctic Bottom Water, CDW: Circumpolar Deep Water (U: upper, L: lower), WW: Winter Water, WDW: Warm Deep Water, WSDW: Weddell Sea Deep Water, WSBW: Weddell Sea Bottom Water. In addition the position of fronts, ice cover and main currents are shown, where ACC means Antarctic Circumpolar Current and CC is the Coastal Current at the antarctic shelf. In the upper panel the dynamic topography of the surface relative to 1500 dbar is shown.

pycnocline isolating the convective layer from the Warm Deep Water (WDW) underneath deepens towards the shelf down to 600 m. At the shelf break less saline waters of the Coastal Current (CC) regime appear which have lower oxygen but higher nutrient concentrations as the surrounding water masses. Depending on ice conditions and incoming solar radiation these values can change rapidly.

The deep ocean (>1000 m) is dominated by the Circumpolar Deep Water (CDW) which is the most extensive water mass with a thickness of more than 3000 m. It can be divided into the Upper CDW (UCDW) with its source in the Indian and Pacific oceans which provide its high nutrient and low oxygen values, and the Lower CDW (LCDW), which is fed in the North Atlantic Deep Water (NADW) moving southward with a maximum in salinity and oxygen and a minimum in nutrients. Entering the ACC the axis of both parts is inclined upward to the south compensating the northward flowing Antarctic Bottom Water (AABW) which spreads as a tongue of cold, fresh water with high oxygen and nutrient values into the great ocean basins. It fills the lowest 500 m above the bottom north of the mid-ocean ridge system at 56°S.

In the deep Weddell basin the oceanic structure looks quite different because of the large vertical extension of the AABW which is always detectable at depths greater than 2000 m with a doming in the gyre centre up to 1200 m. It has the largest silicate values of the world ocean with more than 130.0 µmol/L. Near the bottom at depths of more than 4500 m the influence of the Weddell Sea Bottom Water (WSBW) can be seen from the decreasing temperatures, salinities, and silicate values, and increasing oxygen. Pure WSBW was not detected on this transect.

Between the WW at the surface and the AABW the warm and salty WDW is trapped south of the ACC. It has its origin in the LCDW which circles the cyclonic Weddell Gyre at its eastern end and enters the southern part of the Weddell Gyre above 1500 m (Whitworth and Nowlin, 1987). The heat content of this water mass is used to balance the overall heat loss to the atmosphere south of the Polar Front. The fronts on the Greenwich Meridian are relatively narrow and their signatures are detectable down to greater water depths. Only the Polar Front seems to be smeared out over a larger distance. At the Subantarctic Front for example the sharp horizontal gradients extend from the surface to the bottom (more than 3500 m). South of the Polar Front near Station 577 the transition from the Antarctic Circumpolar Current to the current regime of the Weddell Gyre is also marked by an inrease of the shoaling of isolines.

Calculated baroclinic geostrophic velocities from 50 dbar relative to the bottom are displayed in Fig. 2.1-7. It shows the broad eastward flowing circumpolar current with three bands of strong geostrophic velocities up to 18 cm/s at the surface and of more than 3 cm/s at 2000 m depth. The bands are located between SAF and PF. The complicated flow structure north of the SAF results from the influence of the Agulhas retroflection, the South Atlantic Current (SAC), and the northern limb of the ACC which all form a region of very high eddy activity due to strong horizontal current shear and highly variable water mass composition.

Weddell Gyre (SR4):
Because of the severe ice conditions the cruise track in the Weddell basin had to be modified focusing on two hydrographic sections, one starting at the centre of the gyre (station 623 at 66'S; 33,5'W) running northwest to the South Orkney shelf, and the other closing the gap between the shallow (< 500 m) areas west of South Orkney and east of Clarence Island (Fig. 2.1-2).

As known from previous cruises (Augstein et al, 1991) doming of isolines in the middle of the cyclonic Weddell Gyre (stat. # 626-629) dominate the structure of all oceanic parameters (Figs. 2.1-8a, b, c). The downward slope near the shelf break is not as steep as on the eastern boundary but is clearly visible. The temperature maximum of the WDW ($\Theta > 0.4$°C) is divided into two cores where the western cell has its centre position at 44 W. This was already sampled

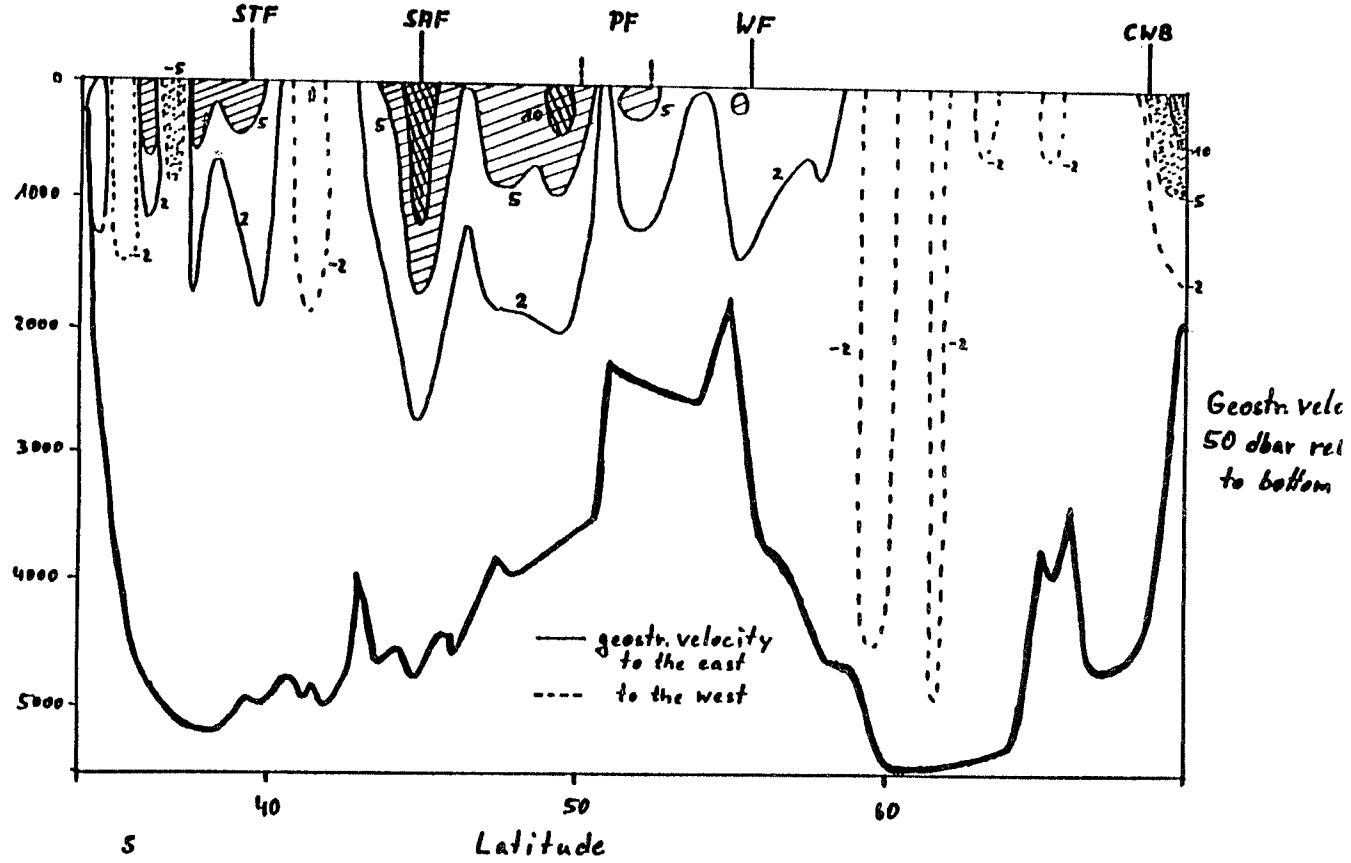

Fig. 2.1-7: Distribution of geostrophic velocities along 0°E, calculated for the 50 dbar level relative to the bottom. Isolines of 2, 5, and 10 cm/s are shown.

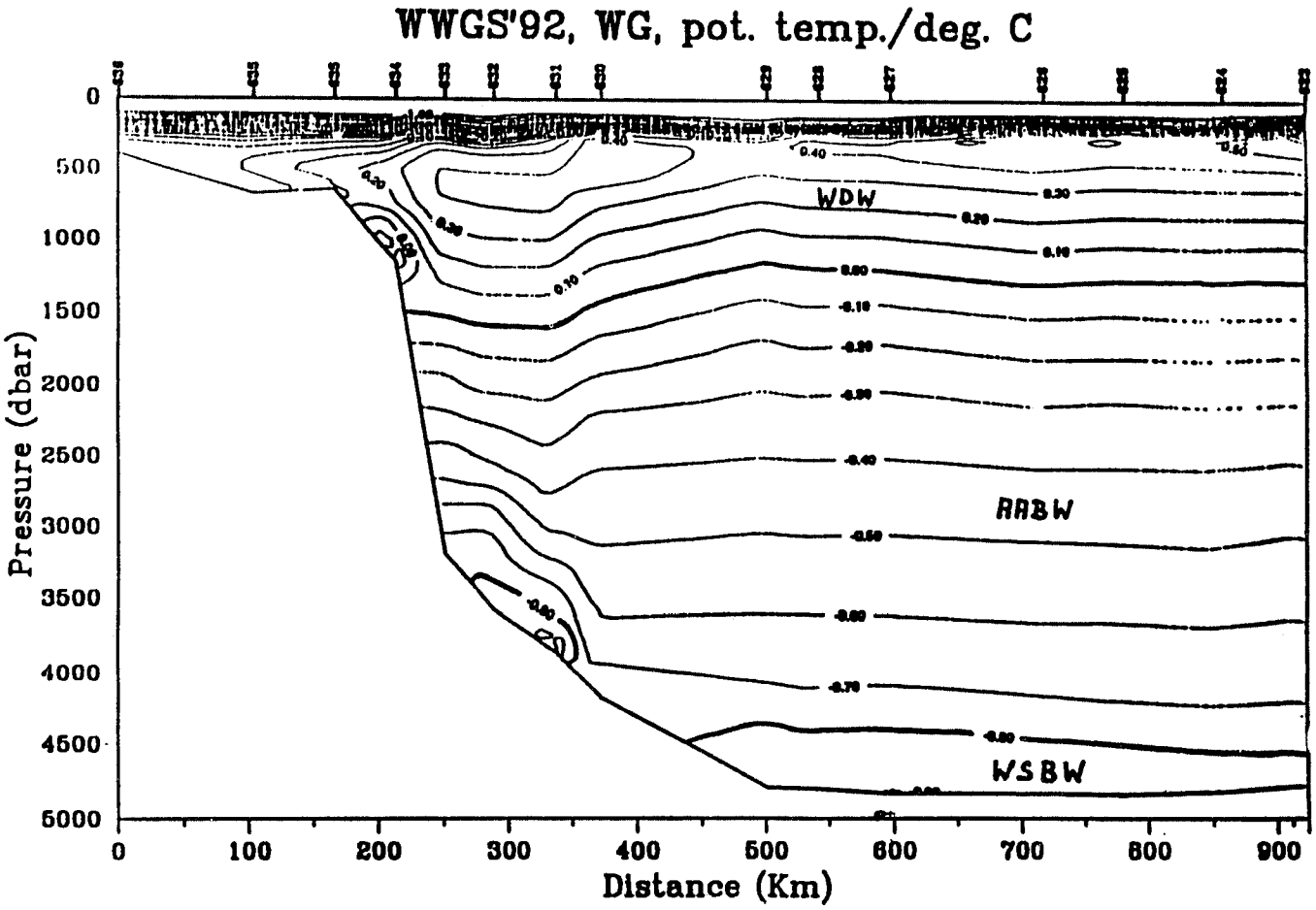

Fig. 2.1-8a: Sections of potential temperature from South Orkney (left) to the centre of the Weddell Gyre (right). See also Fig, 2.1-2 for station numbers.

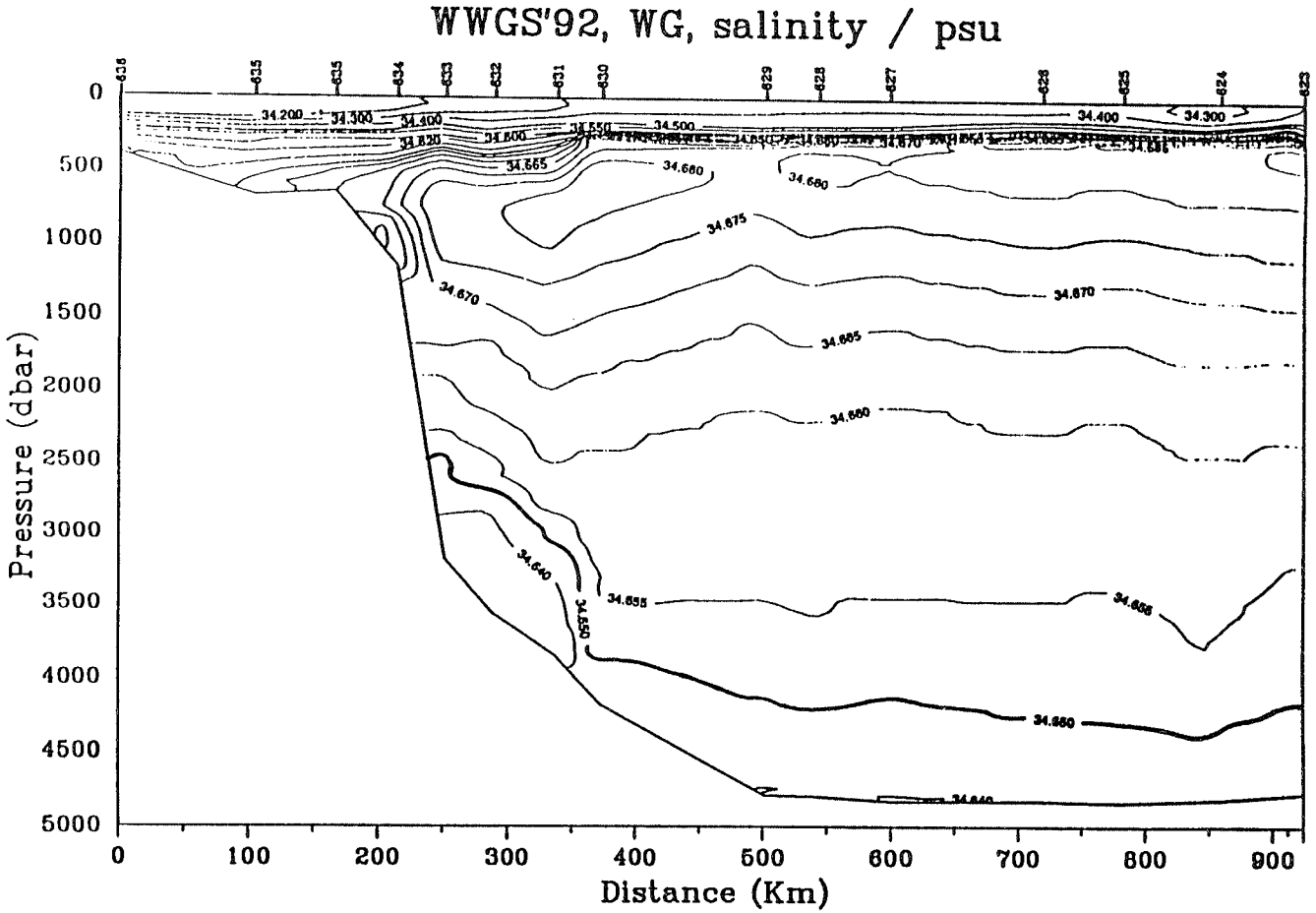

Fig. 2.1-8b: Sections of salinity from South Orkney (left) to the centre of the Weddell Gyre (right). See also Fig. 2.1-2 for station numbers.

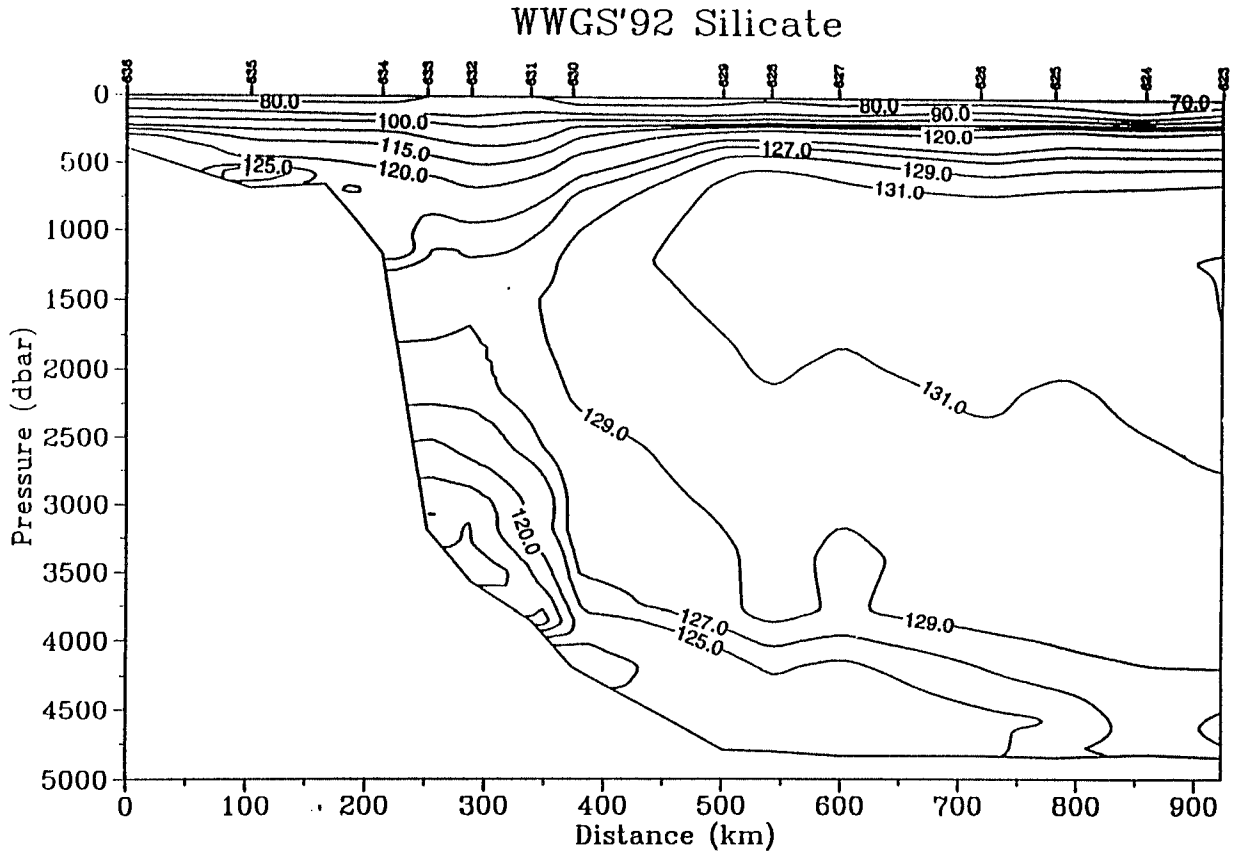

Fig. 2.1-8c: Sections of silicate from South Orkney (left) to the centre of the Weddell Gyre (right). See also Fig. 2.1-2 for station numbers.

in late winter 1989 and summer 1990 by other POLARSTERN expeditions (WWGS´89, SWGS´90).

In the deep ocean Weddell Sea Bottom Water (WSBW) was found between station 624 and 633. It differs from the water mass above (AABW) through lower temperature (Θ < -0.8°C), lower salinity (s < 34.65), lower nutrient values (for example silicate less than 125.0 µM), and higher oxygen values (Ox > 5.7 ml/L).

The most undiluted WSBW is located of a water depth of 2700 - 4000 m at the continental slope as a 100 - 300 m thick lense. A second core fills the flat bottom of the deep Weddell basin at water depths of more than 4500 m. Its thickness is also less than 300 m. This splitting into two branches suggests that different sources of WSBW exist, some of which are known as the Filchner trench and the wide shelf areas along the Antarctic Peninsula. Careful interpretation of the hydrographic parameters together with the analysis of tracer measurements from the water samples should give more information on the pathways and possible source areas

The comparison with previous cruises further south (WWGS '89, SWGS '90, and with the American/Russian drift station ISW '92) will improve our understanding of the formation mechanisms of WSBW.

The northernmost section between the shelfs of Clarence Island and South Orkney was taken to investigate the possible inflow and outflow to/from the Weddell Sea (Figs. 2.1-9a, b). Due to the limited water depth (max. 2400 m) no WSBW is leaving the basin through this gap. In the depth range 200 to 1500 m an outflow of WDW out of the Weddell Sea occurs at the eastern flank of this section. High temperatures and salinities, and low oxygen values indicate that this water originates from the western core of the WDW which is divided by the wide and shallow South Orkney shelf.

Crossing Drake Passage hourly XBT's were launched after leaving the ice edge. These data provide useful information in connection with previous XBT-cruises and with enroute registrations of the ADCP which were run as far as 52°N to calibrate the system via bottom tracking.

Turbulence measurements during the long ice station:
A six hour long timeseries with a fixed acoustic current meter at 1.5 meter below the sea ice was taken to measure the turbulent fluctuations of velocity and temperature in the oceanic boundary layer. The objective of this experiment was to investigate whether a rigid construction can be used to measure physical signals due to Karman vortices around the instrument, without to much noise in the interesting frequency band. The launch and recovery of the instrument through a 10" hole through 2.0 m of ice led to unforeseen difficulties which heavily reduced the measuring time.

References:
Augstein, E. , N. Bagriantsev, H. W. Schenke (eds.), 1991: The Expedition ANTARKTIS VIII/1-2, 1989, with the Winter Weddell Gyre Study of the Research Vessels "POLARSTERN" and "AKADEMIK FEDOROV". Ber. Polarforsch. **84**: 1-134.

Bathmann, U., M. Schulz-Baldes, E. Fahrbach, V. Smetacek, H.-W. Hubberten (eds.), 1992: The Expedition ANTARKTIS IX/1-4 of the Research Vessel "POLARSTERN" in 1990/91. Ber. Polarforsch. **100**: 1-403.

Whithworth,T. III, W. D. Nowlin, Jr., 1987: Water Masses and Currents of the Southern Ocean at the Greenwich Meridian. J. Geophys. Res., **92**, 6462-6476.

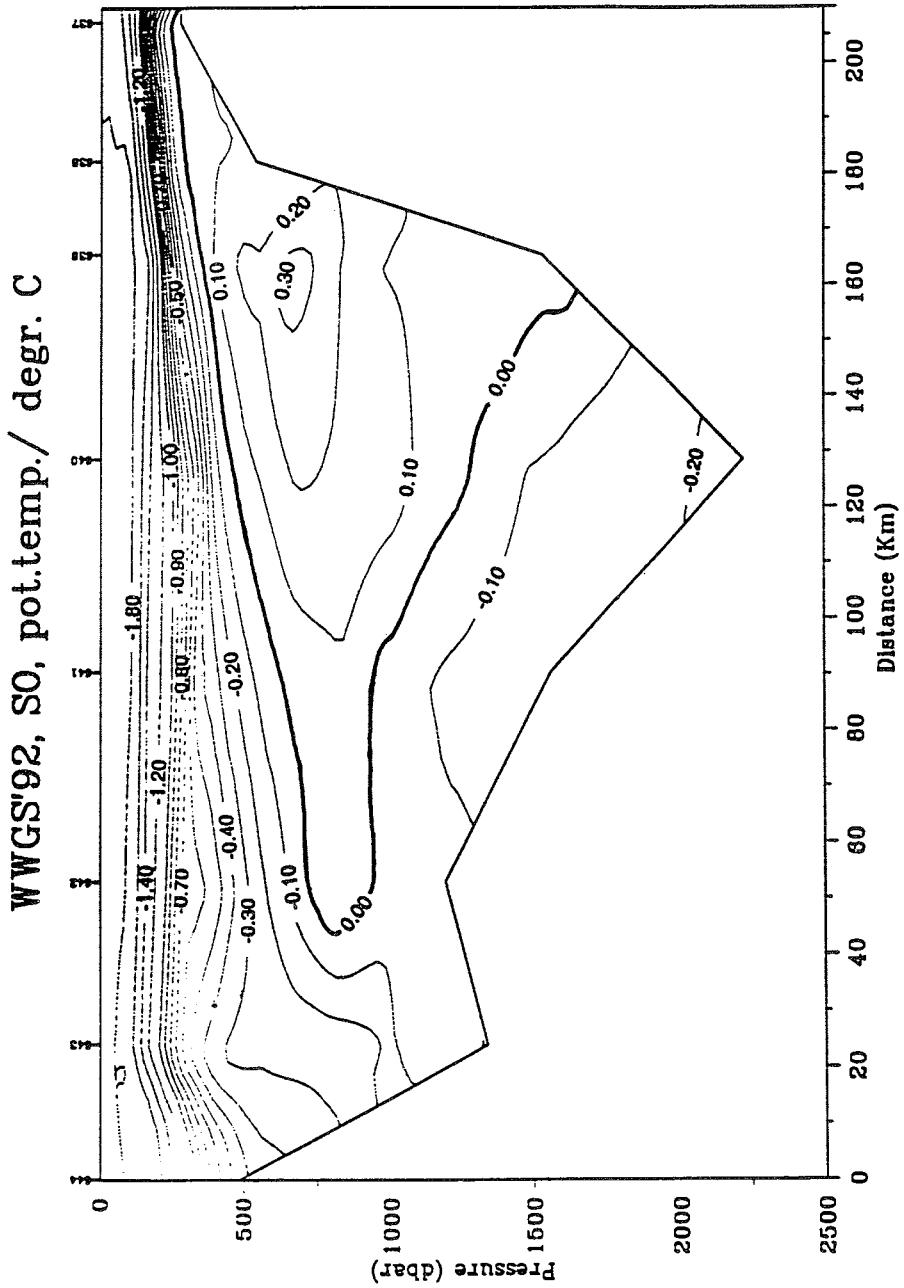

Fig. 2.1-9a: Section of potential temperature west of South Orkney.
See also Fig. 2.1-2.

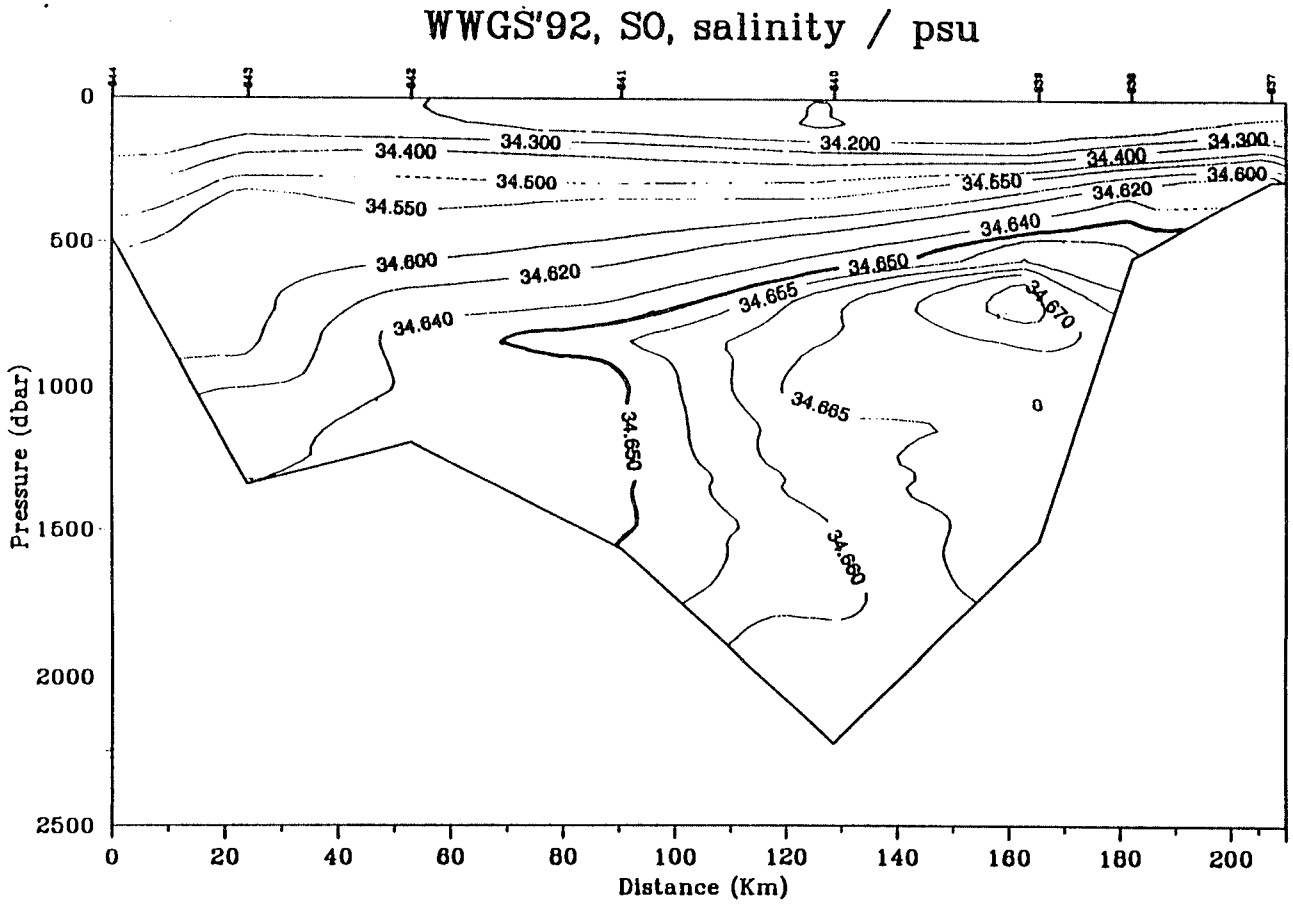

Fig. 2.1-9b: Section of salinity west of South Orkney.
See also Fig. 2.1-2.

2.1.2 Tracer studies

K. Bulsiewicz, W. Plep, H. Rose, J. Sültenfuß (UNIB)

Along the two hydrographic WOCE sections SR2 and SR4 the CFMs Freon-11 and Freon-12 were measured using an automated version of the Bullister and Weiss technique. Furthermore, water samples for tritium and helium were taken. The data sets provide important information about circulation and renewal pathways for all relevant subsurface water masses.

Water samples were taken in the usual way using glass syringes (CFMs), Cu-tubes (Helium), glass bottles (Tritium). For the new technical system to extract helium directly on ship, water samples were taken in 50 ml glass pipettes.

In total 86 tracer stations were occupied. 1600 water samples for the fluorocarbons F-11 and F-12 were analysed during the cruise. In addition, water samples were collected for analysis ashore, including 30 stations for tritium (600 water samples) and 47 stations for helium (880 water samples, 410 with the extraction method).

On the WOCE section SR2 (Cape Town-Antarctica) CFM-free deep water was found at greater depths up to 43°S (see Fig. 2.1-10 for station 557). With this data and a special calibration cast that was made into supposedly CFM-free water in the Drake Passage, the overall blank can be checked. This is important for the precision of the data, since the measurement of water samples require an additional correction for the blank. The measurements of these waters showed consistently low values of 0.01-0.02 pmol/kg for both CFMs, which is a good value in comparision of the measured range of these compounds (approximately 0.1-8 pmol/kg for F-11 and 0.1-3.3 pmol/kg for F-12).

Measurements of near surface waters under the ice, showed that the dissolved CFM concentrations are only about 70% of those predicted for equilibrium with the atmosphere. The undersaturation reflects the restriction of the air-sea exchange due to the sea ice cover.

Measurements at the stations 623-629 indicate unknown water mass at a depth of 2200 m (see Fig. 2.1-11 for station 627). This could be a sign of regional convection processes.

At station 631 the data indicate the presence of high CFM waters (F-11 concentration > 1.8 pmol/kg) at a depth ranging between the bottom and about 3850 m. This is a clear indication of Antarctic Bottom Water.

2.1.3 The carbon dioxide system in Antarctic waters

J.M.J. Hoppema, J.J.M. Belgers (NIOZ)

Of all gases causing the man-made greenhouse effect carbon dioxide (CO_2) is the most important one. A significant part of the excess CO_2 which is brought into the atmosphere is thought to be taken up by the oceans. However, the spatial and temporal extent of the uptake is far from manifest. To gain this important knowledge the data set of oceanic CO_2 measurements has to be enlarged significantly.

Data collected during the cruise constitute an important supplement to the worldwide oceanic data set of CO_2, because winter data of the Weddell Sea are scarse. Particular objectives were to investigate the following features:

1. Contrary to the temperate and tropical oceans the water column in the Antarctic Ocean has a low vertical stability, which could give rise to important vertical fluxes of CO_2. This condition is most pronounced in winter.

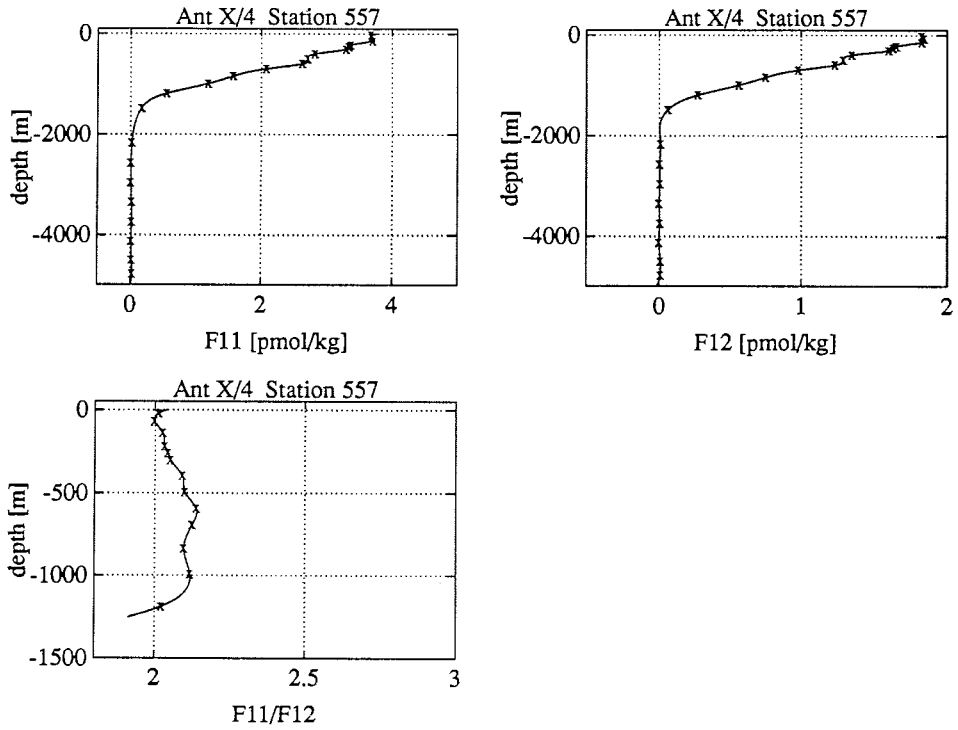

Fig. 2.1-10: Vertical profiles of Freon-11, Freon-12 and the ratio F11/F12 for Station 557.

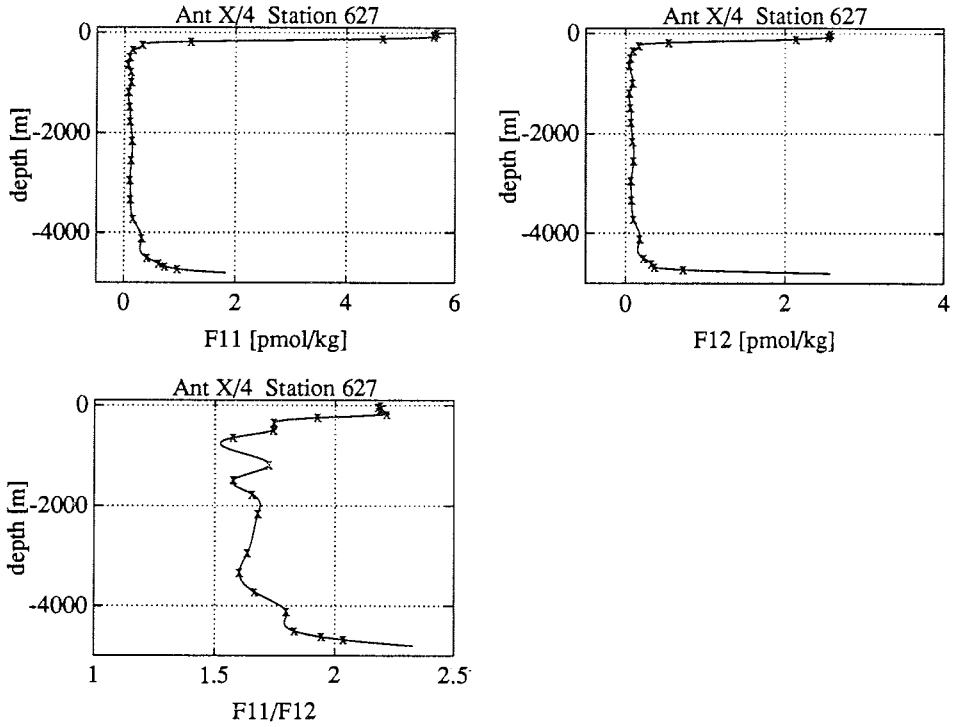

Fig. 2.1-11: Vertical profiles of Freon-11, Freon-12 and the ratio F11/F12 for Station 627.

2. The total CO_2 (TCO_2) content and the alkalinity of a water mass are unique properties, dependent on its history. This renders TCO_2 and alkalinity potential tracers.

3. From TCO_2 and alkalinity the partial pressure of CO_2 (pCO_2) can be calculated. With this property the exchange of CO_2 between ocean and atmosphere can be determined. In the ice-covered areas pCO_2 can tell something about the CO_2 content the water has when it leaves the surface, and thus how much (excess) CO_2 is brought down to deeper waters.

Measurements:
CO_2 in seawater is involved in a series of chemical reactions leading to ionic species. Therefore, to measure CO_2 in seawater one actually needs to determine the CO_2 system. It turns out that by measuring 2 parameters of the system one is able to calculate the whole system. During the cruise TCO_2 and total alkalinity were measured. TCO_2 was measured with a standard coulometric method. Alkalinity was measured by means of a potentiometric acid titration, which consisted of first adding an excess quantity of hydrochloric acid beyond the alkalinity endpoint and then recording the readings of the pH electrode after some small additions of acid. The endpoint was determined with a Gran method.

Water was taken from the Rosette at almost all CTD-stations in Antarctic waters taken during the cruise. For TCO_2 24 samples were normally taken through the whole water column, with samples in the surface layer more closely spaced; at the shallower stations the number of samples was less. Water for alkalinity determination was sampled through the whole water column only at selected stations, while at the other stations only the surface water layer was analyzed. In between stations some continuous on line measurements for TCO_2 were conducted.

Fig. 2.1-12 shows three depth profiles for TCO_2, two within the Weddell Sea and the other one at the Subantarctic Front (SAF) in the Atlantic Ocean. Data on the alkalinity will become available later. All profiles show the feature usually observed in TCO_2 profiles that there is a surface depletion compared to the deep water. However, the extent of depletion was different, in the centre of the gyre it was much less than at the SAF. This is a combined effect of different surface water temperatures and biological activity, which both are higher at the SAF. Also in the deep water there were striking differences between the profiles. In the Weddell Sea a single TCO_2 maximum was observed at about 700-900 m depth, whereas at the SAF the maximum lies at about 1300 m. Furthermore, at the SAF TCO_2 increases again towards the bottom. Here we see the interplay of different water masses of different origin. Between the two Weddell Sea stations there were also some slight differences. The TCO_2 maximum at station 633 was more pronounced than at station 619, while the TCO_2 concentration at the maximum is about equal. Surface TCO_2 concentration in the centre of the gyre was higher. This suggests that the water in the centre of the gyre was in contact with the atmosphere more recently than the water at station 633. A more detailed analysis of the data will include all stations and will also relate to other quantities measured during the cruise.

2.2 Meteorology

R. Brandt, W. Frieden, T. Rothe, O. Schulze, M.Thomas, S. Mai
(IMH, UNIB, AWI)

The main objective of the meteorological program was the investigation of the ice/atmosphere interaction in midwinter. The program consisted of the determination of all components of the energy-budget at the sea-ice surface during longer ice-stations and short period measurements of the turbulent fluxes of sensible heat and momentum at different locations for different surface conditions (ice concentration, flow-size distribution, snow- and ice-thickness).

Particular attention was focused on the spatial variability of the energy balance components over larger leads and polynyas as a ground truth information for the validation of ERS-1 data.

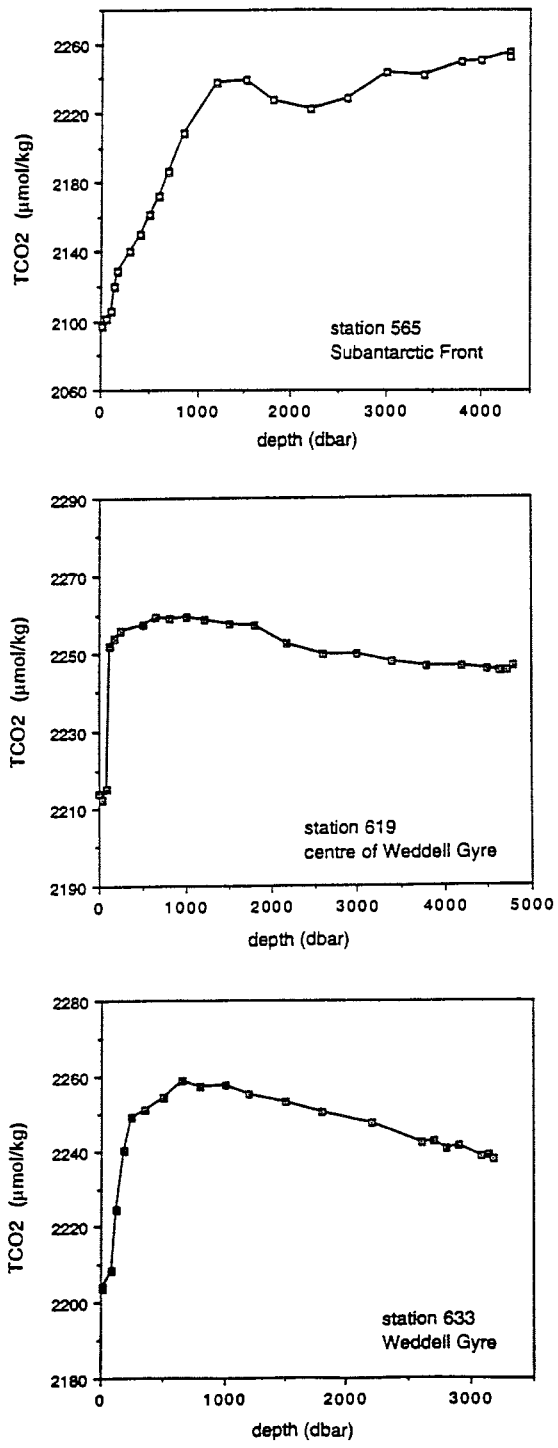

Fig. 2.1-12: Three TCO2-depth profiles as obtained during WWGS '92

Additionally, aerological soundings were taken to obtain information about the vertical thermodynamic and kinematic structure of the boundary layer and the upper atmosphere.

2.2.1 Energy budget

For the determination of the energy-budget the following parameters were measured: the radiation-budget, the turbulent fluxes of sensible and latent heat and the conductive heat flux through the snow/ice cover. In ice-covered areas the turbulent flux of latent heat can generally be neglected. In regions of thin ice or open water this part of the heat flux was estimated using the appropriate bulk formula and ship-borne humidity measurements.

a) Radiation budget
The measurements of incoming shortwave and longwave radiation have been realized with a pyranometer (CM-11, Kipp+Zoenen) and a pyrgeometer (Eppley) mounted at the ship´s boom. The outgoing longwave radiation was calculated from the radiation temperature measured with a radiation-thermometer (KT-4). The albedo of the surface was also measured with a pyranometer (CM-11).

All these measurements, except for the albedo, were performed continuously, beginning on 12 June, when the ship reached the ice-edge and ending on 29 July. The albedo measurements were only made from time to time in periods when the sun was rising above the horizont (12 - 17 June, 11 - 29 July). Due to problems with the data-logger five days of data were loss. In addition to the measurements with the KT-4 the outgoing longwave radiation was measured also with a pyrgeometer (Eppley) during the 3-day-station from 21 - 24 July near the South-Orkneys. This additional data set allows a calibration of the KT-4-measurements. During the long ice-station all instruments were installed on a sledge, placed on the ice-floe in vicinity of the vessel.

As an example Fig. 2.2-1 shows the four components of the radiation-budget during the long ice-station. The curves demonstrate the dependence of the different components on the cloud cover: a clear sky from the beginning of the station until the afternoon of 22 July and a following warm-front passage with an overcast sky until the end of the station, except for 4 hours during the night from 23 - 24 July.

Fig. 2.2-2 contains the net short- and longwave radiation as well as the total net-radiation during the long ice-station. Under clear sky conditions the ice-surface looses up to 80 W/m^2 whereas for overcast sky the components compensate each other and no net radiation energy is available at the surface.

b) Turbulent fluxes
The vertical turbulent fluxes of sensible heat and momentum were derived from wind- and temperature-fluctuations measured during most stations with a sonic-anemometer-thermometer (Metek) at the ship's boom (sampling-frequency 10 Hz). Most of the stations lasted several hours from which we finally got 38 short-period data sets. The measurements were obtained over a variety ice conditions like Nilas, Pancake-ice, first-year-ice and over open water. Two longer time-series were collected during the drifting-periods when the ship was stuck in the ice in Atka-Bay and south of Cape Norwegia. The most important data-set was obtained from the 3-day-station south of the South-Orkneys.

In Figs. 2.2-3 and 2.2-4 the turbulent fluxes of sensible heat and momentum during the long ice-station from the 21 - 24 July (10-min averages) are displayed. The turbulent flux of sensible heat is highly correlated with the air-temperature and the cloud conditions. Due to the clear sky and very low temperatures at the beginning of the station the heat-flux to the surface was very small (positive values denote an energy gain, negative an energy loss at the surface). The energy gain increased with rising temperatures and an overcast sky up to 60 W/qm. The sudden

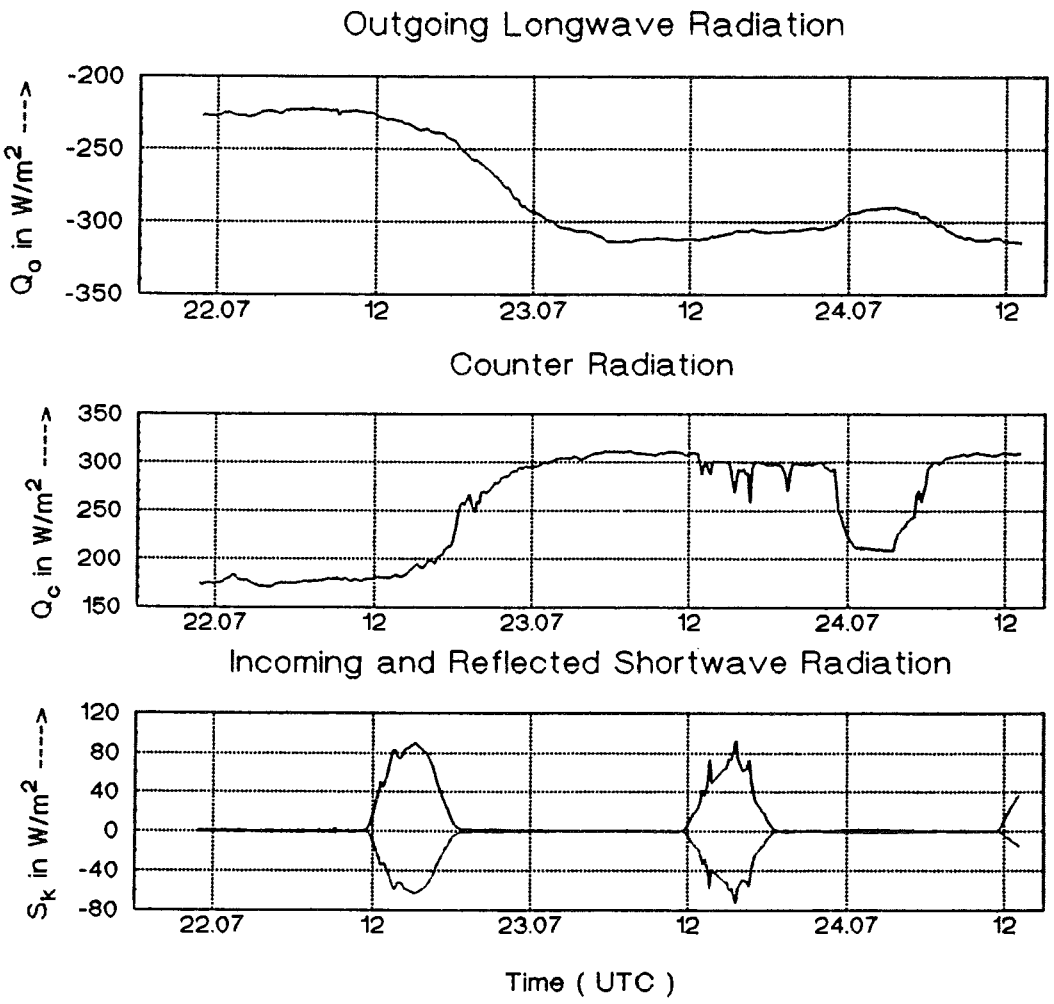

Fig. 2.2-1: Outgoing longwave radiation, counter radiation, incoming and reflected shortwave radiation during the long ice station (21 - 27 July 1992)

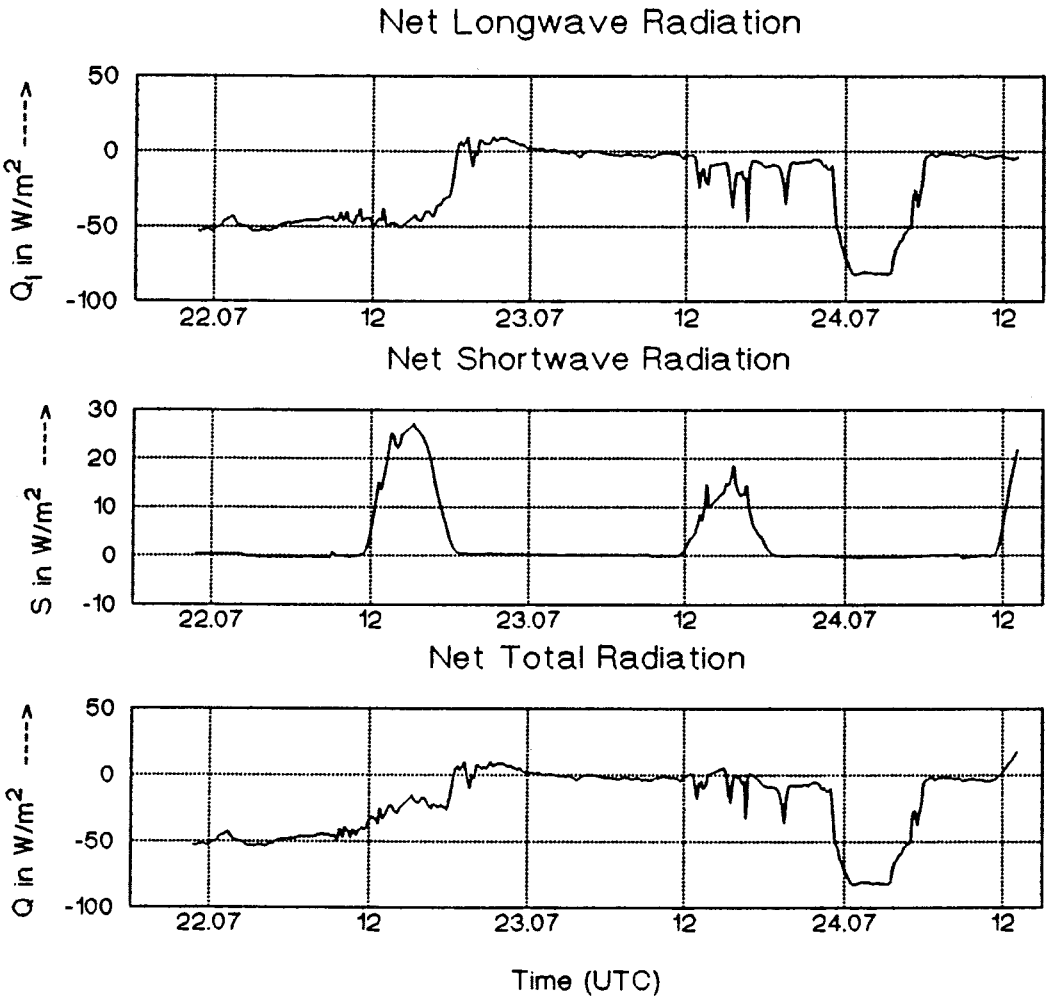

Fig. 2.2-2: Net longwave, net shortwave and net total radiation during the long ice station.

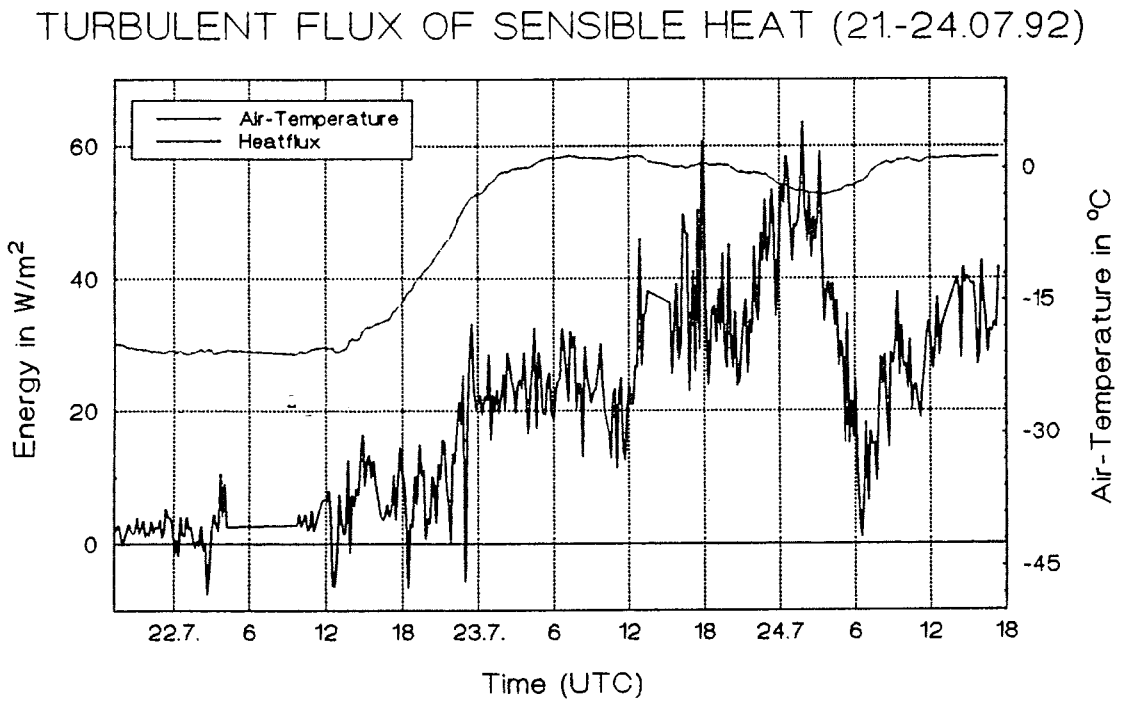

Fig. 2.2-3: Turbulent flux of sensible heat during the long ice station.

and sharp decrease in the morning of the 24 July is due to the clear sky in the night. The turbulent flux of momentum depends on the surface conditions and mainly on the windspeed (see Fig. 2.2-4).

c) Conductive heat flux through the ice
For the calculation of the conductive heat flux a new developed thermistor stick was put into the ice during the 3-day-station to obtain a time-series of temperature profiles. This thermistor stick allowed the simultaneous determination of the ice temperature at seven depth levels ranging from 5 cm to 1.0 m below the ice/snow interface. The sampling rate during the measurements was 1 min.

First results are shown in Fig. 2.2-5. The profiles chosen illustrate the influence of the air temperature on the temperature in the upper layers of the ice. During the station the air temperature rose from -22° C to about 0° C. Simultanously the ice temperature in the first few centimeters increased from -21° C to -5° C. Moreover the profiles show that at the end of the station the temperature at a depth of 0.5 m was about 2 K higher than at the beginning. The light air-temperature drop in the night from 23 - 24 July was not very pronounced in the ice as can be seen in the profiles.

From the temperature gradient the heat flux can be calculated using the thermal conductivity of the ice, which is mainly a function of the salinity. Salinity profiles will be available from the sea ice group.

A first rough estimation of the energy budget, containing the radiation budget Q and the turbulent flux of sensible heat H, at the long ice station is shown in Fig. 2.2-6. In the beginning of the station the surface loss was nearly 50 W/m^2. This energy had to be supplied by freezing processes at the bottom of the ice, which finally had to be transferred to the surface of the sea ice by the conductive heat flux. Later during the station, when the air temperature had increased and the sky was overcast, the surface received about 20 to 30 W/m^2 from the atmosphere.

2.2.2 Radio soundings

In order to get information about the meteorological conditions in the boundary layer and the upper atmosphere a total of 169 radio soundings were performed. Within the sea ice covered region four soundings per day were taken.

As an example of this extensive data set Fig. 2.2-7 shows the wind direction and the wind speed in the lower stratosphere compared to those at the surface level (all soundings at 12:00 UTC from 23 May - 27 July). The mean wind direction in the lower stratosphere is around 270°, while at the surface level two main directions are visible. The more westerly directions were measured in open water and in the subtropical zone, the eastward components are mainly due to the katabatic surface winds near the antarctic continent.

2.2.3 Deployment of Argos buoys

On 10 and 11 July the deployment of six buoys (Metocean) in one array took place. Two small buoys, measuring only air pressure and air temperature, and two highly instrumented buoys were deployed in a distance of 70 km to each other along the track of the vessel. Two additional small buoys were placed by helicopter in a position nearly 70 km away perpendicular to the ship's track. The two central buoys are measuring the air pressure, the air and the sea surface temperature, the snow height and ice temperature profiles with an ice thermistor string. Under these central buoys a 250 m long underwater thermistor cable is fixed with 30 thermistors and also two sensors, measuring pressure, temperature, conductivity and salinity of the

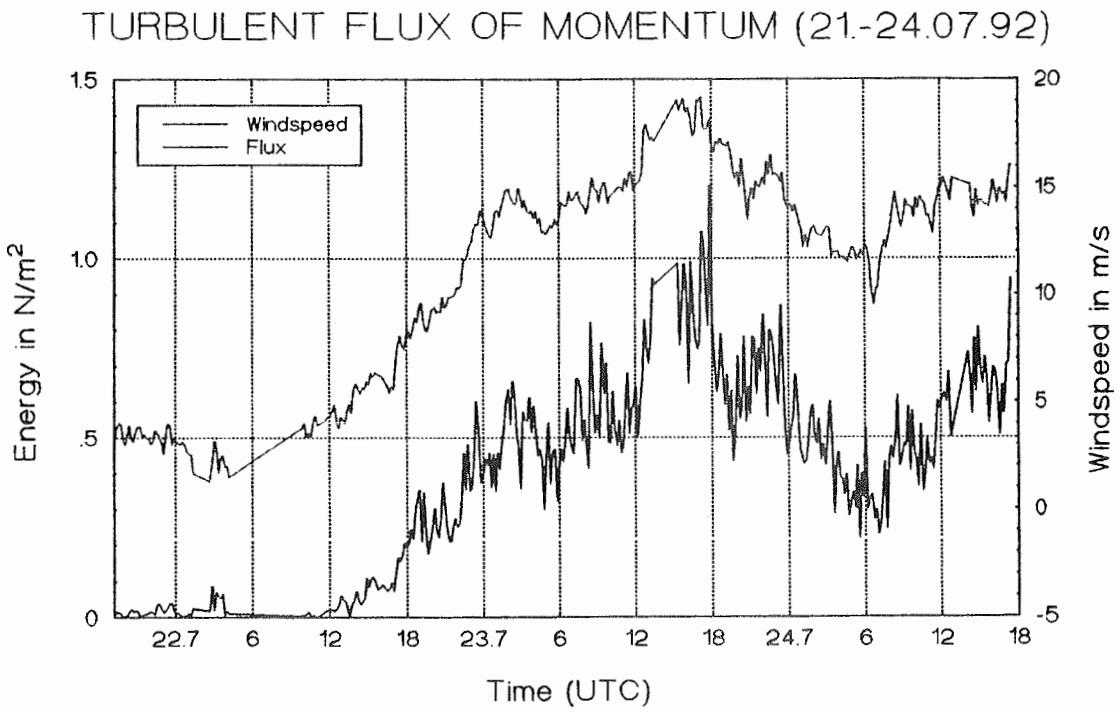

Fig. 2.2-4: Turbulent flux of momentum during the long ice station.

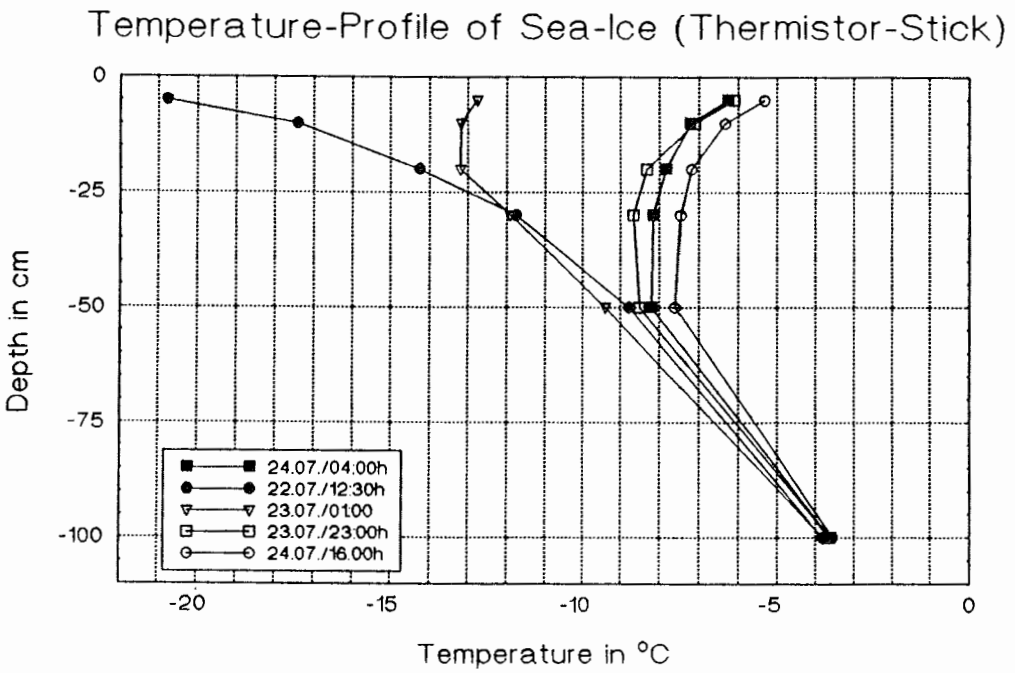

Fig. 2.2-5: Temperature profiles in the ice during the long ice station.

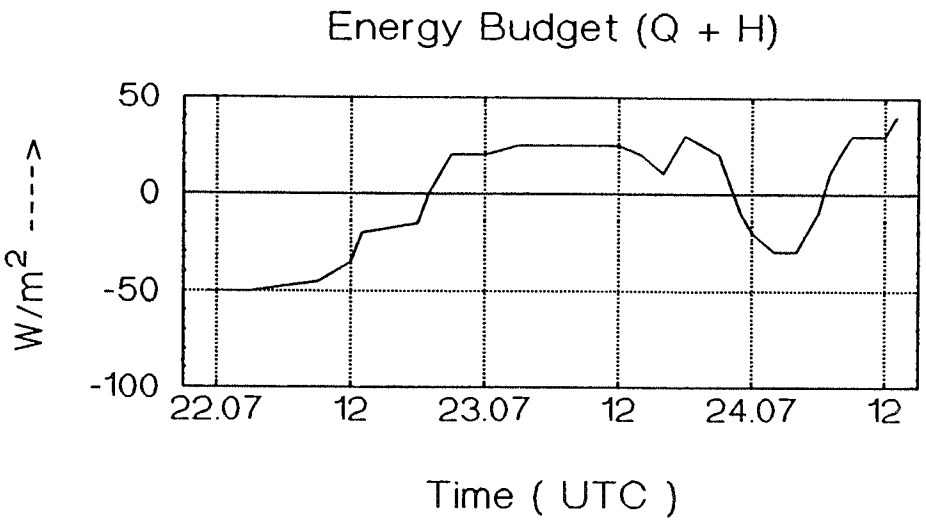

Fig. 2.2-6: Energy budget (radiation budget and turbulent flux of sensible heat) during the long ice station.

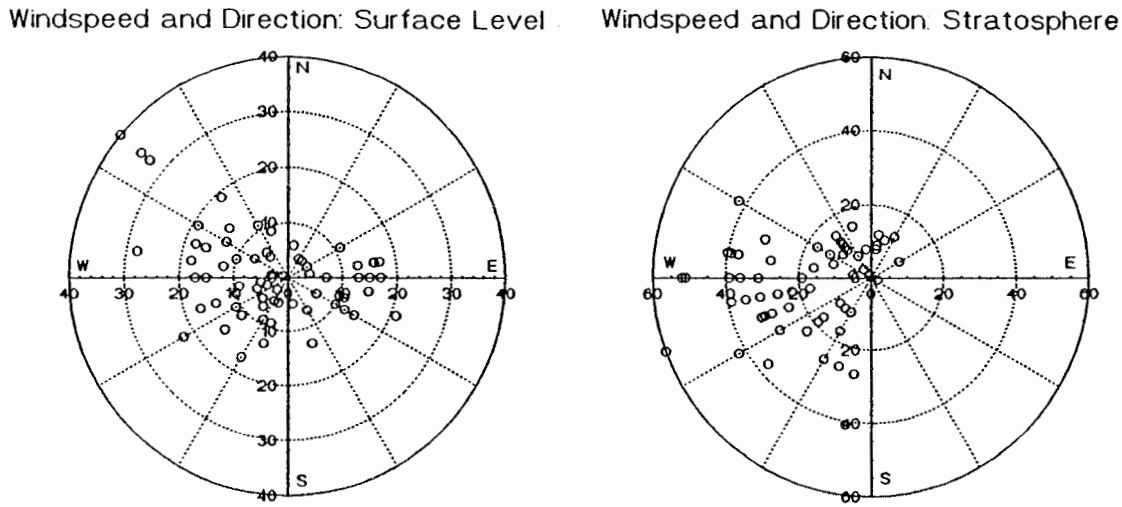

Fig. 2.2-7: Windspeed and directions at surface level and in the stratosphere from aerological soundings (12:00 UTS; 23.05. - 27.07.92)

water in 50 m and 250 m depth. All buoys use the ARGOS system for the transmission of the data. Fig. 2.3-4 shows the initial positions and the drift of the buoy array during the days of this cruise.

2.3 Remote Sensing

Several remote sensing techniques including optical, infrared and passive mircowave sensors as well as active microwave instruments were applied to sea ice investigations. The main scientific aim was to link geophysical characteristics of Weddell sea ice signatures obtained from various remote sensing instruments. These investigations serve as a basis for the interpretation of remotly sensed data in terms of sea ice variables needed in such a way that signatures may be inverted to extract key ice parameters. These ice properties are sought as primary inputs for heat, freshwater and momentum flux calculations, along with 3-dimensional coupled ocean-ice-atmosphere models for the Southern Ocean. Most aspects of these investigations were part of the PIPOR Antarctic project for the validation of Synthetic Aperture Radar data (SAR) from the European Remote Sensing Satellite ERS-1.

The main objectives of the passive microwave program were to study the microwave emissivity and polarization of various types of new ice, the effect of a snow cover on the radiative properties of sea ice and the effect of flooding and the presence of slush at the snow/ice interface. In parallel to the remote sensing activities the temporal and spatial variability of the physical, morphological, chemical, thermal and dielectric properties of snow and sea ice were measured.

The roughness characteristics of sea ice were measured on different scales to constract a data set for validation of sea ice models.

Infrared images were obtained using the shipborne HRPT receiving station and a number of radar reflectors were used to study the large scale ice motion. A data set of floe size distribution and lead statistics was aquired using infrared satellite data as well as helicpoter borne camera data.

Several sources of remote sensing data were used to derive ice information in support of planning navigation, day to day navigation, and scientific investigations.

2.3.1 Measurement of large-scale sea ice motion

T. Viehoff, S. Rasenat (AWI)

The shipborne HRPT receiving station was used to collect data from the Advanced Very High Resolution Radiometers (AVHRR) as well as data from the so called TOVS package system (Tiros Operational Vertical Sounder). During the acquisition period the satellite NOAA-9, NOAA-10, NOAA-11 and NOAA-12 were received. About 10 passes per day were obtained and preprocessed. Out of more than 700 passes acquired 170 data sets were selected and stored on tapes for postprocessing. The antenna system worked well even under very rough sea state conditions and at very low temperatures (< -30° C).

Because of missing daylight at the times of overpasses only the infrared channels 3, 4 and 5 of the AVHRR were be used for sea ice investigations. The data were radiometrically calibrated and geocoded to allow a direct comparison between different passes. The data will be used to describe the large scale ice situation under cloud free conditions. From time series of images the motion of the sea ice was determined using a correlation method similar to the methods used for SAR data analysis. The inertial motion of the ice cover could be measured as well as the mean motion of the ice on time scales of 2-5 days (Fig. 2.3-1). The results were verified by comparison with the drift information from the ARGOS buoys located in the Weddell Sea. The data from the ARGOS system are included in the HRPT data stream.

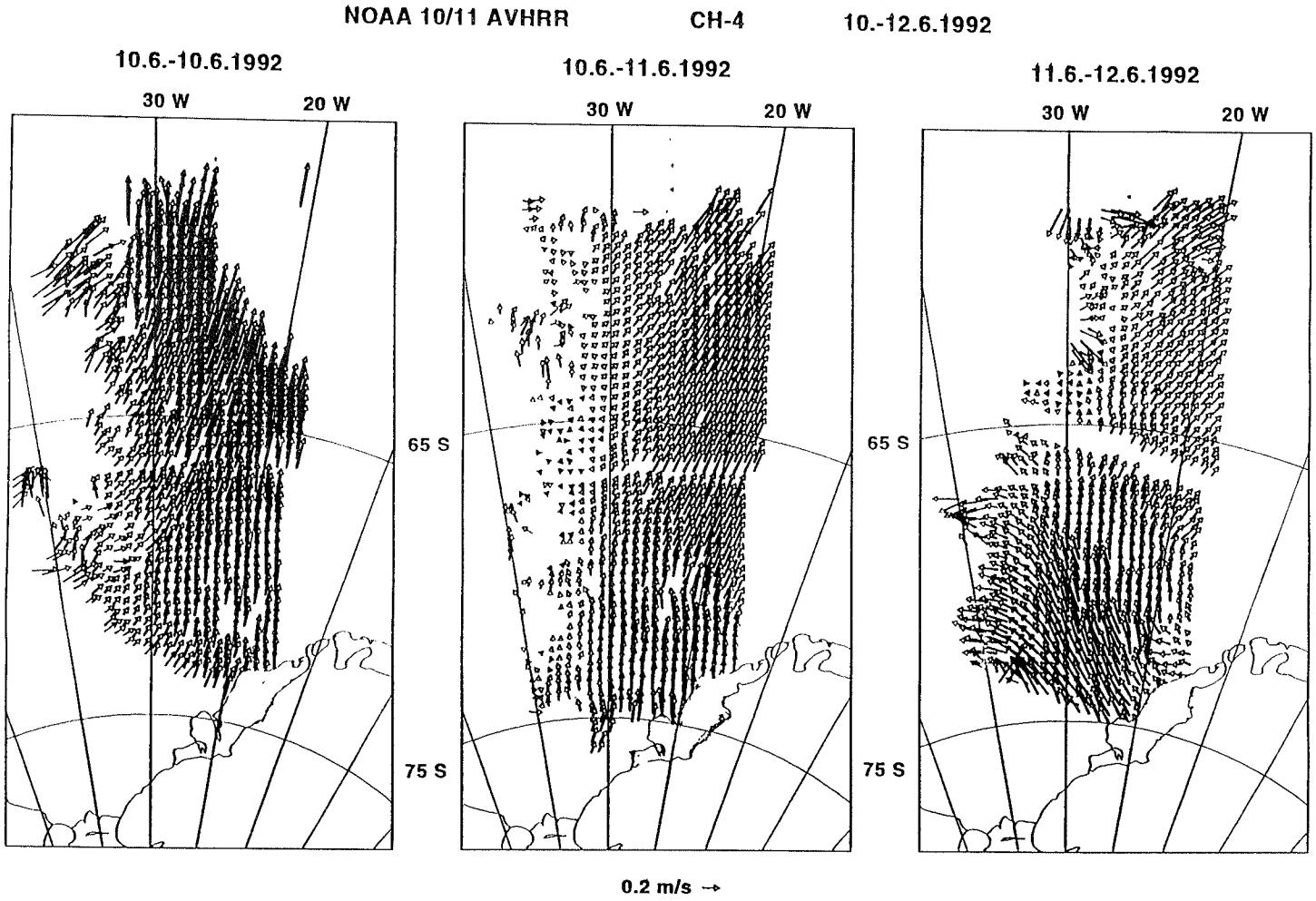

Fig. 2.3-1: Examples of AVHRR derived sea ice velocity fields for the period 10.6.-12.6.1992.

The devolopment of ice shelf edge polynyas were monitored for several cases in the Eastern Weddell Sea (0° Meridian to Gould Bay) as well as off the Filchner-Ronne Ice Shelf.

A very interesting result of the first preliminary processing of the data was the discovery of a number of relative high temperature (>-10° C) patches of 2-20 km in diameter within the sea ice cover in the western and south-western Weddell Sea (Fig. 2.3-2). These features were monitored over a time period of more then 30 days. Their locations and extents were nearly stationary over the entire period although the surrounding ice cover was moving. The location of at least some of these features seem to be correlated with bathymetric features as the shelf edge and/or submarine mountains. Nevertheless a more detailed analysis will be necessary to describe the physical mechanism responsible for the development of these high temperature patches.

Additionally the data from the ARGOS system were acquired to support the ships Meteorological Office with atmospheric information from the drifting buoys in the Weddell Sea as well as from all other Argos-equipped stations in the vicinity of the Weddell Sea.

All together 41 NOAA AVHRR images were used for near real time ice support for the ship. The information extracted from these data was used to navigate the ship through easier ice conditions near the shelf ice edge (Fig. 2.3-3) as well as through open water leads and/or young ice and refrozen leads in the inner pack ice. The processing of the geocoded infrared images was performed within half an hour after acquisition of the passes. Additional software was developed to allow the extraction of useful sea ice information by the ship's officers.

2.3.2 Measurement of infrared brightness temperature

R. Brandt (IMH), T. Viehoff (AWI)

A 44-day time series of snow/ice- and water-radiance was measured with a KT4- radiometer. The data show an instrumental offset of about 4.5°C and an additional air temperature dependence. The data have to be corrected for both effects. The results will be used to calibrate cloud-free data from the NOAA AVHRR infrared channels for atmospheric attenuation effects.

2.3.3 ERS-1 SAR measurements

T. Viehoff (AWI)

In the period 1 July - 31 July the German Antarctic Receiving Station has acquired a large number passes of ERS-1 SAR data. From this data set 246 passes had been requested by the AWI remote sensing group. Caused by the heavy ice conditions and logistical constraints only four direct comparison could be made where the ship was in the SAR swath at the time of overpass. Besides of this a number of surface measurements could be performed in a time window ± 1 day of the overpass.

Some of the SAR images were transmitted to the ship by fax, but the relative poor quality of the fax images prevented an analysis of these data. Due to payload faults in the period 19 July - 24 July 44 data takes were missing. Fortunally the payload could be reactivated to continue the SAR data acquisition.

The receiving station at O´Higgins was supplied with geocoding information as for example frame coordinates etc. to allow a preliminary geolocation of the data at the station. The SAR data will be postprocessed at DLR, Oberpfaffenhofen. The geophysical interpretation of the data with respect to sea ice motion and concentration will be done at the AWI.

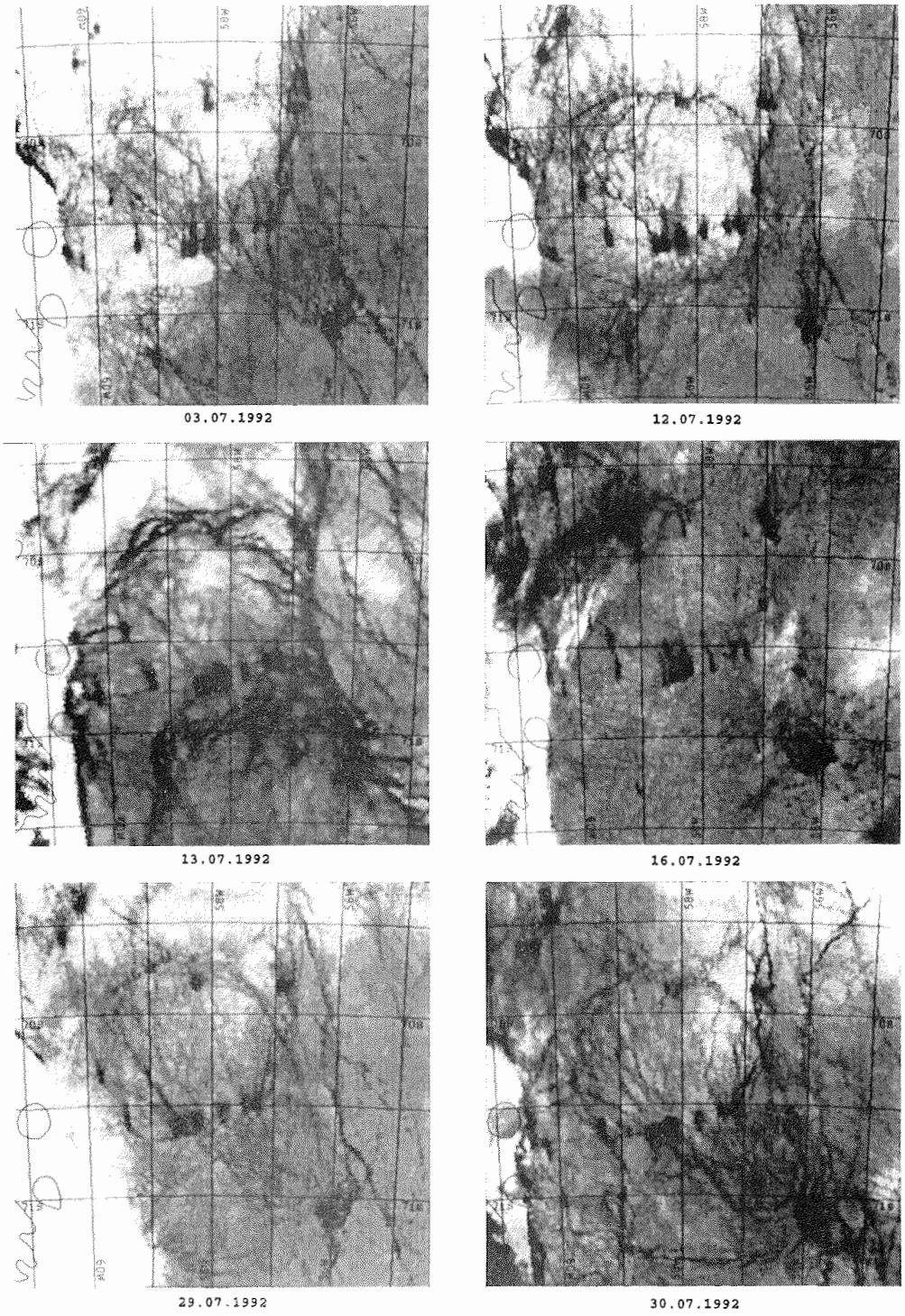

Fig. 2.3-2: Time series of sea ice anomalies in the western Weddell Sea for July 1992 observed by AVHRR infrared sensors. The dark spots represent relatively warm areas (-16°C to -20°C) whereas the bright areas have values between -24°C to -34°C.

NOAA 09 18.6.1992 06:36 UTC

Polarstern Kurs 16.6. 21:00 - 20.6. 01:00

Fig. 2.3-3: Cruise track along the polynya off the shelf ice edge near Atka Bay superimposed over an AVHRR infrared image.

2.3.4 Deployment of radar reflectors

W. Dierking (AWI), M. Drinkwater (JPL)

Twelve radar reflectors were deployed in order to supplement ice tracking capabilities from ERS-1 SAR images (Table 2.3-1). The first two reflectors were placed on the sea ice to test the reflector design and to check if they could be detected in SAR images. Due to unexpected high drift velocities of the sea ice these two reflectors could not be covered by the SAR swathes.

The remaining 10 targets were deployed from the ship as well as from helicopter together with a set of 6 meteorological ARGOS buoys (Table 2.3-2) in an array of about 200 km in diameter (Fig. 2.3-4). The main drift component during the period from the time of deployment until the end of July was to the northeast which coincides with the results of the large scale ice motion extracted from the AVHRR time series. The radar reflector array was covered several times by a SAR swath. According to a first short analysis done by the O'Higgins operating team the targets could be detected in some of the SAR images. However the detailed analysis of the displacement of the targets will be done as soon as the SAR data are available at AWI.

Table 2.3-1 Deployment-Positions of the Radar Reflectors:

No.	Latitude	Longitude	Date	Time (UTC)
#1	70°49.95' S	12°26.15' W	01.07	15:00
#2	71°37.48' S	16°33.47' W	05.07	14:00
#3	69°44.10' S	23°46.70' W	10.07	06:30
#4	69°29.90' S	24°24.60' W	10.07	11:20
#5	69°41.96' S	26°15.47' W	10.07	13:00
#6	69°30.04' S	25°49.61' W	10.07	14:30
#7	68°58.70' S	25°41.30' W	11.07	00:30
#8	68°16.30' S	24°59.10' W	11.07	00:30
#9	68°32.60' S	25°45.70' W	11.07	00:30
#10	68°59.90' S	27°01.60' W	11.07	00:30
#11	68°29.40' S	26°57.00' W	11.07	00:30
#12	68°14.60' S	27°34.60' W	11.07	20:30

Table 2.3-2 Deployment-Positions of the Argos Buoys:

No.	Latitude	Longitude	Date	Time (UTC)
9369	69°44.10' S	23°46.70' W	10.07	06:30
9368	69°41.96' S	26°15.47' W	10.07	13:00
9365	69°14.50' S	25°02.30' W	10.07	18:00
9364	68°43.20' S	26°18.00' W	11.07	09:00
9367	68°16.27' S	24°59.11' W	11.07	14:00
9368	68°14.60' S	27°34.60' W	11.07	20:30

2.3.5 Measurement of sea ice concentration and ice types

T. Viehoff, A. Bochert (AWI)

The sea ice concentration on small scales was estimated during 13 LineScan Camera and/or Video Camera flights (Table 2.3-3 and Fig. 2.3-5). These flights could only be performed during daylight conditions with a sufficient amount of contrast at the sea ice surface. The LineScan data were analysed onboard the ship to distinguish between at least three classes of ice and open water respectively (Table 2.3-4). The main problem of the analysis was to seperate between Light Nilas and Grey Ice and to detect refrozen melt ponds at the surface of floes which was observed at the end of the cruise (flight 12-13) after a significant increase of the air temperature which caused a melting of the snow cover of thinner ice floes.

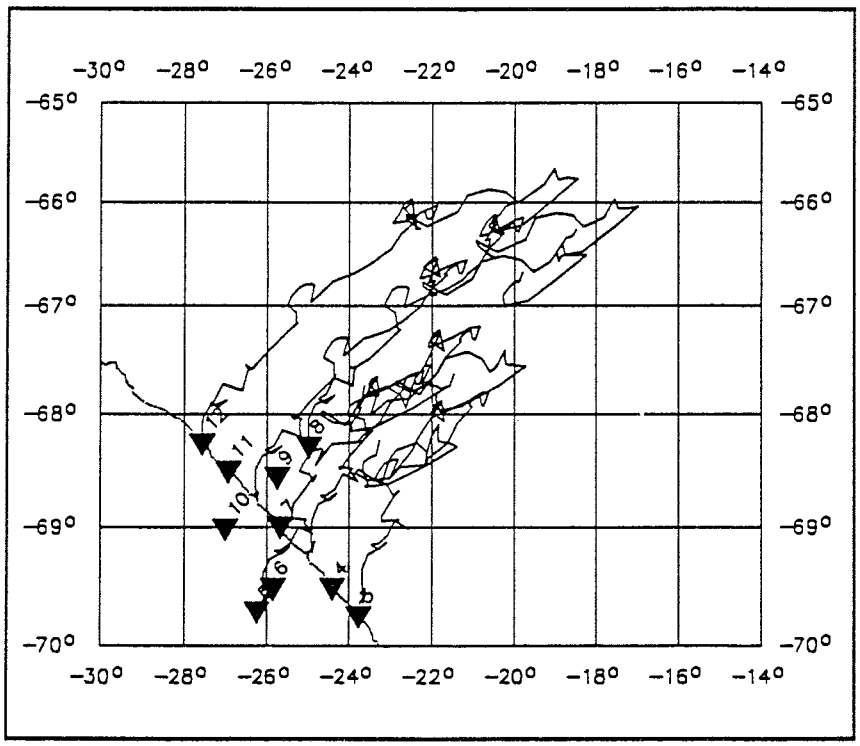

Fig. 2.3-4: Trajectories of the 6 Argos buoys for the period 11.07. - 01.10.1992 and start positions of the 10 radar reflectors (black triangles).

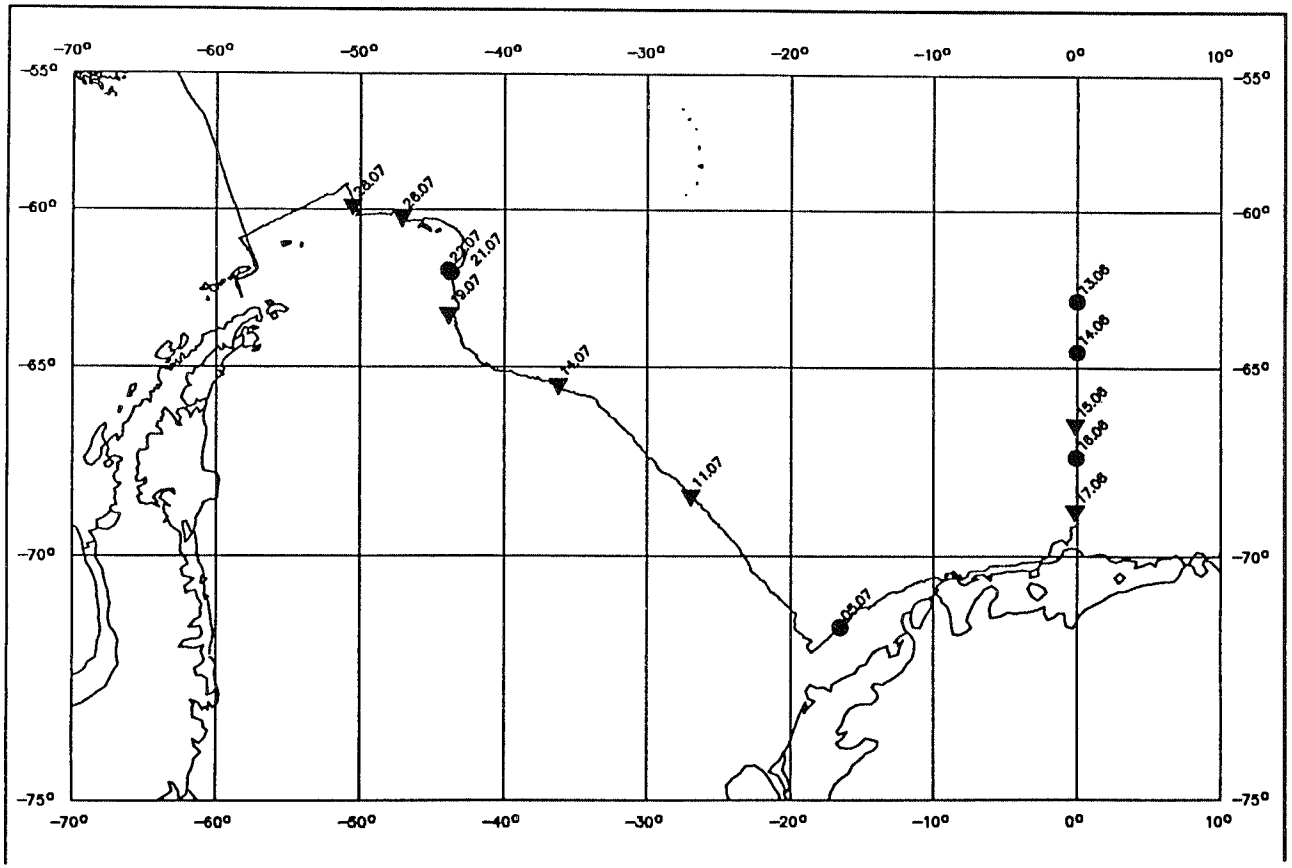

Fig. 2.3-5: Positions of the Video Camera flights (dots) and the combined LineScan Camera/Video Camera flights (triangles).

The preliminary analysis of the data (Table 4) shows the expected result of very high concentrations of white ice in the interior of the Weddell Sea and a more distinctive distribution of the ice classes in the Marginal Ice Zones.

The Video data were not analysed on board the ship but were only visualized to support the LineScan data analysis.

Table 2.3-3 Positions of Video- and LineScan Flights:

No.	Latitude	Longitude	Date	Time (UTC)
1	62° 58.47' S	00° 00.42' W	13.06.	11:00
2	64° 31.50' S	00° 00.40' W	14.06.	11:00
3	66° 29.97' S	00° 00.54' W	15.06.	11:00
4.	67° 30.40' S	00° 00.54 'W	16.06.	11:00
5	68° 44.20' S	00° 04.00' E	17.06.	11:00
6	71° 37.48' S	16° 33.47' W	05.07.	14:00
7	68° 39.92' S	26° 47.00' W	11.07.	13:00
8	65° 29.61' S	36° 12.52' W	14.07.	15:00
9	63° 26.07' S	43° 31.03' W	19.07.	16:00
10	62° 05.65' S	43° 48.46' W	21.07.	16:00
11	62° 00.41' S	43° 55.69' W	22.07.	13:00
12	60° 13.51' S	47° 09.28' W	26.07.	16:00
13	59° 50.18' S	50° 33.77' W	28.07.	15:00

Table 2.3-4 Measured Sea Ice Type Concentrations (%)

Date	Open Water	Dark Nilas	Light Nilas/Grey Ice	White Ice
15.6.	29.1	8.6	8.1 (L.N.)	54.2
17.6.	0.0	2.9	97.4 (G.I.)	0.0
11.7.	0.2	1.0	2.5 (L.N.)	96.2
14.7.	0.2	2.3	1.0 (L.N.)	96.4
19.7.	1.5	1.9	6.5 (L.N.)	88.2
26.7.		has to be analysed		
28.7.	0.3	0.0	14.2 (L.N.) 14.6 (G.I.)	70.2

2.3.6 Measurement of sea ice surface topography

W. Dierking, S. Rasenat (AWI)

A laser profiler mounted on a helicopter was used to measure the surface topography of sea ice along the cruise leg (flight positions see Fig. 2.3-6). The profiles were collected at a sampling rate of 100 Hz. Depending on flight conditions, the horizontal resolution varied between 15 and 25 cm. The effective vertical resolution was 2 cm. At the nominal flight altitude of 30 m the laser footprint on ground was about 8 cm in diameter. Altogether 17 laser flights were performed amounting to a total profile length of 428 nm.

Between 26 and 29 June eight 10 nm-profiles were measured near Atka Bay. During this period a nearly stationary area of rafted and ridged consolidated ice was separated from drifting pack ice by a shear line approximately located 10 nm off the shelf edge. Four of the laser profiles were flown parallel to the shear line (two on either side) at a distance of 2 nm and 4 nm, respectively. The other four profiles were crossing the shear zone. The height and spacing distributions of ice roughness features were investigated separately for the stationary ice area between shear line and shelf edge and the drifting pack ice on the other side of the shear line. The preliminary results show a nearly exponential decrease of ridge frequency as a function of ridge height in the drifting pack ice, whereas the histograms of the stationary ice area reveal a

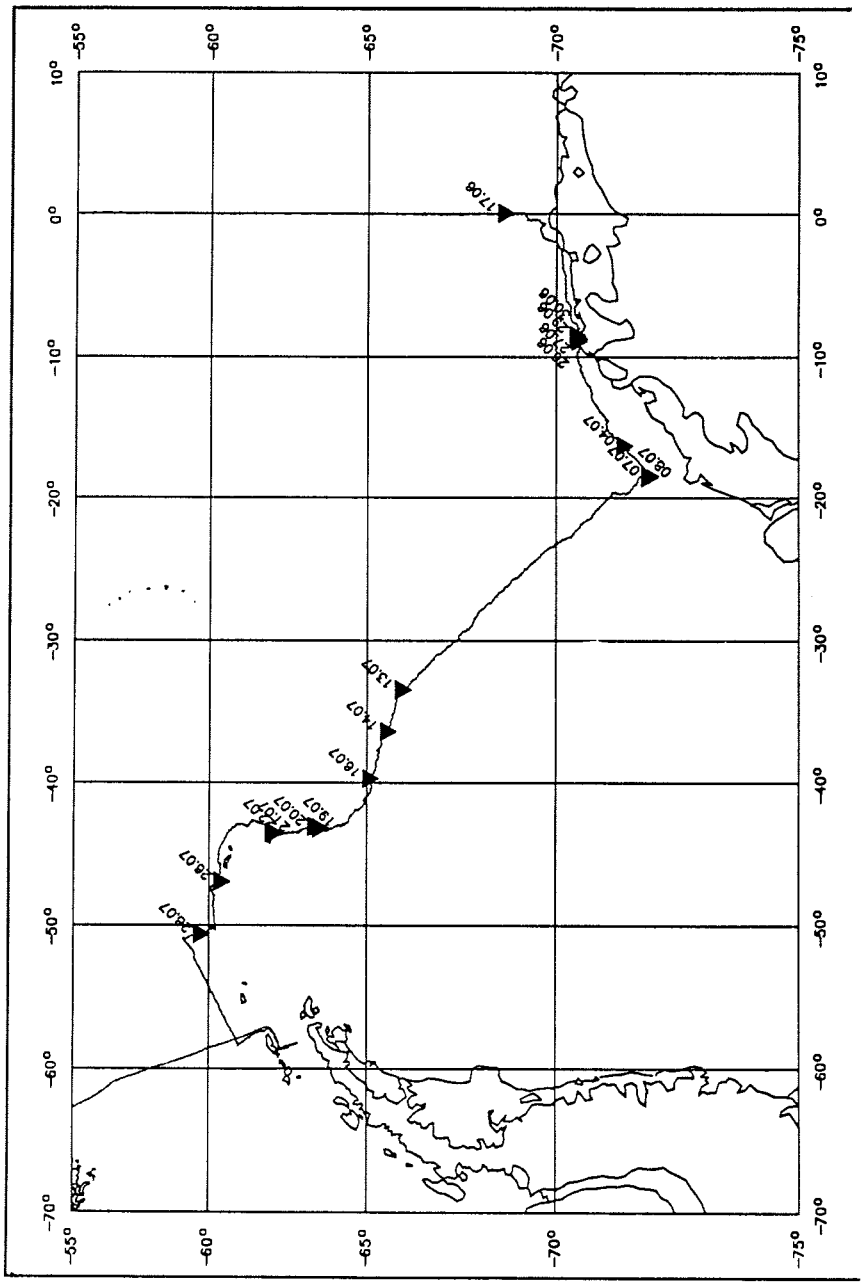

Fig. 2.3-6: Positions of the Laser-Altimeter flights

Rayleigh-shaped distribution function. The mean ridge height, however, is the same on both sides (see Fig 2.3-7). The mean ridge spacing increases with distance off the shear line. In the vicinity of the shear line, the average values are 14m for the stationary ice and 19 m for the drifting ice. At a distance of 4 nm from the shear line the values are 25 m and 40 m, respectively.

The data sets from 13 - 14 July were analysed as an example of the topographic characteristics in an area of divergent ice drift in the center of the Weddell Sea. Both the height and spacing distributions show an exponentially decreasing number of ridges as a function of ridge height and spacing, respectively. The mean ridge heights are 1.4 m and 1.3 m, and the mean ridge spacings are 69 m and 62 m. Floes of undeformed ice as large as 300 to 700 m were observed. A sufficient number of open water leads and areas of thin ice were crossed during the flights to enable an estimate of the freeboard. The mean freeboard, including the snow cover, was 19 and 22 cm, respectively.

2.3.7 Test of NOAA-APT/OKEAN-RAR data acquisistion system

W. Dierking, T. Viehoff (AWI)

A low cost PC-based APT receiving station designed by the DLR Satellite Receiving Station at Neustrelitz for acquisistion of OKEAN RAR data as well as for NOAA APT data was tested. Unfortunally the acquisition of the OKEAN-4 data could not be carried out because of a delay of the satellite launch. The NOAA-APT data were received and processed successfully. This was done parallel to the data acquisition by the ship´s Met Office.

2.3.8 International Space Year (ISY) activities

C. Garrity (AWI/AES), A. Bochert (AWI)

As part of the International Space Year (ISY), ice maps were transmitted by INMARSAT facsimile to FS "Polarstern" during the expedition. The ice information originated from two sources: Defense Meterological Satellite Program (Special Sensor Microwave/Imager (SSM/I)) and the European Space Agency Remote Sensing Satellite (ERS-1) (Synthetic Aperture Radar (SAR)). The SSM/I brightness temperatures (T_B) were obtained directly from the Fleet Numerical Oceanographic Center in Monterey, USA to the Alfred Wegener Institute (AWI) using a computer modem. The data transfer to AWI was funded by ISY. R.O. Ramseier, who was on secondment from AES for one year, processed T_B's using the AES algorithm, providing the ship with ice maps of total, thin and old ice concentrations within 4-6 hours after the satellite overpass. These maps proved to be very useful for planning purposes, especially in order to avoid high concentrations of old ice. The SAR data was received directly from the ERS-1 satellite by K.W. Asmus and K. Strübing, at a german receiving station located at O'Higgins, at the tip of the Antarctic peninsula. The reception of data was successful, however, the SAR images received on the ship were poor quality. Only sketches showing the interpretation of the original images were of interest. The captain did not use the ERS-1 SAR derived ice information for navigation of the ship. The SSM/I products combined with images received directly on the ship from the NOAA satellites (Advanced Very High Resolution Radiometer (AVHRR) images) proved to be a good combination to aid navigation of a ship through the ice. However, cloud free conditions were required for the AVHRR images to be useful for ice information.

It is the ultimate aim to combine ice information obtained from the 30 m resolution SAR with the 25 km resolution SSM/I maps. However, further understanding of backscatter from snow and ice are required before features on a SAR image can be interpreted. It is for this reason that measurements of the snow and snow/ice interface, ship-based T_B's and quantitative ice concentrations obtained from a helicopter in an area of the satellite footprints were completed.

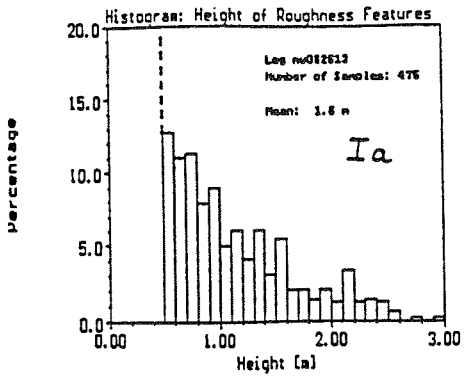

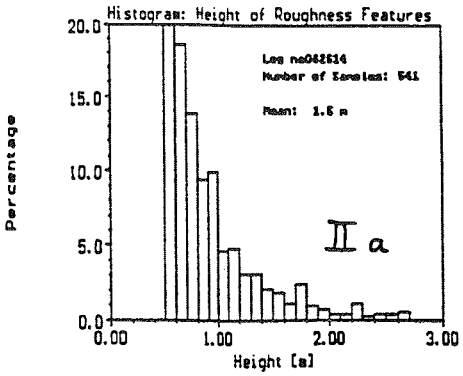

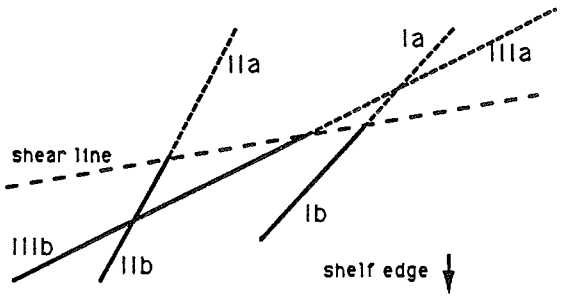

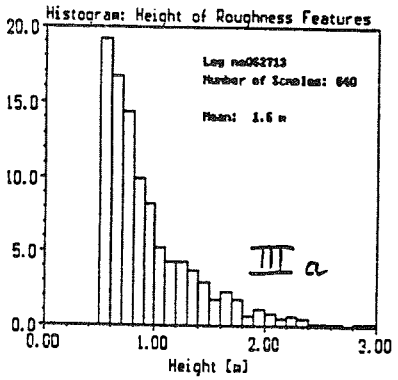

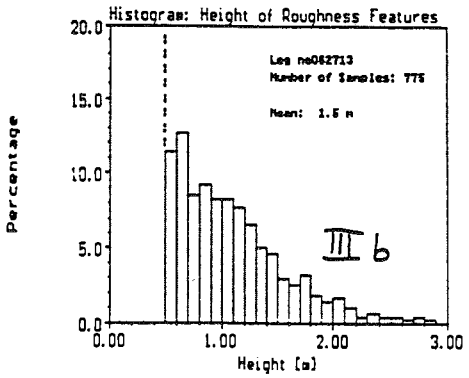

Fig. 2.3-7: Histograms of roughness features derived from three Laser-Altimeter flights near Atka Bay. The graph shows nearly exponential decrease of ridge frequency in the drifting pack ice whereas in the stationary ice the histograms reveal a Rayleigh-shaped distribution function.

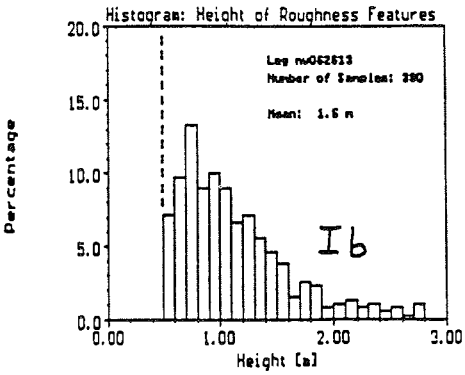

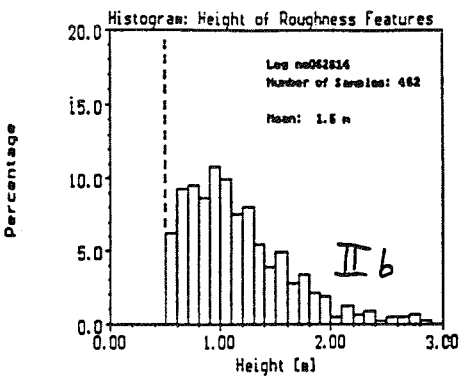

a) Snow Characterization
Vertical profiles of the dielectric properties, structure, free water content, salinity, temperature and to a less extend grain size of snow will have an affect on the microwave signatures from snow covered sea ice. Variation of ship-based and satellite T_B's in the Arctic and Antarctic due to a snow cover in the spring, summer and fall have been documented by Garrity [1991]. Based on 177 vertical snow profiles characterizing the snow, 38 of these profiles with dielectric property measurements, combined with snow depth profiles on 100 ice floes, an understanding of the snow cover can be established during the 1992 winter in the Weddell Sea. Preliminary results show similar conditions to what was found during the spring of 1989 [Garrity, 1991] where old ice floes, characteristic of the western Weddell Sea, had snow covers near 1m thick. Except for thick fast ice (4 m plus), there was often slush found at the snow/ice interface due to the heavy snow load causing a negative freeboard. The slush and thick snow cover caused a low emissivity measured by the ship-based 37GHz dual polarized radiometer which is an explanation of why the AES algorithm classified these areas as old ice using SSM/I data. It appears that these thicker ice floes with a significant amount of snow also caused a low radar return on the SAR images.

Comparison of snow properties and ice type with T_B measurements made during the 12 ice stations will be used as "control points" for the numerous T_B's measured as the ship moved through the ice. A T_B will be assigned to a particular ice type and snow cover.

b) Time-of-Flight Laser Ice Profilometer
Micro-roughness of the ice and/or snow surface were measured on 8 ice floes using a laser system with a resolution of 0.7 mm and 1.4 mm. This cruise provided the opportunity to test the system and there is a lot to be learnt about the interpretation of the data.

c) Ship-Based Brightness Temperature Measurements
The 37GHz dual polarized radiometer measured T_B from open water (wind speed dependence) and sea ice continuously from May 23 to August 1. The primary frequency used in the AES algorithm is 37GHz, thus the choice of frequency for the ship-based radiometer. Each day, T_B's from different ice types were collected and used as "control points" for the transect T_B's which were averaged over a 10s period every minute as the ship moved. The resolution of the radiometer for the 10s averaging is 1.0K. Scatter plots of T_B, that is the vertical versus horizontal polarization, will serve as "control points" for microwave signatures for different ice types providing "tie points" for updating the AES algorithm during the Antarctic winter condition. A preliminary analysis of the scatter plots using ship-based T_B's collected from the ice edge to the fast ice (May 12-19), before heading westwards, shows what can be expected for ice type classification using the AES algorithm. First year ice is radiometrically similar to grey ice, but is some what lower in T_B. The older fast ice with near a metre of snow, showed low T_B's, some even lower than open water. For calm water, dark nilas and open water can have similar T_B's. However, the vertical polarized signature from dark nilas is often higher than that from water. Pancake ice shows a very good separation from open water and can be distinguished from other ice types. The vertical polarization is lower for pancake ice compared to the radiometrically similar dark nilas. Light nilas shows a higher horizontal T_B compared to dark nilas and is larger in both polarizations compared to pancake ice. Grey ice and pancake ice may overlap, however grey ice generally shows a higher T_B. These scatter plots were based on 1s radiometric averaging, thus the resolution is poor (3.4K) compared to the 10s averaging. Scatter plots using the better resolution and for the total data set across the Weddell Sea will provide a confident conclusion. Polarization plots, that is, the vertical minus horizontal channels will also provide useful information.

Once the correct "tie points" are obtained and used in the AES algorithm, error in the ice fractions obtained from the algorithm during winter conditions could then be mainly attributed to atmospheric effects. Using the radiosonde data collected during the cruise by the Institute for

Meteorology and Climatology, Hannover, Germany, a correction for the atmosphere will eventually be determined.

d) Infra-red and Line Scan Camera Helicopter Flights
In order to determine if ice fractions obtained from the AES algorithm are correct, at least three ice types were quantified for each helicopter flight pattern using the Infra-Red (IR) Line Scanner Reconofax, developed by A. Bochert, as well as an older system, the Line Scan Camera (LSC) which operates in the visible range (400-800nm). Eleven flights covering a total area of 650km^2 have been processed and will be compared not only to SSM/I derived ice fractions but also will aid the interpretation of the SAR images.

This cruise provided the opportunity for six test flights of the IR system. The system proved to be an excellent instrument for quantifying ice fractions when the lighting conditions were too low for the LSC to operate. A snow surface temperature compared well to that measured from the IR system and thicker ice types did correspond to colder IR temperatures. An example of thick "cold" ice due to ice under pressure, thus rafting and ridging, compared to "warm" less pressured, thinner ice is shown in Figure 2.3-8. The shear line marks the border between these two areas.

Acknowledgements
The authors acknowledge Dr. B. Pfeiffer for financial support towards this aspect of the International Space Year. We are grateful to the crew, in particular Captain Jonas, for guiding the ship through some difficult situations. The field team is sincerely grateful to the Helicopter Service Wasserthal for a good service in getting us to different ice floes. We also thank the people from various institutions who helped us on the ice digging snow pits, which were sometimes deep and hard.

Reference:
Garrity, C., Passive microwave remote sensing of snow covered floating ice during spring conditions in the Arctic and Antarctic, doctorate dissertation, York University, Centre for Research in Experimental Space Science, North York, Ontario, Canada, September, 1991.

2.3.9 Optical and thermal infrared measurements

R. Massom (GSFC)

The research objective of this investigation was to relate measurements collected in the optical and thermal infrared regions of the electromagnetic spectrum to the nature, state and structure of sea ice and its snow cover. The overall aim is to use these data to help develop improved techniques for extracting information on surface temperature and type from NOAA AVHRR data, with particular attention being paid to regions of thin ice. Such data are virtually non-existent from over Antarctic sea ice, especially during the austral winter.

A field-portable SE-590 spectrometer, measuring in 252 wavelengths between 0.37 and 1.1mm, was semi-permanently mounted on the ship's port rail (alongside a PRT-5 and KT-4, a radar scatterometer and passive microwave radiometers). It was also taken down to the surface on a limited number of occasions. The PRT-5 is a thermal infrared radiometer that operates at wavelengths equivalent to channels 4 and 5 of the AVHRR/2. Being totally dependent upon the availability of sunlight (and ideally clear skies), the optical measurements were limited to the early and later stages of the cruise. Spectrometer data were taken over a variety of scan angles, both towards and away from the sun. The PRT-5 operated almost continuously from June 12 onwards (at an incidence angle of 40°, although this was adjusted on a number of occasions to examine the effect of the angular dependence of surface emissivity on temperature). Data were collected both while the ship was in motion and stationary.

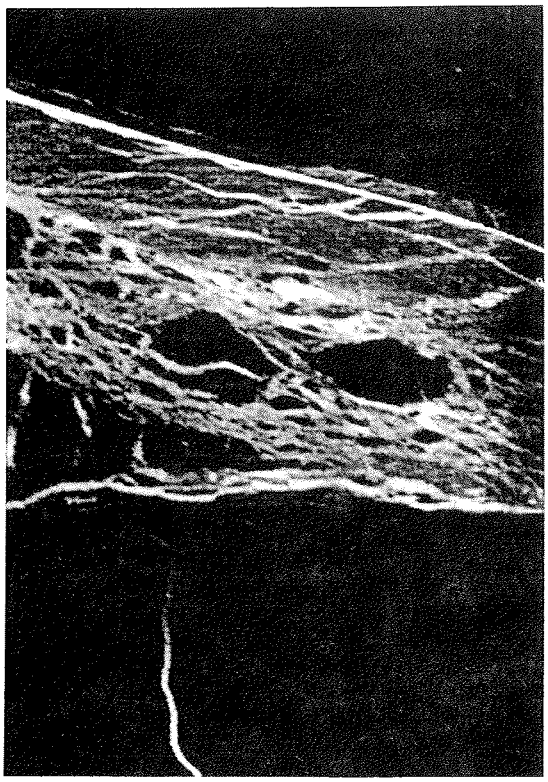

Fig. 2.3.-8: Shear line at S70°27'W08°31' measured with Infra-red Line Scanner Reconofax (bright: warm, dark: cold)

Surface properties affecting the thermal and optical properties of the snow cover i.e. grain size distribution, stratigraphy, wetness, and density (and salinity), were measured close to and within the footprint of the instruments on short ice stations, and also by means of helicopter "floe hopping". These measurements were carried out in collaboration with Al Lohanick, Caren Garrity, Mark Drinkwater, Axel Bochert, Christian Haas and Markus Thomas. Snow temperature profiles were also made in at least two snow pits per ice station. The 3-day station, from July 21 - 24, 1992, coincided with a large increase in air (and thus surface) temperature, air humidity and wind speed and enabled time series observations to be carried out of the response of the surface. Measurements were taken of the resultant increases in snow cover wetness, granularity and "crustiness".

The winter-time traverse of the pack afforded a unique opportunity to monitor the evolution of the Weddell Sea ice and its snow cover in various stages and states. Of particular significance in terms of remote sensing was the prevalence of hard barchan snow dunes and other ripple features on flat white ice, large fields of metamorphosed frost flowers on the centimetre scale, and, from mid-July onwards, the widespread occurrence of ice nodules and crusts on the snow surface, thick (up to 3 cm) ice lenses within the snow mass, and "melt ponds" caused by submergence due to ridging/rafting.

2.3.10 Microwave Radar Scatterometry

M. Drinkwater (JPL)

During the WWGS '92, a C-band (4.8 GHz) frequency-modulated continuous-wave (FM-CW) radar scatterometer was operated from the port rail of "Polarstern" to obtain the first shipborne measurements of the microwave scattering properties of Antarctic sea ice. The radar had dual polarization, enabling like- (VV) and cross-pol (HV) data to be acquired at a variety of incidence angles (10-70°). When the ship was stationary, and on station by an ice floe, the radar was scanned to obtain backscatter measurements as a function of both angle and polarization.

The objective of this investigation is to provide validation data for the ERS-1 C-band synthetic aperture radar (SAR) observations (at 23° incidence) and to obtain a detailed microwave backscattering dataset for computer modelling purposes. In support of this programme, detailed surface measurements were made within the footprint of the radar, each time a radar scan was completed. This information comprises snow and ice physical and chemical properties measurements together with structural information.

At short ice stations combined radar and snow and ice measurements were made of a number of ice types characteristic of the Weddell Sea during the wintertime: these include undeformed snow-covered grey and white first-year ice, together with second-year and possible fast ice forms each with extreme snow loading; other ice forms included ridged and rafted white ice and hummocked second-year floes.

A 3-day long ice station from 21 - 24 July, 1992 offered the possibility of making time-series observations of the sea ice with the scatterometer. In addition to periodic scans of data over the complete range of incidence angles, the radar was operated at frequent intervals (approximately 4 hourly) at a fixed incidence angle of 45°, and at both polarizations. The angle was chosen because the radar responds sensitively to the surface reflectivity and roughness, and is also sensitive to volume scattering from the snow and ice surface layers. Preliminary results indicate that the radar backscatter shows strong correlations with surface properties measurements and especially the thermal conditions in the upper ice and snow. Large temperature changes noted during the ice station offer the possibility of future modelling studies which demonstrate links between the combined active and passive microwave characteristics and the heat flux component in the surface energy balance.

2.3.11 Multi-frequency passive microwave observation of sea ice

A. Lohanick (NRL)

The primary aim was to obtain a comprehensive set of high-spatial-resolution sea ice brightness temperature (T_B) data in the Weddell Gyre in winter, and include coincident ground-based measurements characterizing the surfaces encountered. The data are gathered for: (1) comparison with SSM/I imagery for algorithm development, (2) comparison with surface measurements for model development, and (3) comparison with coincident scatterometer data for improvement of models and algorithms.

a) Observations completed
Stations: T_B as a function of frequency (10, 37, and 85 GHz), polarization (H and V) and incidence angle (35 to 75 deg in 10 deg increments). Snow samples for bulk snow salinity and density, and later observation and photography. Snow stratigraphy observations. Ice surface scrapings for determination of ice surface salinity (top 5 mm). Snow grain photography for determination of snow grain size and shape.

Ship in motion: T_B (mainly 10 H, 37 H and V, and 85 H, at 55 deg incidence angle) as a function of time (distance) along track, with notation of various pure and mixed ice types for a "catalog" of ice type signatures.

Sky T_B: Sky brightness temperature as a function of angle from zenith, for a determination of sky contribution to T_B of each sea ice signature.

b) Preliminary look
Brightness temperatures in most cold (< -10 C) cases appear high and have the small angular dependence expected of the first-year sea ice found in the Weddell Sea. We have not as yet calibrated the deep snow cases seen in cold weather. These should show low polarization (T_B difference at H and V) and lower T_B at the higher frequencies (37 and 85 GHz) due to volume scatter.

Surface snow grains appear small and eroded, consistent with being wind-blown in cold conditions. Depth hoar has been found in most cases of snow deeper than 100 mm, as expected with the large temperature gradients encountered. Snow has been found to have at least 3 ppt salinity in most cases, and much higher at the base of even the thinnest snow covers in most instances. Snow densities have ranged from 0.06 to about 0.55 g/cm^3, and so cover virtually the entire range of possible densities.

During the long ice station we obtained the first good simultaneous active/passive data set during a warming-melt event with very good surface characterization. T_B's behaved as expected, becoming higher and less polarized, with disappearing angular dependence as the snow became warmer and wetter.

Sky T_B profiles appear strongly dependent on cloud conditions, as expected, and a comparison of these with the many radiosonde soundings (kindly provided by the "Polarstern" meteorological crew) should prove very useful in modelling the contribution of the sky to T_B of sea ice in this region and season.

2.4. Properties of Sea Ice and Snow

Chr. Haas (UNIK), M. Thomas (UNIB)

The main goals of the sea ice work during WWGS'92 were to investigate the energy- and mass-balances of Antartic sea ice in winter, to improve our knowledge of the growth mechanisms and ice dynamics, and to provide ground truth data for the different remote sensing

methods which were carried out simultaneously. In addition, comparisons will be made with data collected in the same region by previous investigations (e.g. WWGS'89). The programme consisted of the following main parts:

- Ice coring and subsequent analysis
- Snow and ice thickness measurements
- Standardized ice observations from the ships bridge

a) Ice Core Processing
Ice cores were obtained from a total of 33 stations to measure several physical and chemical parameters. On the ice, temperature profile measurements were carried out. Detailed analyses were then performed in a -25°C cold lab on the ship, including texture analysis and qualitative pore size and -distribution discription with the aid of thick sections. For subsequent quantification, thin sections were produced. In addition, salinity, chlorophyll-a and nutrient concentrations were measured. Subsamples were retained for later δO^{18} and density measurements.

Fig. 2.4-1 shows the observed spatial distribution of several ice texture classes along the cruise track. While the ice was mostly of frazil origin in the Eastern Weddell Sea, according to the so-called "pancake cycle", congelation growth seems to dominate in the central Weddell Sea. The following table gives a summary of the observed proportions of the different textural classes:

Ice Texture	**Frequency of occurrence**
polygonal granular	1%
orbicular granular	47%
mixed columnar/granular	9%
intermediate columnar/granular	3%
columnar	38%
platelet	2%

Compared with the observations during WWGS'89, the ratio of columnar/ orbicular granular is virtually the opposite due to the fact that in the early winter most of the ice has recently formed and congelation growth hasn't taken place yet. It is also partially an artefact of the different distributions of stations during the two investigations.

Fig. 2.4-2 shows the composite mean salinity profile of all analysed cores together with the standard deviation and a 2nd order degree polynomial fit. Although many cores showed an S-type shape, the C-type shape which is typical of first year ice in the Weddell Sea can be clearly seen in the composition of all of the cores. The mean salinities for all of the cores was 5.67 ppt for true and 6.76 ppt for normalized lengths, respectively.

b) Thickness Measuremsents
Along several profiles up to 100 m length, snow and ice thicknesses and draft/freeboard were measured by drilling with a spacing of 1-2 m.The measurements were made to obtain information about ice mass, isostasy and roughness, which are important parameters in the ocean-ice-atmosphere interaction processes. Additional randomly-spaced drillings on one floe or by means of helicopter "floe hopping" gave information about the thickness distributions over a wider range. The mean ice thickness for all measurements was found to be 0.88 m (with 0.13 m snow and 0.05 m freeboard).

In Fig. 2.4-3 the mean ice thicknesses are given for the longitudinal transect. Ice thickness increases with increasing longitude due to the larger amount of second- and multi-year ice which is transported within the Weddell Gyre to the northwestern Weddell Sea. Fig. 2.4-4 presents the overall probability density functions (PDF's) for all of the data. Closer inspection of the

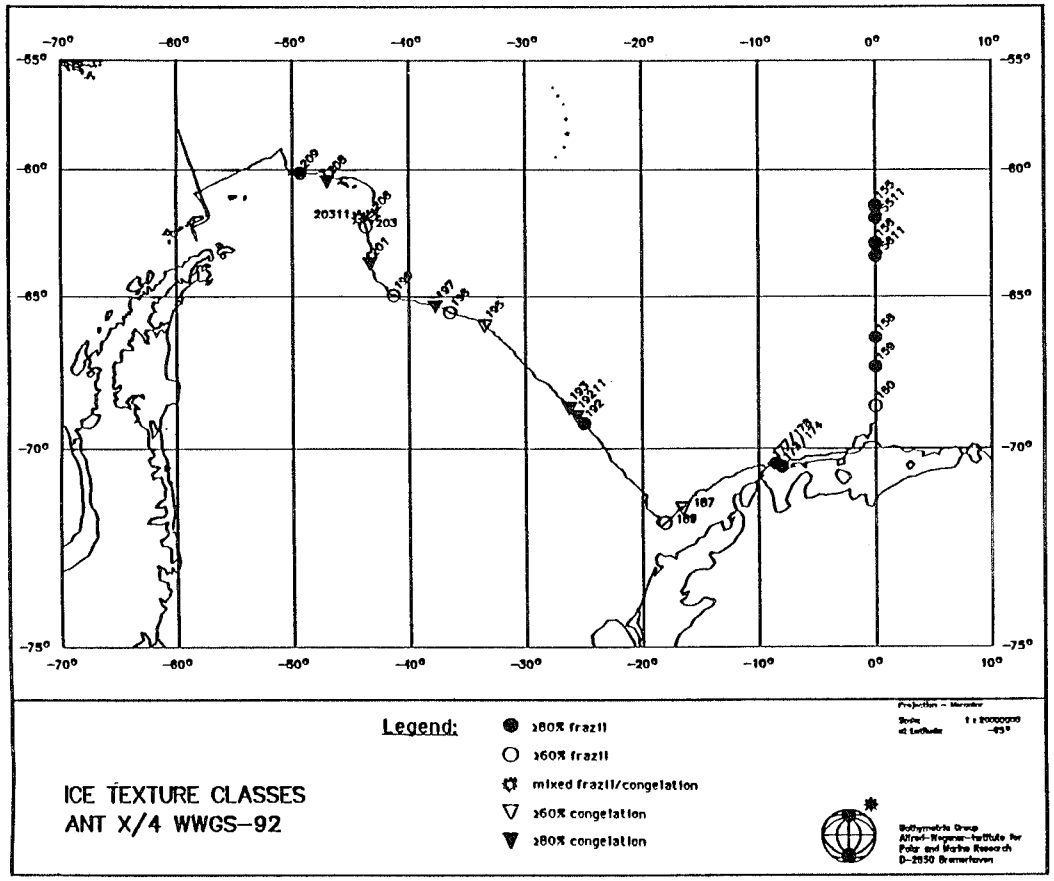

Fig. 2.4-1: Spatial distribution of sea ice texture classes along the cruise track

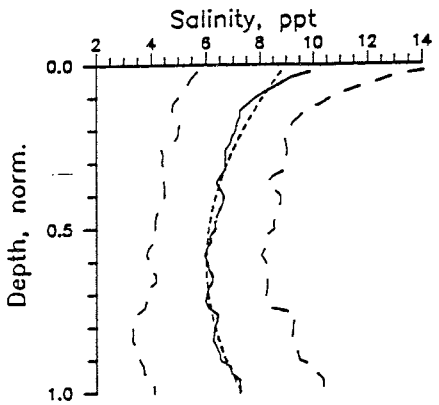

Fig. 2.4-2: Composite mean salinity profile of all ice cores (solid: mean, long dashes: std. dev., short dashes: 2nd deg. polynomial fit)

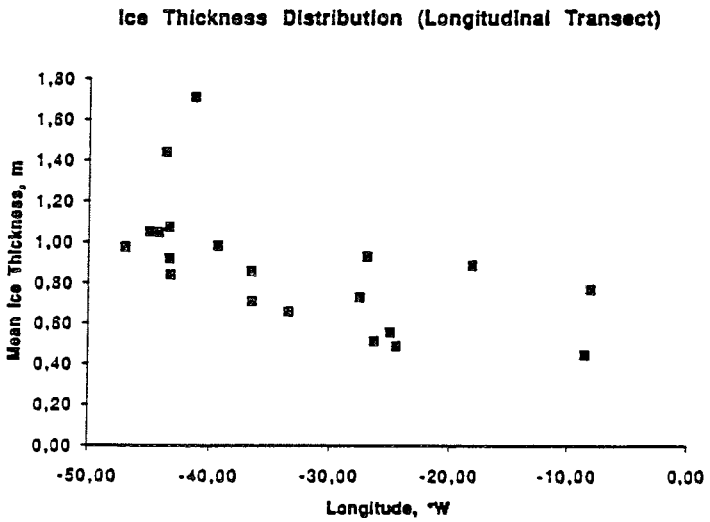

Fig. 2.4-3: Mean ice thickness along the zonal transect

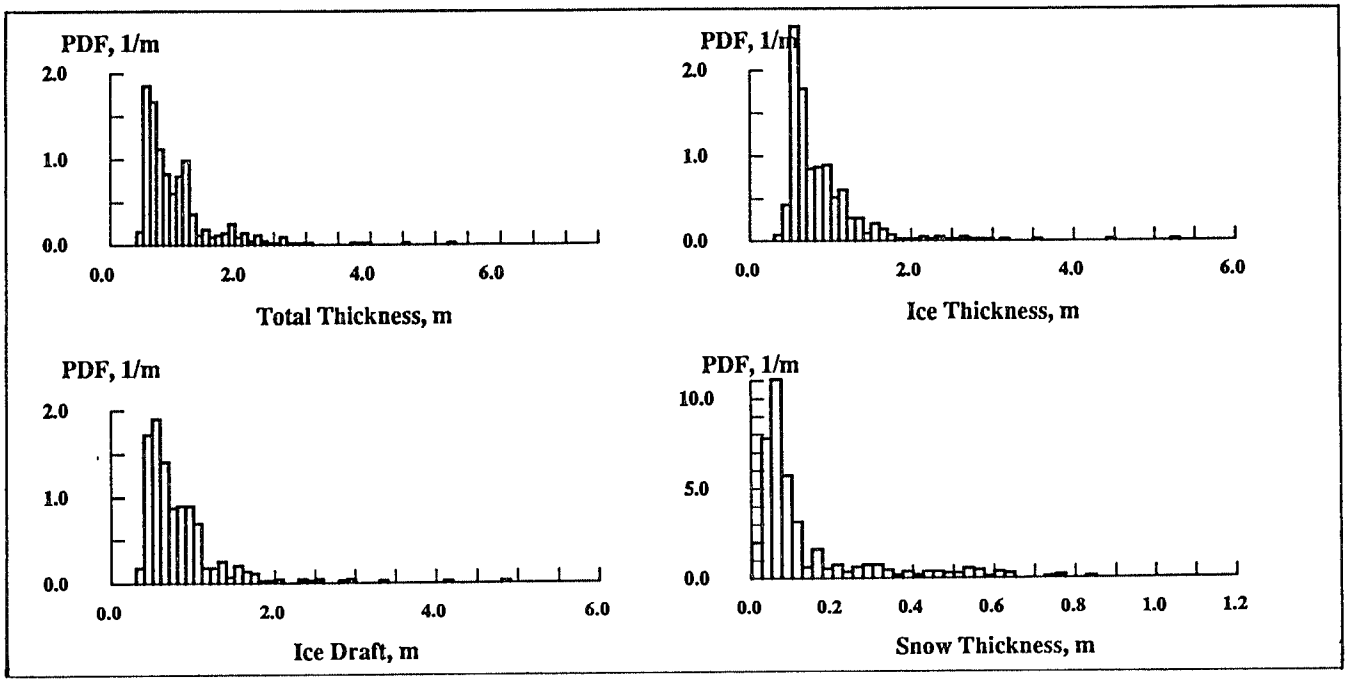

Fig. 2.4-4: Probability density functions for several parameters for the complete dataset

dataset suggests that the sampled floes were mainly composed of deformed first-year ice (0,89 m mean thickness) and undeformed first- (0.72 m) and second- (1.23 m) year ice which may be identifiable in the total thickness PDF.

c) Ice Observations
Hourly standardized ice observations (following the protocol for observations of sea ice in the framework of Southern Ocean (SO) JGOFS-activities) were performed from the ship´s bridge in cooperation with other scientists on board.This procedure gives important general information about the ice conditions along the cruise track and provides ground truth data for satellite-borne SSM/I, AVHRR and SAR sensor data. The results will be edited in a small booklet and distributed afterwards. Additionally, helicopter-borne video, optical and infrared linescan camera recordings were made along standardized flight patterns.

d) Further Investigations
The permeability or effective porosity of the ice column is an important factor for brine drainage and exchange and for sea ice organisms. In order to obtain an estimate of this parameter, water level measurements were performed in drill holes which didn't break through the ice underside (i.e. did not penetrate totally through the ice column to the underlying ocean). An example of a measurement in a 0.54 m deep hole (icethickness 0.67 m, freeboard 0.05 m) is shown in Fig. 2.4-5. The observed curve fits quite well to a logarithmic function, which provides information on the permeability to be calculated. For the central Weddell Sea, permeabilities were nearly always negligible and increased only to the north of 62.5°S.

The propagation of seismic waves provides valuable information about elastic parameters and thickness of a floating icesheet. With a 12 channel seismograph, two recordings were carried out over a 200 m profile on flat ice 80 cm and 120 cm thick. Compressional as well as horizontal shearwaves were generated with a 6 kg sledgehammer and recorded with vertical and horizontal geophones respectively. While the attenuation of direct waves was relatively high, a well developed flexural wave was observed on each record. After some computational processing, the dispersional behaviour will enable estimates of ice thickness.

2.5 Biology

2.5.1 Plankton ecology in and under sea ice

E.-M. Nöthig (AWI), V. Spiridonov (AARI), P. Jahn, Chr. Schulte (AWI)

a) Main scientific goals
Many investigations on plankton ecology have been carried out in the Weddell Sea area and adjacent waters in the last ten years with RV "Polarstern". However, the knowledge of the seasonal patterns in different regions is still limited. Almost nothing is known on species composition and biomass distribution in the water column and for sea ice organisms during the winter time. It is still not clear, for instance, whether algae from the water column choose the ice as an overwintering habitat. What are the overwintering patterns of zooplankton species (particularly copepods and euphausids), and how do they differ in different areas of the Weddell Sea? It seems evident that the sea ice might have an important influence on the whole pelagic environment in winter. Therefore, ecological investigations should be based on a comparative study on both habitats simultaneously.

In order to obtain answers to some of the open questions, the biological activities during WWGS'92 focused on three major fields which are essential for the biological and biochemical understanding of the annual cycles of the ecosystems and their organisms within the Weddell Gyre.

Water column:
Phyto-, protozoo- and mesozooplankton abundances and species compositions in the marginal ice zone (0° transect) and across the Weddell Gyre as well as the

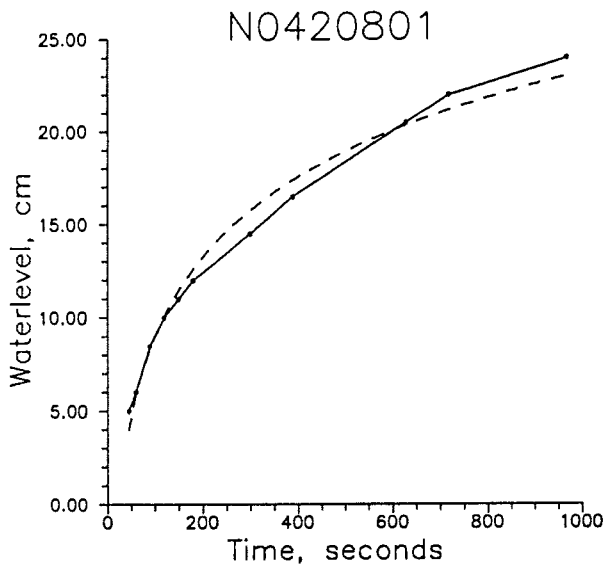

Fig. 2.4-5: Waterlevel rise within a drill hole, allowing the calculation of sea ice permeability (dashed: logarithmical fit)

biochemical composition within the water column should record the conditions of the pelagic systems in early winter.

- Sea ice:
  Investigations of the sea ice ice algae, microheterotrophs as well as biochemical composition within ice cores should resolve variations on the horizontal scale and the vertical scale.

- Experimental work:
  Growth experiments of simulated biological spring with algae should add information of the potential growth capacities of algae in winter.

  Simulated formation of sea ice with phytoplankton cultures and observed development of species composition and changes in biochemical parameters in the ice should give information of algal behavior during freezing. Grazing experiments with copepods should give information on heterotrophic activity and life cycle strategies of some dominant hebivorous organisms.

b) Measurements

Water samples from Niskin bottles of the oceanographic rosette sampler were taken to determine the following parameters: phyto- and protozooplankton species composition and abundances, chlorophyll a (chla), particulate organic carbon (POC), and nitrogen (PON) and biogenic silica (PSi). Samples for species analyses were taken down to 150 m; the biochemical parameters were recorded to a depth of 300 m whenever possible down to 1000 m. In addition phytoplankton species composition (> 20 µm) of the surface layers were obtained by means of an Apstein net (20 µm, 0 - 10 m) and short video-sequences of some samples were taped by a video sytem attached to an inverted microscope.

Zooplankton was collected with a Multinet (Hydrobios,100 µm) within the upper 1000 m and occassionally 2000 m. We always towed the homogenous layer of the Winter Water, the main thermocline and several layers of the Deep Water, including the T-max stratum. At some stations a Bongo net was used (in most cases down to 500 m). The catch of the 100 µm net cone was preserved for routine examination, whereas the catch of the 335 µm net cone (protective cod end container), was used for obtaining living animals for experimental work, lipid analyses, dry weight determination and ecotoxicological studies.

A total of 17 Multinet tows and 12 Bongo net tows were performed. When being stuck in the ice, west of the Kapp Norwegia, 5 Nansen net tows were successfully made through the moon pool with a hand winch ("4 men power") down to 500 m. The samples collected at the 0° transect and a part of the other samples were examined on board. All developmental stages of *Calanoides acutus*, *Calanus propinquus*, *C. simillimus*, *Rhincalanus gigas*, *Metridia gerlachei* and Euphausiid species were counted.

The data set of ice core parameters comprises on mainly the vertical (cm) distribution of autotrophic and heterotrophic species analysed by means of light microscopy. Samples were taken for particulate organic carbon, nitrogen and biogenic silica of defined layers of the ice cores. The vertical distribution of chlorophyll a was determined in relation to ice texture. Occassionally inorganic nutrient distribution were measured. The under water morphology of part of the ice floe at the long ice station was recored on Video-tape .

In the experiments carried out on board, algae from 10 m (STN 586, 592) and algae released from upper, middle and bottom parts of an ice core by melting in filtered sea water (< 0.2 µm) were incubated at temperatures of -0.5 °C at about 50 µE m^{-2} s^{-1}.

Two different algal cultures (pelagic, sea ice) were transferred into 1 L bottles and frozen and stored either in the light (ca 30 50 $\mu E\ m^{-2}\ s^{-1}$) or in the dark at -10° C. In addition experiments on solution of amorphous biogenic silicia in sea ice which was hid once a day to simulate crashing were carried out.

Zooplankton experiments were done in a laboratory container (-1°C), particulary with *M. gerlachei* in order to study its ability for feeding on different food sources in winter. Larvae of *Euphausia superba* and *E. crystallorophias* were kept individually in 250 ml glasses in order to examine their moulting and feeding activity. For their feeding artificial blocks of ice with frozen algae were prepared.

c) Preliminary Results
Pelagic Biology
i) Phytoplankton

The biological properties along the 0° transcet showed the influences of the different oceanographic fronts. From the Subantarctic Front to the Polar Front phytoplankton biomass was relatively evenly distributed and attained chlorophyll a values of 0.2-0.3 µg/L in the upper mixed layer (STN 565-573). Biomass decreased at the Polar Front (574) but increased again shortly behind it at the border of ACC and Weddell Water reaching highest values during the entire cruise of 0.44 (STN 576). Towards the south phytoplankton biomass decreased down to about 0.1 µg chla/L (STN 581-606) with a slight maximum at STN 589 to 596. Closest to the shelf-ice coast relative high values were encountered down to 300 m due to deep vertical mixing in the coastal current area. Figure 2.5-1a gives an overview of the biomass (integrated values from 0 - 300 m) along the transect.

Along the east-west transect across the Weddell Gyre the influence of the coastal current on both ends of the transect could be seen as higher chlorophyll a values. Lowest values of the entire cruise were encountered in the central Weddell region (STN 624 - 629; < 0.01 µg chla/L). Biomass concentrations along this transect never reached values above 0.1 µg chla/L. The whole area was extremely poor of phytoplankton. (Fig. 2.5-1b). Biogenic silica, particulate organic carbon and nitrogen as well as detailed species composition will be analysed in the home laboratory.

Net phytoplankton composition in the upper 10 m of the water column reflected the different water masses. In the heavy pack ice zone of the central Weddell Sea, species abundance was low and many empty frustles were found in the net samples. The most common forms were *Dactyliosolen antarcticum*, *Dactyliosolen tenuijunctus*, *Chaetoceros dichaeta*, *Chaetoceros criophilum*, *Distephanus speculum*, *Thalassiosira spp.*, *Asteromphalus spp.*, *Rhizosolenia truncata*, *Nitzschia spp.*, and *Nitzschia kerguelensis* and some other *Chaetoceros spp.* Some ice algae were found in the upper water column and few ciliates, tintinnids and dinoflagellates; the most prominent protozoans were radiolarians of the genus *Protocystis*.

ii) The distribution and composition of the common zooplankton species

Zooplankton sampling at the 0° transect was started with crossing the South Polar Front. There *C. simillimus* and *R. gigas* were extremely abundant (respectively 72000 and 26000 ind/1000 m^3 in the 500-0 m layer). The population of *C. simillimus* consisted mainly of the V copepodites. This subantarctic species was not found south of 55°S. The southern periphery of the ACC was characterizied by the presence of considerable numbers of *C. acutus*, *C. propinquus* (the youngest parts of their populations) in the Winter Water; in greater depth mostly older copepodite stages (also for *R. gigas*) predominated (Figs. 2.5-2a-c). However, total abundances of these copepods were low (in the range of 1000 ind/1000 m3). In the southern ACC zone the Antarctic krill (*Euphausia_superba*) larvae were sometimes even more abundant than *C. acutus* and *C. propinquus* (Fig. 2.5-2d). The percentage of young larvae (calyptopis) was very high (55-100%). These observations could indicate the very prolonged period of the herbivorous zooplankton reproduction in the waters, close to the ACC/Weddell Gyre boundary. This cor-

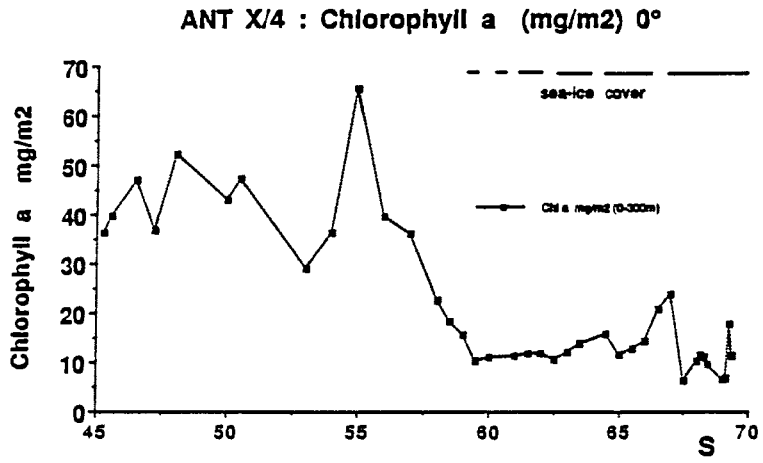

Fig. 2.5-1a: Chlorophyll a values integrated over a 300 m water column along the 0° transect

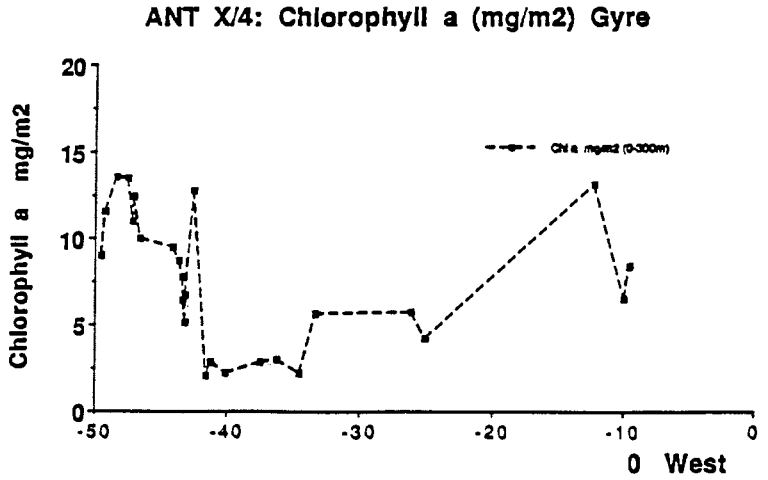

Fig. 2.5-1b: Chlorophyll a values integrated over a 300 m water column along the Gyre transect

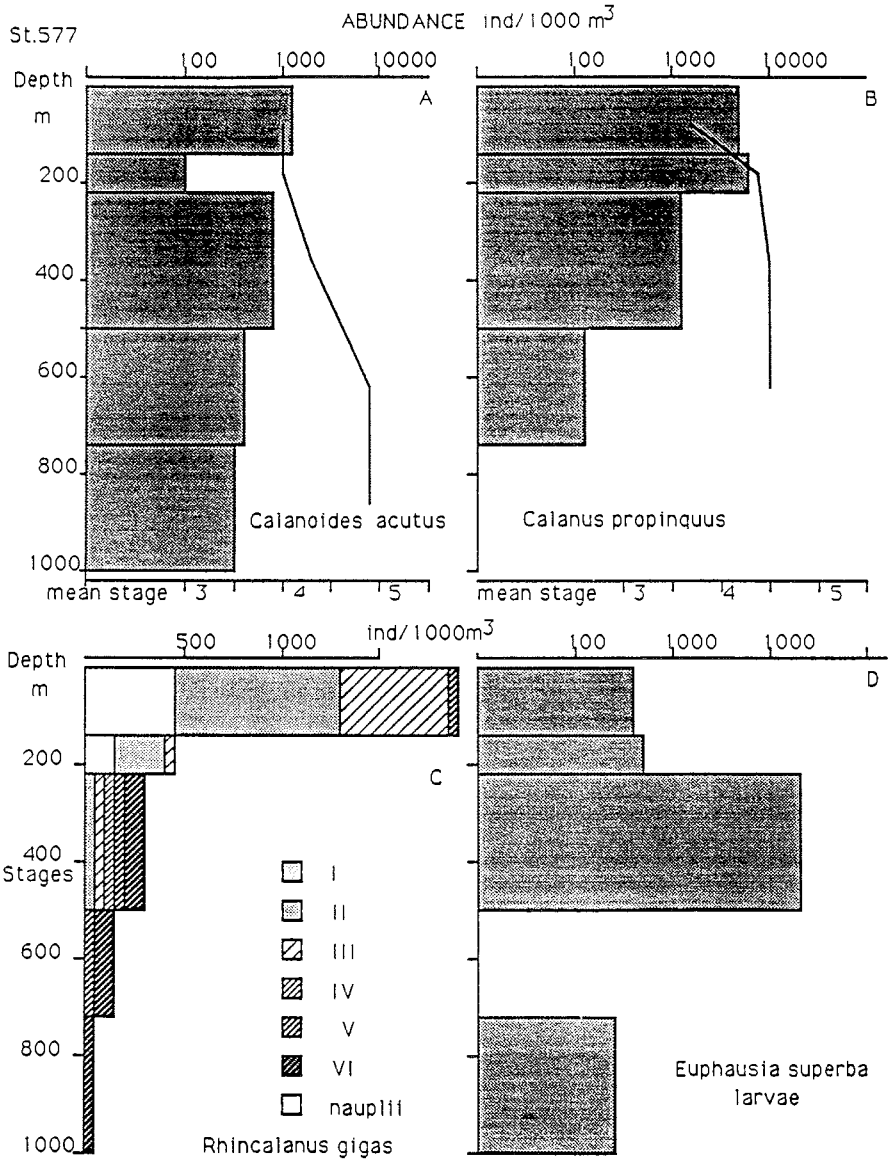

Figs. 2.5.-2a-d: The vertical distribution of 3 copepod species and the Antarctic krill (Euphausia superba) larvae at the Station 577 (Antarctic Circumpolar Current). For C. acutus and C. propingus mean developmental stages (solid line) are shown.

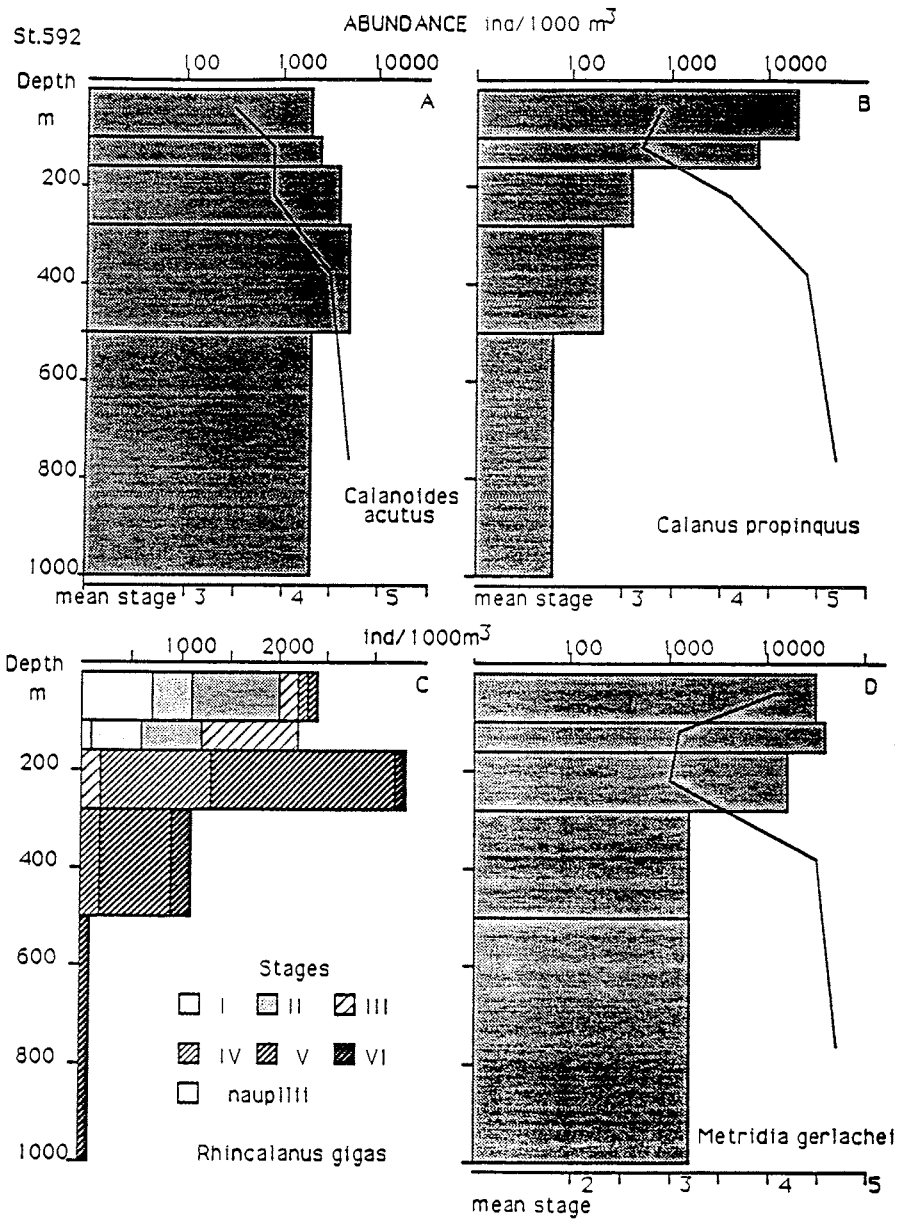

Figs. 2.5-3a-d: The vertical distribution of 4 common copepod species at the station 592 (area of Warm Circumpolar inflow). The mean development stage are shown by solid lines.

responded well with the relatively high phytoplankton concentrations found in that area in the early winter.

In the Weddell Gyre System, the zone of Warm Deep Water inflow around Maud Rise showed some similarity in the state of the populations of *C. acutus* and *R. gigas* with the southern ACC waters, which also could indicate their prolonged reproduction in autumn (Figs. 2.5-3a-c). But krill larvae with an abundance of one order of magnitude lower than near the ACC/Weddell Gyre boundary consisted of more older stages (furcilia).

In the Weddell Gyre itself the vertical distribution and composition of the large Calanidae fitted well the winter situation. Thus the whole population of *C. acutus* was mostly in the Deep Water and consisted of the satges IV and V (Fig. 2.5-4a) (however 68-78% of the population were in the upper 1000 m layer at the Sts 589 and 598). *C. propinquus* was very abundant in the Winter Water. The older stages, especially the copepodites V dwelled the Winter Water, but they also predominated in the deepest layers sampled, while in the main thermokline and the Tmax strata mostly the younger copepodites (III) occured (Figs. 2.5-3b, 2.5-4b).

Particulary new was the finding of high abundance (up to 25000 ind/1000 m^3) of *M. gerlachei* in the Winter Water (mostly the stage V). The younger (II-III stages) occurred generally in the main thermocline and Tmax strata. Deeper (also below 1000 m) the older stages (V and VI) were again more abundant (Figs. 2.5-3d, 2.5-4d).

In the western transect the high abundances of *C. acutus* and *C. propinquus* in the central area of the Weddell Gyre (where the phytoplankton was very poor) and low abundance in the northern Weddell Gyre zone (where there was more chlorophyll in the water) were noted.

Of particular interest was the occurrence of the Antarctic krill on this transect, including the central part of the Weddell Gyre, where it was supposed to be very scarce. At the St. 625 the abundance of 324 ind/ m^2 was recorded. The main age group was rather uniform in size (mean length 28.2 mm, SD = 1.85) with external genitalia just started to develop. It was likely the generation of 1990/91 which should form the so-called intermediate group in the spring-summer 1992/93. There were also few older furcilia and large (40-49 mm) subadult specimens. The moulting activity of these krill population was rather high, 64% of them were premoult and 2 of 3 animals kept in the laboratory had moulted on the 9th and 12th days after catching. Thus, it can be concluded, that the northward drift of krill in the western part of the Weddell Gyre, postulated in early years of the study of this species and then rejected by some authors, apparently can take place.

Ice Biology

Most of the general observations and physical parameters were done by the ice working groups (see 2.4)

Whereas most of the floes broken by the ship showed only slight brown colouration in the east we found almost choclate brown sea ice in the middle and western part of the Weddell Sea indicating high abundances of diatoms in the sea ice. Fig. 2.5-5 gives an example of biomass distribtuion of four cores sampled at regionally different places. The first three cores (left) were first year ice of this year which is reflected in the distribution pattern of chlorophyll a. The core obtained in the Atka Bay must have been formed fairly late, probably in a lead, since the chlorophyll concentrations were extremely low reflecting the poor phytoplankton concentration in winter. Most of the cores obtained in the eastern part of the Weddell Sea showed the same pattern. In contrast, ice cores obtained in the western Weddell Sea were either first year or second year ice. The core from July 19 showed a distinct band layer and a bottom layer which is a common feature for sea ice older than one year.

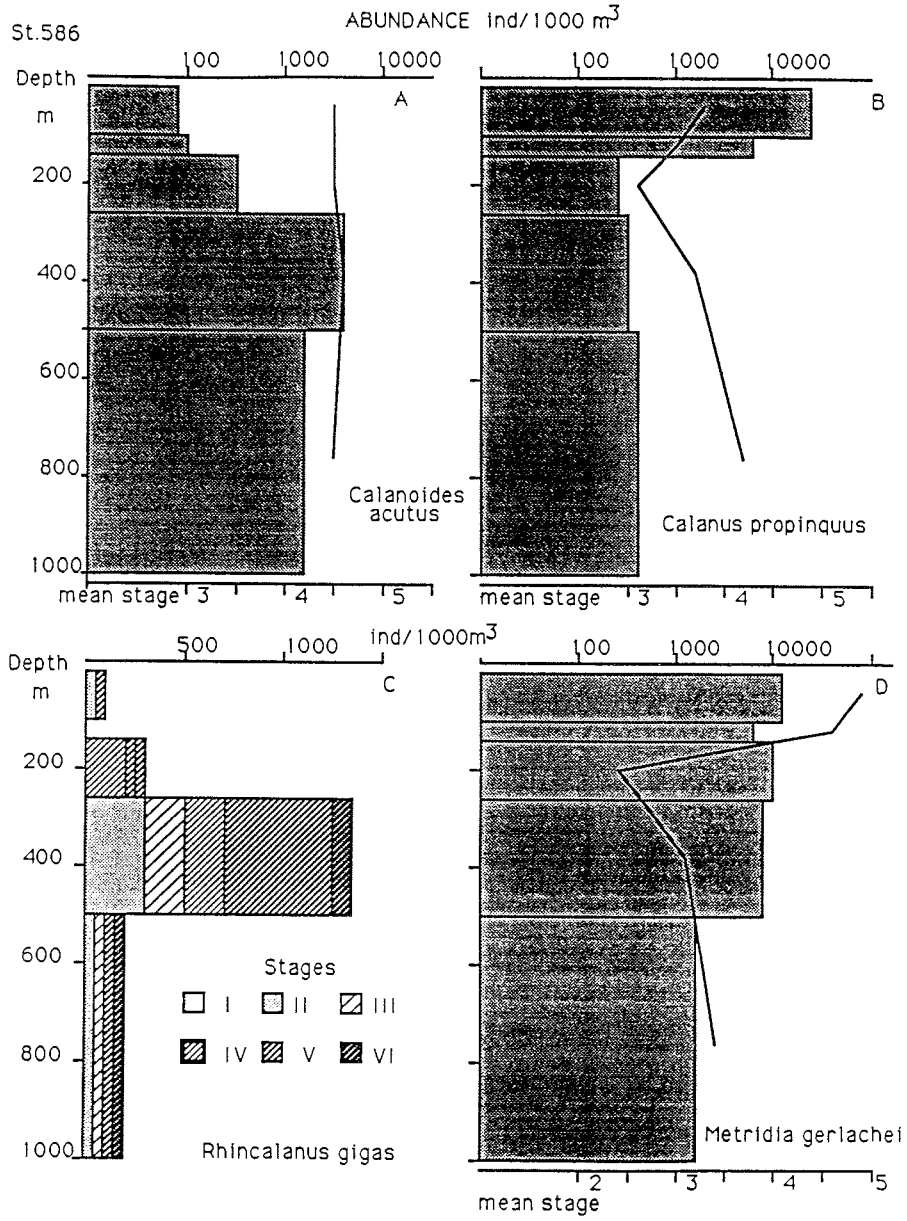

Figs. 2.5-4a-d: The vertical distribution of 4 common copepod species at the station 586 (central part of the Weddell Gyre). The mean development stages are shown by the solid lines.

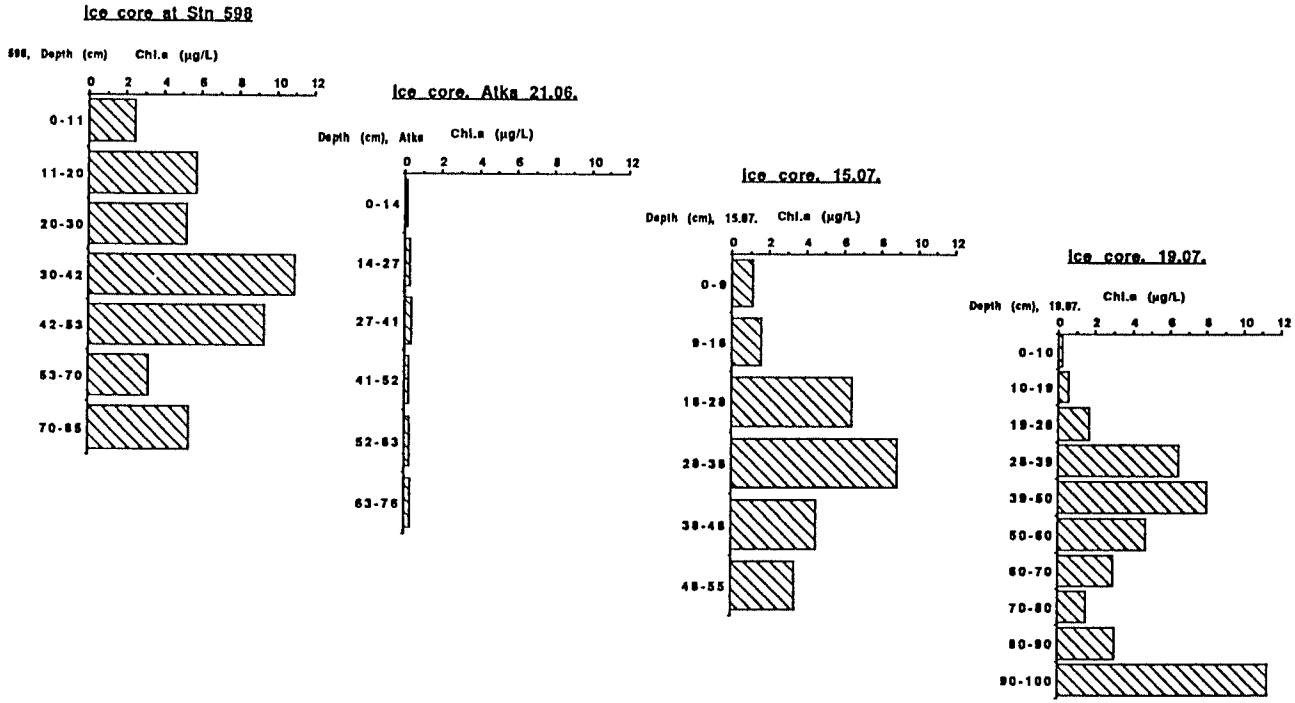

Fig. 2.5-5: Vertical distribution of chlorophyll a in four different ice cores. Left to right: core taken at station 598, core taken in the Atka Bay, two cores taken of different ice types in the western Weddell Sea.

Compared with the pelagic system an ice floe of 1 m thickness contains about five times higher biomass as the 300 m water column below indicating the significant importance of the sea ice as a reservoir for herbivorous food.

Further analyses of the samples obtained during this cruise will focus on an detailed species analyses of the diatoms and flagellates using microscopical techniques. The abundances of the different compartments of the ice communities will be analysed in comparison to abiotic parameters like ice texture, temperature, salinity or nutrient concentrations. This should lead to a detailled insight of both structure and development of the ice community by using all available data.

Experiments
Growth experiments with planktonic algae and ice algae were run in 10 L glas bottles. The results showed that the algae in the ice are able to grow as fast as pelagic forms when they were melted into sea water. Therefore they should be regarded as an important source to the total primary production per unit sea area in addition to the pelagic algae. The algae incubated seem to obtain their growth capacities during the dark winter time and can immediately react to changing conditions in the environment.

The simulation of freezing and crashing the algae seemed not be very harmful since only a slight decrease in chlorophyll a concentration was observed. Thus, algae incorporated in sea ice seem capable to survive at least in the first months.

The grazing experiment with *M. gerlachei* from the Winter Water gave some indications that this species is able to graze the phytoplankton in winter, but because of high mortality of the copepods the estimation of grazing rates was impossible. *M. gerlachei* is also capable to feed on other copepods, including their own young copepodites and as large forms as the III stage of *C. propinquus*.

In the experiment with Euphausid larvae feeding behaviour of both species *E. superba* and *E. crystallorophias* close to the undersurface of the ice blocks was observed. The mortality of the larvae was also high. No moults were recorded for the 2 week interval.

2.5.2 Bird and Seal Watch

L. Holsbeek (VUB)

Whereas summer distributions of birds and sea mammals (seals and whales) of the Antarctic and the Sub-Antarctic are largely studied, much less information is available on winter distributions and migratory movements. The ANT X/4 expedition was an excellent opportunity to gather new information on these subjects. Special interest was thereby given to the migratory behavior of penguins and seals.

During the first leg of the expedition - Cape Town to the shelf near Sanae - information was gathered about winter distributions of pelagic bird species in relation to environmental parameters such as water temperature and ice coverage. 183 half hour standardized counts were made from the bridge (which stand for 1129 km of observations); the observed numbers of birds can be recalculated into densities taking into account the ship's speed and position on one hand and specific species-linked factors on the other (larger birds recognizable at larger distances). A total number of 27 pelagic bird species were observed (n = 7668). Most of them show a clear restricted latitudinal distribution, resulting in 'bands' of species being replaced by related species further south (Fig. 2.5-6). In the case of the albatrosses (n = 566), the more northern Wandering and Black-browed Albatrosses were gradually replaced by Grey-headed and Light-mantled Sooty Albatrosses. All albatrosses disappeared long before the polar front was reached. Local high concentrations of mainly Blue Petrel, Antarctic Prion, Cape Pigeon and Antarctic Fulmar were found at the sub-tropical as well as at the sub-polar and polar front.

Once in cold polar waters, all previous seen species disappeared while Antarctic Petrels started to appear, being at their turn replaced by Snow Petrel once the ice edge was reached. The growing closed pack ice more south was characterized by the complete absence of birds and sea mammals. No seals, only 1 Minke whale and 2 unidentified greater whales were seen during the whole of this first leg.

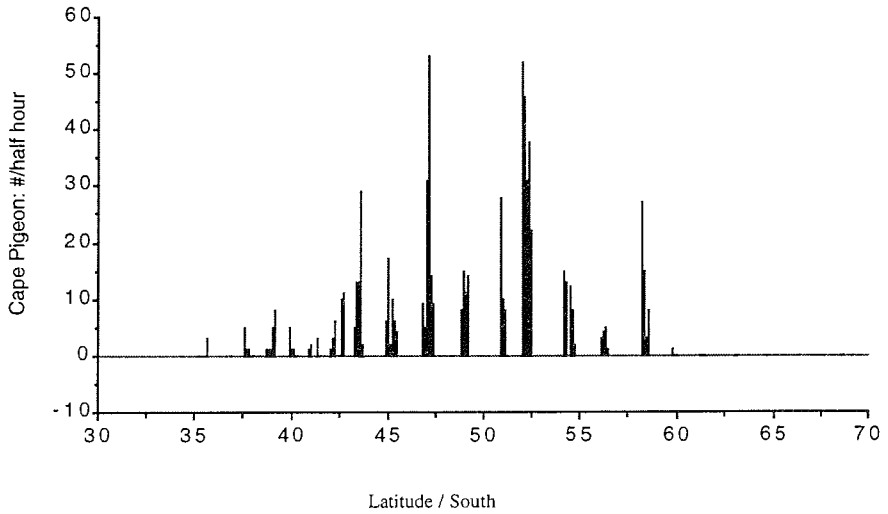

Fig. 2.5-6: 1992 Winter distribution of Cape Pigeon in the eastern South-Atlantic sector.

Because of the almost complete absence of flying birds, the second - partially overlapping - leg in the Weddell Sea pack ice concentrated on penguin and seal distribution. A total of 2256 penguins (172 Emperor; 2084 Adelie) were seen during 140 half-hour counts, as well as 345 seals (9 Weddell, 286 Crabeater, 7 Leopard and 43 Fur). Additionally to these standardized counts, observations were made during station time, while travelling in the darker hours of the polar winter days, and during several helicopter flights. Another 2589 penguins (135 Emperor, 2454 Adelie) and 335 seals (52 Weddell, 279 Crabeater, 4 Leopard) were thus observed.

No penguins or seals were seen in the growing pack ice in the western Weddell Sea. Only in the vicinity of the shelf the first Emperor penguins started to appear. After contacts with the Neumayer station, a helicopter flight was carried out to estimate the status of Emperor penguin colonies near the shelf in the Atka Bay. In the northeastern bight (70°32'4/08°38'8) a small colony of 1000 to 1500 males was found, an estimate based on a comparison with the 9000 couples 'Neumayer'-colony which is constantly observed from Neumayer. The location of the colony is very close to the place were it was first found during the PS-1986 winter expedition, though numbers were at that time estimated to be even larger then at the 'Neumayer'-colony. On the way north, Emperor penguins were found, scattered all over the pack but clearly in larger numbers once the polar circle was reached. They usually appeared in small groups ranging from 5-15 and were observed at several occasions feeding in leads or in small patches of open water.

Adelie penguins were found in growing numbers once over 66° though large numbers (groups from 50 to 1000) were only seen NW of the South Orkneys, migrating through the broken

pack, often clearly following relative small pathways through the pack (helicopter observations). Smaller groups were observed as long as the ship was in the ice.

No large concentrations of Chinstrap penguins were found, not even when leaving the pack heading towards Drake Passage. Only three small groups were encountered, all in open water close to the ice edge (total n = 16). Flying birds were rarely seen in the pack, except for low numbers of Snow Petrels when approaching the South Orkneys and larger numbers in the polynia north of them (n = 130).

Weddell seals were rare. A large group of 50 animals was observed from the helicopter on the fast ice at 71°37'S/16°25'W. Nine animals were seen near 64°, appearing from under the closed pack ice after the passing of the ship. Crabeater seals started to appear when approaching the South Orkneys, though larger numbers were only seen to the NW of the islands. A rather high concentration (n = 149) was found on the fast ice South of King George Island. Crabeater seals were mostly seen on the ice in small groups from 2 up to 5 individuals. A striking feature was that these groups were mostly found in larger assemblies, suggesting sort of a contact. Leopard seals were only encountered south of King George Island. The only Fur seals were also found near King George, most of them lying on relative small flows in open water. No Ross seals were seen during the expedition.

In general, most of the vertebrate activity in the pack ice was concentrated around leads and polynias; except for Weddell seals or some lonely Emperor Penguin, almost no sightings were done in closed pack ice regions.

Whales were rarely seen; 36 Minke whales were counted during the half hour counts, usually appearing in small groups up to 6 animals. During helicopter flights, another 18 Minke whales as well as 4 Orcas were seen. On the other hand, Minke whale blow-holes in 5-10 cm thick ice were seen all over the more northern section of the expedition.

2.6 Lipid investigations

K. Fahl (AWI)

The main goal of this cruise wasthe investigation of the lipid metabolism of the endemic antarctic copepods, mainly the 3 species *Calanoides acutus, Calanus propinquus* and *Metridia gerlachei*. The herbivorous or respectively omnivorous copepods incorporate the polyunsaturated fatty acids of the phytoplankton into the storage and the membrane lipids. With the aid of these high unsaturated fatty acids as markers, it is possible to obtain information on physiological adaptations to the environment and food supply. No previous measurements have been taken during Antarctic Winter, and therefore this cruise should complete the seasonal and geographical data set.

a) Measurements
The copepods were caught with a Bongo - or Nansen - net on different stations. The investigations, which were made during the cruise, consisted of 4 parts:

- Feeding of the different copepod species and developmental stages with radioactive-labeled phytoplankton material (use of $NaH^{14}CO_3$). This experiment gives information on the turnover of the lipids which depends on the stage of developement and species.

- Feeding experiment with non-labeled algae where the food supply was changed. By this means, it is possible to obtain information about the flexibility of the feeding behaviour of the copepods.

- Additional experiments with *Metridia gerlachei*. This species was fed with radioactive-labeled *Calanus propinquus* (C III) to obtain information on the turnover of lipids through the next step of the food web.

- Some experiments with *Calanoides acutus* as an interesting species in winter, because it is known that this copepod sinks down into deeper water layers to survive the cold and dark periods in a kind of hibernation without feeding. But it is not known whether this "non-feeding" behaviour depends only on the missing food supply in winter.

b) Preliminary Results
Most of the validation of the experiments will be carried out in the home institute because the analytical methods are too complex to be conducted on board the ship. The preliminary results from scintillation measurements indicate that *Calanoides acutus* is able to feed in winter as well as *Calanus propinquus* and *Metridia gerlachei*. During this season *Calanoides acutus* is not able to feed on all kinds of phytoplankton. The results indicate that it likes to eat only the small species of diatoms. By way of contrast, *Calanus propinquus* and *Metridia gerlachei* prefer to eat large diatoms such as *Thalassiosira antarctica.*

I want to thank Evi Nöthig for the microscopical investigations and for her help in matters of biological understanding and Vassily Spiridonov, who helped to determine both the different species and developmental stages of the copepods.

2.7 Marine geology

Chr. Haas (UNIK)

Sampling of surface sediments for marine geological investigations was performed at 19 selected CTD-stations on the transect between Cape Town and the sea ice edge. For the collection of surface sediments a micro-corer (MIC) was applied, which consisted of a weight bomb and four tubes (ø 6 cm) installed 20 m below the CTD. At 17 stations undisturbed surface sediment cores were collected with lengths of up to 60 cm (see Table 2.7-1). The samples are used for the completion of data sets in the South Atlantic, which form an important background for the field work of the Sonderforschungsbereich 261. The calcareous (foraminifera) and siliceous (diatoms, radiolarians) microfossils as well as their chemical composition and the composition of abiogenic particles (e.g. clay minerals) will be determined quantitatively at a later stage. These data sets represent the basis for the reconstruction of environmental conditions during earlier geological epochs.

Table 2.7-1: Station list of sediment samples

Station	GEO-Station PS	Date	Latitude	Longitude	Water depth (m)	Recovery
21/539	2230-1	22.5.92	34°45,206' S	17°21,409' E	2575	20 cm
21/541	2231-1	23.5.92	35°36,316' S	16°22,079' E	4285	16 - 24 cm
21/543	2232-1	24.5.92	36°35,071' S	15°15,070' E	4807	-
21/545	2233-1	25.5.92	37°32,344' S	14°06,816' E	4929	22 - 51 cm
21/556	2234-1	30.5.92	41°59,917' S	6°03,988' E	4778	19-35 cm
21/557	2235-1	30.5.92	42°14,962' S	5°13,148' E	4797	34 cm
21/559	2236-1	31.5.92	42°41,494' S	3°32,033' E	4562	-
21/563	2237-1	1.6.92	44°15,210' S	1°32,651' E	4450	23 cm
21/564	2238-1	2.6.92	44°53,394' S	1°32,651' E	4688	20 - 34 cm
21/565	2239-1	2.6.92	45°30,027' S	1°14,067' E	4291	23 cm
21/568	2240-1	3.6.92	46°46,034' S	0°37,004' E	4186	15 - 23 cm
21/569	2241-1	3.6.92	47°24,053' S	0°17,429' E	3748	0 - 15 cm
21/571	2242-1	4.6.92	49°59,897' S	0°02,635' E	3680	0 - 18 cm
21/576	2243-1	8.6.92	54°59,859' S	0°01,506' E	1757	0 - 23 cm
21/577	2244-1	9.6.92	56°00,519' S	0°02,582' E	3547	25 - 41 cm
21/578	2245-1	9.6.92	57°00,593' S	0°02,132' E	3802	18 - 60 cm
21/579	2246-1	10.6.92	58°00,009' S	0°00,215 E	4529	30 cm
21/581	2247-1	10.6.92	59°00,470' S	0°00,248 E	4607	33 - 36 cm
21/583	2248-1	11.6.92	60°00,055' S	0°01,981 E	5373	30 cm

3. Stationsliste/Station list

Station No.	Date	Start Time (GMT)	Start Position		Depth (m)	Work
21/535	22.05.92	05:55	34°16.5'S	17°20.9'E	2000	CTD
21/536	22.05.92	11:05	34°11.8'S	17°58.1'E	244	CTD
21/537	22.05.92	14:09	34°22.8'S	17°45.8'E	438	CTD
21/538	22.05.92	17:19	34°34.0'S	17°33.0'E	2110	CTD
21/539	22.05.92	21:15	34°45.3'S	17°21.2'E	2579	CTD/MIC
21/540	23.05.92	03:27	35°07.0'S	16°56.0'E	3411	CTD
21/541	23.05.92	12:06	35°36.2'S	16°22.0'E	4284	CTD/MIC
21/542	23.05.92	21:11	36°05.9'S	15°48.8'E	4636	CTD
21/543	24.05.92	06:25	36°35.0'S	15°14.9'E	4809	CTD/MIC
21/544	24.05.92	20:05	37°03.8'S	14°40.7'E	4910	CTD
21/545	25.05.92	07:14	37°32.8'S	14°06.8'E	4940	CTD/MIC
21/546	25.05.92	16:49	38°03.0'S	13°33.0'E	5041	CTD
21/547	26.05.92	02:48	38°32.0'S	12°59.0'E	5034	CTD
21/548	26.05.92	20:05	39°21.9'S	11°58.9'E	4775	CTD
21/549	27.05.92	06:07	39°51.1'S	11°24.1'E	4816	CTD
21/550	27.05.92	17:26	40°20.0'S	10°47.8'E	4670	CTD
21/551	28.05.92	04:40	40°50.1'S	10°12.8'E	4647	CTD
21/552	28.05.92	19:11	41°03.9'S	09°24.1'E	4695	CTD
21/553	29.05.92	04:33	41°18.9'S	08°33.9'E	5241	CTD
21/554	29.05.92	16:10	41°32.0'S	07°43.5'E	4493	CTD
21/555	29.05.92	23:19	41°45.8'S	06°53.7'E	4879	CTD
21/556	30.05.92	06:38	42°00.0'S	06°04.0'E	4781	CTD/MIC
21/557	30.05.92	14:00	42°14.2'S	05°12.8'E	4793	CTD/MIC
21/558	31.05.92	06:00	42°28.0'S	04°23.0'E	4644	CTD
21/559	31.05.92	13:54	42°41.5'S	03°32.0'E	4563	CTD/MIC
21/560	31.05.92	22:56	42°56.2'S	02°40.9'E	3878	CTD
21/561	01.06.92	04:41	42°59.6'S	02°20.3'E	825	Pegel 4u.3
21/562	01.06.92	12:31	43°36.7'S	02°08.1'E	4481	CTD
21/563	01.06.92	21:48	44°15.0'S	01°49.4'E	4449	CTD/MIC
21/564	02.06.92	06:02	44°53.4'S	01°32.6'E	4488	CTD/MIC
21/565	02.06.92	14:53	45°30.0'S	01°14.0'E	4288	CTD/MIC
21/566	02.06.92	20:00	45°49.2'S	01°04.8'E	4364	CTD
21/567	02.06.92	23:53	46°08.0'S	00°55.7'E	4452	CTD
21/568	03.06.92	08:05	46°46.1'S	00°36.7'E	4186	CTD/MIC
21/569	03.06.92	15:42	47°24.0'S	00°17.6'E	3773	CTD/MIC
21/570	03.06.92	23:35	48°00.3'S	00°00.3'E	3946	CTD
21/571	05.06.92	00:00	49°59.9'S	00°02.4'E	3621	CTD/MIC/BO
21/572	05.06.92	06:41	50°29.9'S	00°00.3'E	3473	CTD
21/573	05.06.92	12:20	50°59.9'S	00°00.6'W	2289	CTD
21/574	07.06.92	19:28	53°00.4'S	00°00.2'E	2550	CTD
21/575	08.06.92	06:08	54°00.3'S	00°01.0'E	2591	CTD/BO
21/576	08.06.92	17:38	55°00.1'S	00°00.5'E	1743	CTD/MIC/MN
21/577	09.06.92	08:27	56°00.1'S	00°00.1'E	3760	CTD/MIC/MN/BO/ APN/SD
21/578	09.06.92	18:31	57°00.2'S	00°00.6'W	3891	CTD/MIC
21/579	10.06.92	06:04	58°00.0'S	00°00.0'W	4533	CTD/MIC/BO/APN
21/580	10.06.92	13:22	58°30.1'S	00°00.3'W	4181	CTD/MN/APN/SD
21/581	10.06.92	22:19	59°00.4'S	00°00.3'W	4614	CTD/MIC
21/582	11.06.92	08:16	59°36.9'S	00°00.3'W	5189	CTD/APN

21/583	11.06.92	14:17	60°00.0'S	00°00.3'W	5370	CTD/MIC/MN/APN
21/584	11.06.92	23:13	60°30.2'S	00°01.0'W	5351	CTD
21/585	12.06.92	05:25	61°00.3'S	00°00.8'W	5375	CTD/APN
21/586	12.06.92	11:40	61°30.0'S	00°00.7'W	5379	EK/CTD/MN/APN/SD
21/587	12.06.92	19:45	62°00.5'S	00°00.2'W	5357	CTD/APN/EK
21/588	13.06.92	02.01	62°30.2'S	00°00.1'W	5335	CTD
21/589	13.06.92	08:10	63°00.2'S	00°00.4'W	5299	EK/CTD/MN/APN
21/590	13.06.92	17:06	63°30.3'S	00°00.4'E	5233	EK/CTD/APN
21/591	13.06.92	23:35	64°00.5'S	00°00.4'W	5186	BO/CTD
21/592	14.06.92	06:45	64°30.3'S	00°00.0'E	4659	CTD/APN/SD/MN/BO
21/593	14.06.92	15:28	65°00.2'S	00°00.8'E	3718	CTD/BO/APN
21/594	14.06.92	22:35	65°30.1'S	00°00.1'E	3980	CTD
21/595	15.06.92	04:10	66°00.1'S	00°00.8'E	3418	CTD/APN/MN
21/596	15.06.92	11:27	66°30.1'S	00°00.9'E	4531	CTD/APN/SD/MC
21/597	15.06.92	19:08	67°00.0'S	00°00.4'E	4697	CTD
21/598	16.06.92	06:16	67°30.2'S	00°00.4'E	4621	CTD/MN/APN/SD/ MC
21/599	16.06.92	17:55	67°59.9'S	00°00.8'E	4502	CTD/APN
21/600	16.06.92	23:25	68°15.1'S	00°00.3'W	4440	CTD
21/601	17.06.92	05:18	68°30.0'S	00°00.9'E	4251	CTD
21/602	17.06.92	12:03	68°44.7'S	00°01.5'E	3641	BO/APN/CTD/ICE
21/603	17.06.92	21:05	69°00.3'S	00°00.5'E	3393	CTD/APN/MN
21/604	18.06.92	10:00	69°14.6'S	00°02.7'W	2605	CTD/APN/ICE
21/605	18.06.92	20:35	69°29.8'S	00°22.9'W	1820	CTD
21/606	19.06.92	00:13	69°42.6'S	00°40.8'W	2139	BO/APN/CTD
21/607	21.06.92	08:48	70°32.3'S	08°02.1'W	197	ICE
21/608	22.06.92	07:11	70°32.3'S	08°02.3'W	196	ICE
21/609	25.06.92	14:30	70°27.5'S	08°31.8'W	317	ICE
21/610	30.06.92	06:00	70°31.7'S	09°09.9'W	404	CTD/BO
21/611	30.06.92	09:30	70°29.4'S	09°44.9'W	970	CTD
21/612	30.06.92	12:24	70°29.5'S	09°54.2'W	1462	CTD/APN/MN
21/613	01.07.92	11:59	70°48.8'S	12°18.4'W	2028	CTD/APN/ICE
21/614	05.07.92	13:00	71°38.0'S	16°35.0'W	2428	ICE
21/615	07.07.92	09:45	72°03.0'S	18°06.6'W	2771	ICE/NAN
21/616	10.07.92	06:00	69°44.1'S	23°46.7'W	4591	ICE/DEPL-9369/RR
21/617	10.07.92	10:40	69°30.1'S	24°24.7'W	4670	ICE/RR
21/618	10.07.92	14:18	69°15.2'S	25°03.2'W	4696	CTD/ICE/DEPL-9365/ DEPL-9368(Heli)
21/619	11.07.92	00:06	68°58,7'S	25°41.5'W	4740	RR
21/620	11.07.92	05:32	68°44.3'S	26°18.8'W	4739	CTD/ICE/DEPL-9364/ DEPL-9367(Heli)
21/621	11.07.92	13:49	68°29.7'S	26°57.6'W	4741	ICE
21/622	11.07.92	19:58	68°14.6'S	27°34.8'W	4729	ICE/DEPL-9366/RR
21/623	13.07.92	14:30	65°59.4'S	33°29.8'W	4777	CTD/MN/ICE/APN
21/624	14.07.92	02:47	65°47.5'S	34°52.6'W	4763	CTD
21/625	14.07.92	19:05	65°35.1'S	36°27.1'W	4769	ICE/CTD/APN/BO
21/626	15.07.92	13:12	65°17.2'S	37°40.6'W	4769	CTD/MN/APN/ICE
21/627	16.07.92	21:45	65°08.5'S	40°13.1'W	4767	CTD
21/628	17.07.92	14:21	64°56.0'S	41°20.3'W	4741	CTD/BO/APN/ICE
21/629	18.07.92	06:20	64°41.8'S	41°56.9'W	4731	CTD
21/630	19.07.92	07:12	63°43.5'S	43°24.5'W	4060	CTD/MN/APN/ICE
21/631	19.07.92	16:40	63°25.3'S	43°33.0'W	3827	CTD
21/632	20.07.92	16:54	62°59.5'S	43°20.6'W	3554	CTD
21/633	20.07.92	23:20	62°40.1'S	43°33.4'W	3194	CTD

21/634	21.07.92	07:21	62°20.5'S	43°41.1'W	1174	CTD/BO/ICE
21/635	21.07.92	19:00	62°01.2'S	44°17.8'W	656	CTD/APN/BO/ICE-LST
	24.07.92	13:11	61°54.2'S	43°07.5'W	703	CID
	24.07.92	18:00	61°52.9'S	43°00.3'W		Ende ICE-LST
21/636	25.07.92	11:05	60°59.1'S	42°58.6'W	400	CID
21/637	26.07.92	04:09	60°25.0'S	46°58.0'W	285	CID
21/638	26.07.92	15:07	60°13.7'S	47°11.0'W	569	CTD/APN
21/639	26.07.92	19:03	60°05.5'S	47°18.9'W	1536	CTD/MN
21/640	27.07.92	03:39	60°09.9'S	47°57.7'W	2245	CID
21/641	27.07.92	10:55	60°10.2'S	48°39.2'W	1575	CTD/APN/MN
21/642	27.07.92	16:50	60°10.3'S	49°19.4'W	1214	CTD/ICE
21/643	27.07.92	21:30	60°12.3'S	49°50.8'W	1358	CID
21/644	28.07.92	00:28	60°13.9'S	50°16.9'W	496	CTD/BO
21/645	28.07.92	08:00	60°05.6'S	50°18.5'W	2793	ICE/MU
21/646	28.07.92	13:35	59°51.8'S	50°31.9'W	3830	ICE
21/647	28.07.92	17:30	59°39.3'S	50°29.9'W	3818	ICE
21/648	29.07.92	08:20	59°08.1'S	50°57.4'W	2830	ICE/CTD/MN
21/649	30.07.92	10:20	61°00.2'S	58°25.2'W	5209	CTD/MN
21/650	01.08.92	07:10	59°48.4'S	58°43.6'W	2173	XBT
21/651	01.08.92	07:50	59°48.0'S	58°47.0'W	1814	XBT
21/652	01.08.92	08:57	59°35.7'S	58°56.6'W	4084	XBT
21/653	01.08.92	09:57	59°23.3'S	59°05.5'W	3774	XBT
21/654	01.08.92	10:59	59°10.7'S	59°14.5'W	3819	XBT
21/655	01.08.92	11:59	58°57.7'S	59°22.8'W	4182	XBT
21/656	01.08.92	13:59	58°31.6'S	59°39.9'W	3773	XBT
21/657	01.08.92	15:00	58°18.1'S	59°48.3'W	3359	XBT
21/658	01.08.92	15:55	58°05.5'S	59°54.6'W	3792	XBT
21/659	01.08.92	16:57	57°53.1'S	60°04.7'W	3664	XBT
21/660	01.08.92	17:58	57°40.7'S	60°13.5'W	3151	XBT
21/661	01.08.92	18:56	57°28.5'S	60°21.7'W	3272	XBT
21/662	01.08.92	21:57	56°47.1'S	60°49.6'W	3923	XBT
21/663	01.08.92	23:00	56°33.8'S	61°01.9'W	4121	XBT
21/664	02.08.92	00:00	56°23.0'S	61°17.3'W	4097	XBT
21/665	02.08.92	02:18	55°58.5'S	61°49.3'W	4095	XBT
21/666	02.08.92	02:52	55°51.5'S	61°57.8'W	4049	XBT
21/667	02.08.92	03:53	55°39.2'S	62°11.5'W	4106	XBT
21/668	02.08.92	04:50	55°27.3'S	62°20.5'W	4153	XBT
21/669	02.08.92	05:57	55°13.6'S	62°33.8'W	4285	XBT
21/670	02.08.92	06:58	55°00.4'S	62°46.5'W	3192	XBT
21/671	02.08.92	07:57	54°50.2'S	62°58.7'W	1864	XBT
21/672	02.08.92	08:19	54°44.2'S	63°03.7'W	624	XBT

BO = Bongo-Net, MN = Multi-Net,ICE = ice station, APN = Apstein-Net, SD = Secchi-Disk, EK = Eiskorb, MC = Mummy Chair Coring, NAN = Nansen-Net, DEPL-XX = deployment of drifting buoy, RR = deployment of radar-reflector, XBT = expandable bathythermograph

4. Beteiligte Institute/Participating institutions

Adresse/address		Teilnehmer/participants
Federal Republic of Germany		
AWI	Alfred-Wegener-Institut für Polar- und Meeresforschung Postfach 12 01 61 27515 Bremerhaven	21
HSW	Helicopter Service Wasserthal GmbH Kätnerweg 43 22393Hamburg	4
IMH	Institut für Meteorologie und Klimatologie der Universität Hannover Nienburger Straße 6 30167 Hannover	5
UNIB	Universität Bremen Bibliothekstraße 28334 Bremen	4
UNIK	Universität Kiel Institut für Geophysik Leibnizstr. 2418 Kiel	1
SWA	Seewetteramt Deutscher Wetterdienst Bernhard-Nocht-Str. 76 20359 Hamburg	2
Belgium		
VUB	Vrije Universiteit Brussels Laboratory for Ecotoxicology Pleinlaan 2 B-1050 Brussel	1
Canada		
AES	AES/Cress Microwave Group Petrie 214-York University 4700 Keele Street North York, Ontario Canada M3J 1P3	1

Netherlands

NIOZ	Nederlands Instituut voor Onderzoek der Zee PO Box 59 1790 Ab den Burg, Texel	2

Russia

AARI	Arctic and Antarctic Research Institute 38 Bering Street 19226 St. Petersburg	1

United States of America

NRL	NOAA Research Laboratory 72 Lyme Road Hanover, NH 03755	1
GSFC	NASA/Goddard Space Flight Center Laboratory for Oceans, Code 61 Greenbelt, Maryland, 20771	1
JPL	Jet Propulsion Laboratory 4800 Oak Grove Drive Pasadena, CA 91109	1

5. Fahrtteilnehmer/Participants

Belgers, Jan J.J.M.	NIOZ
Bochert, Axel	AWI
Brandt, Rüdiger	IMH
Brey, Heinz	HSW
Brunken, Nicole	AWI
Büchner, Jürgen	HSW
Bulsiewicz, Klaus	UNIB
Dierking, Wolfgang	AWI
Dietrich, Helmut	AWI
Drinkwater, Mark	JPL
Ewald, Horst	HSW
Fahl, Kirsten	AWI
Frieden, Wolfgang	IMH
Garrity, Caren	AWI/AES
Haas, Christian	UNIK
Hansen, Imke	AWI
Heil, Petra	AWI
Holsbeek, Ludo	VUB
Hoppema, Mario	NIOZ
Jahn, Petra	AWI
Köhler, Herbert	SWA
Kreyscher, Martin	AWI
Lemke, Peter (chief scientist)	AWI
Lohanick, Alan	NRL

Massom, Robert	GSFC
Mai, Stephan	AWI
Moschner, Stephan	AWI
Nöthig, Eva-Maria	AWI
Plep, Wilfried	UNIB
Rasenat, Steffen	AWI
Richter, Klaus-Uwe	AWI
Riewesell, Christian	HSW
Röd, Erhard	SWA
Rose, Henning	UNIB
Rothe, Thomas	IMH
Schröder, Michael	AWI
Schulte, Christian	AWI
Schulze, Olaf	IMH
Spiridonov, Vasili	AARI
Steiner, Nadja	AWI
Sterr, Uta	AWI
Sültenfuß, Jürgen	UNIB
Thomas, Markus	IMH
Viehoff, Thomas	AWI
Wisotzki, Andreas	AWI

6. Besatzung/Crew

Kapitän	Jonas
1. Offizier	Gerber
Naut. Offizier	M. Rodewald
Naut. Offizier	Grundmann
Naut. Offizier	S. Schwarze
Arzt	Dr. R. Thoennies
Ltd. Ingenieur	K. Müller
1. Ingenieur	G. Erreth
2. Ingenieur	R. Fengler
2. Ingenieur	O. Ziemann
Elektriker	G. Schuster
Elektroniker	H. Elvers
Elektroniker	M. Arndt
Elektroniker	H. Muhle
Elektroniker	J. Roschinsky
Funkoffizier	H. Geiger
Funkoffizier	K.H. Wanger
Koch	E. Kubicka
Kochsmaat	M. Dutsch
Kochsmaat	H. Hüneke
1. Steward	H. Vollmeyer
Steward,/Krankenschw.	M. Reitz
Stewardess	M. Hoppe
Stewardess	K. Helpap
Stewardess	J. Hasler
2. Steward	Ch. L. Yu
2. Steward	K. Yu
Wäscher	Ch. Chang
Bootsmann	R. Zulauf
Zimmermann	K. Marowski

Matrose	J. Novo Loveira
Matrose	B. Iglesias Bermudez
Matrose	J. Soaga Curra
Matrose	J. Pousada Martinez
Matrose	F. Garcia Martinzez
Matrose	M. Winkler
Lagerhalter	K. Müller
Maschinenwart	M. Lesch
Maschinenwart	U. Husung
Maschinenwart	M. Reitz
Maschinenwart	G. Dufner
Maschinenwart	G. Fritz